SYSTEMS, STRATEGIES & RESEARCH FOR LUBRICATION PROFESSIONALS

AN STLE PUBLICATION | APRIL 2014

TLT

TRIBOLOGY & LUBRICATION TECHNOLOGY

10 YEARS
of publishing excellence

PUTTING BEARINGS TO THE TEST

New technology has improved (but not perfected) our ability to predict failure.

Split or Squeak?
Stick-slip explained

Q&A with Michael Forgeron
Future challenges in oil analysis

ASTM Tests
Evaluating industrial lubricants

Revolutionary New Oil
Report from Dr. Loof Lirpa

Download 2014 STLE Annual Meeting App. Sponsored by Sea-Land Chemical.

INTRODUCING

**IN PLACES FEW WILL EVER SEE –
WHERE THE WORLD'S INDUSTRIAL LUBRICATION IS DONE –
THE MICROBOTZ™ DO THEIR WORK.**

WHERE TEMPERATURES SOAR AND PRESSURE IS INTENSE, WHERE THE ENEMIES ARE MANY AND RESPITES FEW.
PATROLLING AND PROTECTING OUR CUSTOMERS' LUBRICANTS, DEEP INSIDE THE EQUIPMENT THEY SERVE.
THIS IS THEIR WORLD. NEVER SEEN, NEVER TIRING, NEVER BEATEN.

THROUGH OUR PASSION FOR SOLUTIONS®, WE HAVE CREATED SEVEN UNIQUE GUARDIANS.
THEIR MISSION: TO GUIDE YOU THROUGH THE INDUSTRIAL LANDSCAPE. EXPLAINING THE BENEFITS OF AFTON'S ADDITIVE TECHNOLOGY TO YOUR BUSINESS AND INTRODUCING YOU TO NEW SOLUTIONS. EACH IS AN APPLICATION EXPERT; FROM TURBINE TO SLIDEWAY, INDUSTRIAL GEAR TO METALWORKING, WIND TURBINE, HYDRAULIC AND GREASE.

SEVEN CHAMPIONS. SEVEN HEROES OF PROTECTION AND PERFORMANCE.
IN THE MONTHS AHEAD, THEIR STORY WILL UNFOLD...

www.aftonmicrobotz.com

INDUSTRIAL

Afton CHEMICAL
Passion for Solutions®

Contents

TLT / APRIL 2014 / VOLUME 70 / NO. 4

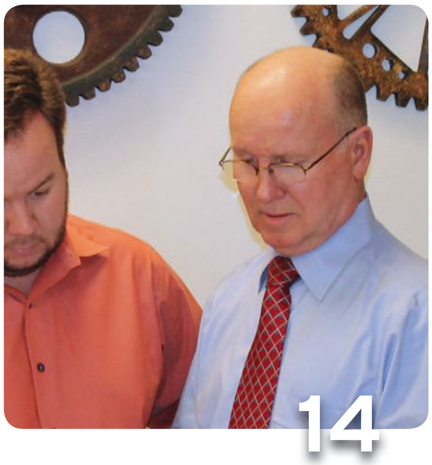

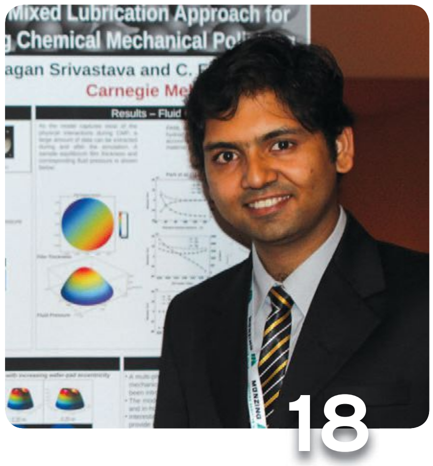

FEATURES

Contents

4

8

DEPARTMENTS

COLUMNS

TRIBOLOGY AND LUBRICATION TECHNOLOGY (USPS 865740) Vol. 70, Number 4, (ISSN-1545-858), is published monthly by the Society of Tribologists and Lubrication Engineers, 840 Busse Hwy, Park Ridge, IL 60068-2376. Periodicals Postage is Paid at Park Ridge, IL and at additional mailing offices. POSTMASTER: Send address changes to Tribology and Lubrication Technology, 840 Busse Hwy, Park Ridge, IL 60068-2376.

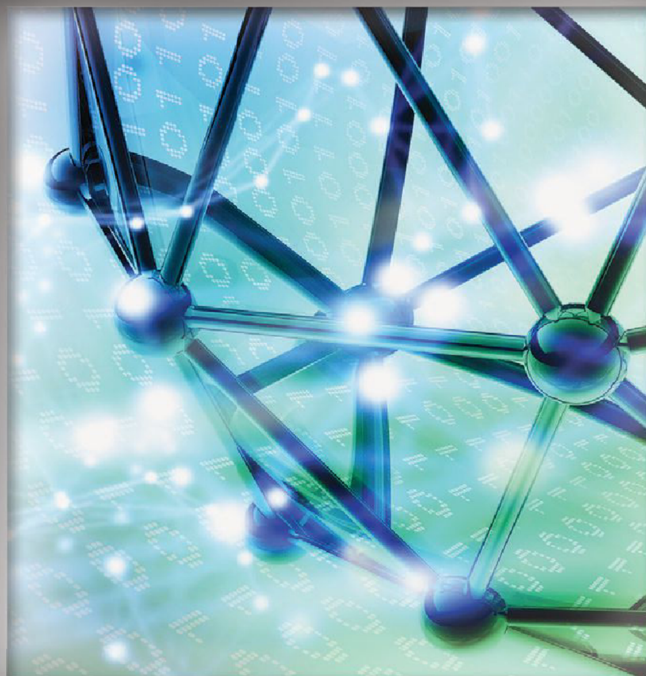

Robert D. Heverly

Tribological Tea Leaves

You don't need a fortune teller to see that STLE's 2014 Annual Meeting & Exhibition just might be our biggest in years.

In olden days seers would read tea leaves to predict someone's future. Here at STLE, we've updated that ancient approach. Every year we look for indicators about the health of our upcoming annual meeting and exhibition.

I'm happy to report that the omens for our 2014 conference are overwhelmingly positive. The early indicators are that the event, May 18-22 at Disney's Contemporary Resort in Lake Buena Vista, Florida, about 19 miles from Orlando, could be our biggest in years.

Let's take a look at the tribological tea leaves.

First, STLE is offering more than 400 technical presentations. Anything over 350 is a very encouraging sign. This many presentations ensures that anyone who comes to the meeting will have access to a broad range of the finest industry-specific technical research available in the world.

Technical education and training has always been STLE's strong suit, and our 2014 conference is no exception.

Another good indicator of strong meeting attendance is the number of room nights, because reserving a room is usually the first action a member takes when planning a convention itinerary. Bookings for the Contemporary and for two additional hotels have been running more than 50 percent ahead of what we would normally expect to see.

Two other key indicators of a strong annual meeting are sales of exhibit booths and the Commercial Marketing Forum (CMF). For our Corporate Members, both events are opportunities to openly promote their products and services in a way the society doesn't allow at technical sessions. For attendees, the two events are where you can find the kind of technical solutions that can save you thousands of dollars or help you better serve your employer and customers.

Normally, STLE sells booth space right up to the start of the meeting. This year the trade show sold out in early February. We added another row of booths, and they sold out in a day. The same was true of time slots for the CMF. All spaces sold out *months* ahead of the norm. STLE added another day of the 30-minute slots, and they were purchased immediately. We are running wait lists for both the trade show and CMF, so if you are interested please contact national sales manager Tracy VanEe at (630) 922-3459, **tnicholas@stle.org.**

So we know there will be a lot of people in Lake Buena Vista. Our estimate is that some 1,400 members of the lubrication engineering and tribology-research communities from all over the world are attending.

Of course, the key component of any industry event is content. Fortunately, technical education and training has always been our society's strong suit, and our 2014 conference is no exception.

In addition to the 400 technical presentations, STLE's meeting offers 12 one-day education courses taught by the industry's most knowledgeable experts. For the first time, you may take a course without registering for the meeting.

A traditional highlight of an STLE annual meeting is the keynote speaker. This year we are very pleased to have Dr. Don Hillebrand with Argonne National Laboratory in suburban Chicago. Don's topic is "Advanced Vehicle Technology Research," and he'll update us on such issues as the electrification of the automobile, the smart grid, advanced combustion methods, new fuels and autonomous vehicles. I know I'm looking forward to Don's talk.

STLE remains the industry's premier source for technical education and training, but please remember that our annual conference also is a networking event. That means the most important element of any annual meeting is *you*. Please join us for an invaluable and unique experience that just can't be replicated anywhere else. To register, just log on to **www.stle.org** up to and even during the meeting.

When you see me at the show, please be sure to say hi. I look forward to meeting you.

Representing the Houston area, Rob Heverly is a technical sales representative for Vanderbilt Chemicals, LLC, in Norwalk, Conn. You can reach him at ***rheverly@vanderbiltchemicals.com.***

 We've all heard the term "vernal equinox." Vernal means "spring" and equinox means "equal night." Both words are Latin.

Evan Zabawski

Dr. Loof Lirpa's Revolutionary New Oil

A sense of humor is a good thing.

Oddly enough, German cars do actually require 730 oil.

"DID YOU HEAR ABOUT THE NEW OIL PUT OUT BY…" is a sentence that will not end well when spoken on April 1 or, for that matter, when spoken any time of year to someone new to the industry. Let's face it, we all enjoy some gentle ribbing, but sometimes the prankster won't own up to the ruse.

One of the most popular setups I have heard was likely started by a mechanic when speaking to an apprentice. The innocuous request is for the apprentice to fetch "710 oil." After rummaging through the inventory of oils in the shop and returning empty handed, the apprentice will likely break down and admit defeat. At that point, the mechanic will implore it must be found because the filler cap clearly states the correct name for the required oil.

The prank becomes a *fait accompli* when the apprentices checks the cap and realizes that 710 is merely OIL when viewed upside down. Oddly enough, German cars do actually require 730 oil. Don't believe me? Just check the cap. By the way, did you know the German word for oil is OEL?

I almost had you there. The folks over at Honda Motorcycles who assign part numbers definitely have a sense of humor. For the past 30 years, the part number for the relatively universal oil filler cap, which is embossed OIL, remains 15611-KA4-710 (actually true).

A less common setup, which can only be pulled off once a year, is to invoke chemist Dr. Loof Lirpa's name in conjunction with some extravagant new development from a major chemical, additive or oil company. I can admit my high school chemistry teacher got most of my class with this one, but I still hear it occasionally all these years later. Loof Lirpa is not a real person, just April Fool spelled backwards.

The line between fact and fiction can be crossed by those pushing aftermarket additive products. Many of us have been to a trade show where someone will demonstrate the "lubricity" of commonly used engine oils by using an apparatus that attempts to stop a rotating spindle by using a lever to push a small block of steel against it. The engine oil is applied to the spindle and some small amount of weight is hung from the end of the lever, thus pressing the block against the spindle, which quickly stops. The next step is to apply some of the additive, whereby the spindle remains spinning despite significant addition of weight.

The fact is that the test rig is real (conforms to ASTM D2509 and D2782); it evaluates the load-carrying capacity of extreme-pressure (EP) lubricants. The fiction comes from the fact that no engine oil will have, nor require, significant EP properties, but the additive obviously does. By describing the demonstration as a lubricity evaluation, the viewer is lured into a very real but misleading setup. The jig is up, so to speak, if an honest and educated or experienced individual calls out the demonstrator.

This is a luxury not afforded to the average shopper in the oil section of an automotive parts store with another staged lubricity demonstration. The mini test rig involves two baths of oil, each with a series of interconnected plastic gears arranged vertically. Turning the crank on each of the bottom gears yields only one or two oil-wetted gears in the plain oil bath but a veritable reverse-waterfall in the additized oil bath. Without a human demonstrator, nobody can challenge that the property being demonstrated has more to do with tackiness (again, not required in engine oils) or that the additized oil bath ends up with significant air entrainment (undesirable in any lubricated application).

It can be a lot of fun to joke with our colleagues but only when done good naturedly. It is unacceptable to perpetrate a deception publicly, especially if it has the potential of harming the very asset it promises to protect.

Evan Zabawski, CLS, is a reliability specialist in Calgary, Alberta, Canada. You can reach him at ***evan.zabawski@gmail.com.***

Edward P. Salek, CAE / Executive Director

Mastering the art of networking

Some thoughts on what to do if "working the room" doesn't come naturally.

IT HAS BEEN REPORTED that former U.S. President Bill Clinton would say, "It's show time!" before stepping foot into any event. This was indicative of his focus on the art of networking—he knew the people who would be there, he came with the intent of forming relationships and he made his time purposeful.

With the networking opportunities that are available at the STLE Annual Meeting & Exhibition in May, and other events throughout the year, most of us would love to have the skill set of a naturally extroverted networker like President Clinton. But for those who, like me, are not adept at "working the room," there is hope for some improvement in the form of a new white paper published by The National Conference Center (NCC), which is located in the Washington, D.C. area.

Titled *The Power of Networking*, the report is based on interviews with eight business leaders and meeting professionals who offer tips on how to be a better networker. This is crucial, they contend, because there is simply no substitute for face-to-face connections, even in this age of Facebook and LinkedIn.

The guidance starts by defining what we mean by networking. According to these experts, networking can and should be more than chit chat over a glass of Chardonnay or a bottle of beer. Instead, we should think of it as the process of cultivating people who can be helpful, both professionally and personally.

Networking superstars dissect this concept and approach it strategically. The NCC white paper advises that this requires "work, practice, concentration and good habits. It's asking who is going to be there, what do I want to accomplish and what do I want to walk away with?"

Once you are at an event, the article recommends coming up with an introductory line that sparks conversation and invites more than superficial dialogue. One of the contributors suggests, "Instead of asking where someone works, ask 'What has you the most engaged today?' It shifts the focus to them." Thought-provoking questions are another good conversation starter. At your next networking event, try asking: "What person in history do you most admire and why?"

The NCC white paper offers many other practical ideas to power up your networking skills. Three of my favorites are:

- Have a goal set and know who you want to meet prior to attending. Come prepared with business cards, but only give them to people who you can either help or that you feel have a strong interest in your product or service.
- Do less talking and more listening! We love to hear ourselves talk. Show interest. You draw interest when you show interest.
- Don't focus on the people you know, use the people you know to connect with other people.

You never know when even a casual conversation at an STLE meeting could lead to a technical solution, a new opportunity or a business relationship.

While primarily a technical-education conference, STLE's upcoming annual meeting is loaded with networking opportunities. The Welcoming Party, Presidents Luncheon and trade show are the most obvious examples. But remember that even casual conversations during refreshments breaks and in the hallways between technical sessions or education courses are opportunities for you to apply your networking skills. Some 1,400 people from around the world are attending the event, and you never know when a casual conversation will lead to a technical solution, a new opportunity or a business relationship.

The Power of Networking is available for complimentary download from The National Conference Center's Website (**www.conferencecenter.com**). For more in-depth reading, check out *Eat, Drink and Succeed: Climb Your Way to the Top Using the Networking Power of Social Events* by Laura Schwartz. It's available on Amazon and through other booksellers.

*You can reach Certified Association Executive Ed Salek at **esalek@stle.org.***

Dr. Neil Canter / Contributing Editor

Potential for windmills at the microscale

Micro-windmills can operate without even standing up.

THE CHALLENGE IN FINDING LONG-TERM LUBRICATION solutions for wind turbines is well known and documented. One approach that has been discussed involves finding ways to reduce the stress on individual wind turbines in a farm in order to improve their longevity.

In a previous TLT article, researchers used a technique known as Simulator for Offshore /Onshore Wind Farm Applications to examine an existing wind farm and studied five scenarios in which the turbines are spaced in a different manner from each other.[1] The results from these scenarios indicate that staggering wind turbines leads to a significant improvement in the efficiency of each individual unit. A second factor is that reduction of the number of wind turbines also results in greater efficiency.

A good deal of attention has also been paid to determining how lubrication occurs at the nanoscale and what types of materials should be used to improve the performance of devices such as microelectromechanical systems (MEMS). One concern with small electrical devices is how to effectively dissipate the heat they generate.

Developing a device that can assist with this process is one of the reasons why work was initiated to design a turbine that functions on the microscale. J.C. Chiao, Greene and Garrett Professor of Electrical Engineering at The University of Texas-Arlington in Arlington, Texas, says, "We have been working to develop MEMS turbine devices for the past six to seven years. My group is involved in the design of new MEMS platforms and we felt that placing a turbine on a silicon chip will have two benefits. The turbine can harness energy that passed by the chip in the form of air circulation or cool the silicon chips operating in an electrical device."

Initial attempts at developing a micro-windmill did not work. Chiao says, "Our initial micro-windmills were fabricated in silicon, which is a very robust material. But under the conditions of strong wind force, the silicon-based micro-windmill became brittle and shattered immediately once wind speed picked up."

The benefits of a micro-windmill can only be achieved if a more durable material can be used. Such a material has now been found.

KEY CONCEPTS

- Micro-windmills with blades that are approximately 0.9 millimeters in length have been developed from a nickel alloy.
- In contrast to macro-windmills, micro-windmills do not need to stand up and can be placed flat on a surface.
- One important application for micro-windmills is to dissipate heat buildup in MEMS.

NICKEL ALLOY

Chiao and his research associate, Dr. Smitha Rao, produced durable micro-windmills through the use of a nickel alloy. Chiao says, "After consultations by one of our research partners, we found that they fabricated micro-machined devices using a nickel alloy instead of silicon. The advantage of the nickel alloy is that it has a lower Young's modulus and is more flexible than silicon. This property enables the alloy not to shatter when it bends."

> *'The advantage of the nickel alloy is that it has a lower Young's modulus and is more flexible than silicon. This property enables the alloy not to shatter when it bends.'*

Fabrication of the micro-windmill was not easy because there was no existing tool to run simulations to evaluate potential designs. Chiao says, "We tried more than 20 different ideas, but finally settled on a design that was inspired by Dr. Rao's daughter who likes to run around with a pinwheel on her head."

The design combines origami concepts with conventional wafer-scale semiconductor device planar layouts. Chiao says, "We fabricated the nickel alloys in a multilayer fashion. Five layers of the nickel alloy with sacrificial layers provide us with required thickness in 3-D structures."

The manufacturing cost is independent of the number of micro-windmills prepared in a wafer. A micro-windmill blade is approximately 0.9 millimeters in length, which means that it will turn with a diameter of 1.8 millimeters. Figure 1 provides a perspective on the size of a micro-windmill relative to a penny.

The dimensions for the initial micro-windmills are purely intuitive at this point. Chiao says, "We need to optimize the length of the blades. Longer blades will lead to more torque, which will increase the speed and effectiveness of the device. But it will reduce the number of windmills in a defined area. So we need to optimize its size to get the maximum combined power."

In contrast to macro-windmills that are built vertically above the ground to use wind blowing horizontally, air patterns on the micro level are different. Chiao says, "Air moves orthogonally to the micro-windmill, which means that the device does not need to stand up and can be placed flat on a surface. Holes are placed in the micro-windmill to enable air to flow through."

Chiao is unsure about how the air velocity fluctuates at the micro-level.

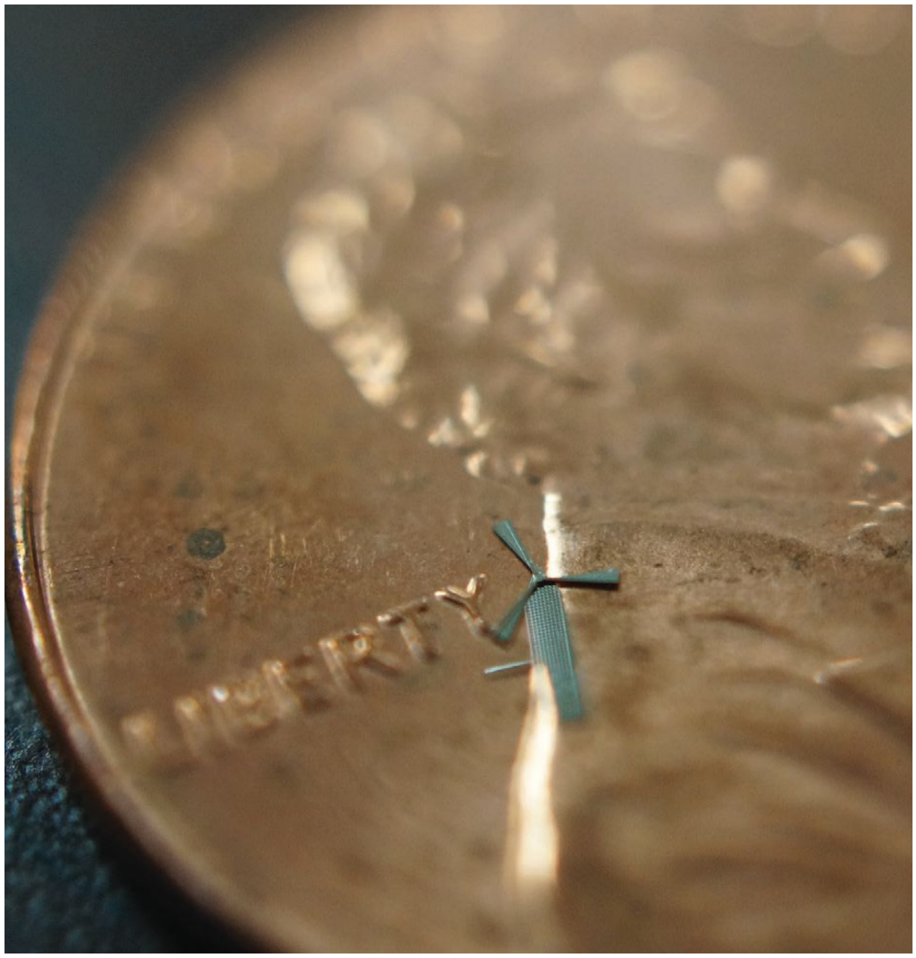

Figure 1 | **The small size of a micro-windmill is shown relative to a penny and means that this device can potentially be used to dissipate the heat buildup in MEMS.** *(Courtesy of The University of Texas-Arlington)*

'We do not know at this point but believe to maximize the benefit of the micro-windmill in a specific application, the mechanical configuration for that application must be designed around the turbine.'

He says, "We do not know at this point but believe to maximize the benefit of the micro-windmill in a specific application, the mechanical configuration for that application must be designed around the turbine. The wind gradient at the micro-level is much different from what is seen in a conventional wind tunnel that is several meters wide. This is due to the narrower dimensions at the micro-scale."

Evaluation of the micro-windmill is in progress at this point. Chiao says, "We did some elementary tests to make sure the device works such as using a tiny vacuum tube to blow air on it and also using a hair dryer. Currently, we are in the process of building an apparatus to more systematically evaluate the micro-windmill."

When asked about the use of lubricants, Chiao indicates that currently none are in use for such MEMS devices. He says, "We believe lubricants will be needed to run the micro-windmills in the future. One area where lubricants will be needed is to protect the micro-windmill from water. Moisture can be a big problem that leads to an increase in friction at the micron or submicron scale."

Chiao believes that micro-windmills can be used in a number of applications including remote sensors to evaluate the health of infrastructure. He says, "Maintaining infrastructure is a big issue, and the micro-windmills could be used in a wireless sensor to monitor the health of infrastructure such as bridges in a cost-effective manner."

The researchers have applied for a provisional patent on this technology. Further information can be obtained by contacting Chiao at **jcchiao@uta.edu.**

REFERENCES

1. Canter, N. (2014), "Staggered wind turbines," TLT, **70** (2), pp. 12-13.

Modeling of sudden fluid thickening

A new model explaining discontinuous shear thickening focuses on the frictional contact between particles.

DUE TO THE LARGE NUMBER OF COMPONENTS used in formulating, lubricants can be considered complex fluids. With some of the components in suspension, there can be times when the fluid may suddenly thicken in response to changes in parameters such as shear and viscosity.

In a previous TLT article, a related process in which fast shear or sudden impact to a dense suspension of cornstarch in water was studied.[1] The net effect of applying such stress to a 50 percent suspension of cornstarch in water was the immediate formation of a solid. Stress in the form of an aluminum rod striking the cornstarch suspension leads to the formation of a propagation front of solidification that is similar to how a snow plow operates.

KEY CONCEPTS

- Discontinuous shear thickening (DST) occurs when high shear is applied to a concentrated suspension, leading to a dramatic increase in thickening.
- A new model has been developed to explain that DST involves the formation of a three-dimensional force chain network.
- Once stress is applied, hydrodynamic forces force the particles together to initiate contact and friction.

> *'DST is very abrupt once sufficient shearing is done to a concentrated suspension. A small, say factor of two, increase in shear rate can lead to orders of magnitude rise in fluid viscosity.'*

Application of high shear to a concentrated suspension can lead to a dramatic increase in thickening through a phenomenon known as discontinuous shear thickening (DST). Jeffrey Morris, professor of chemical engineering at The City College of New York in New York, N.Y., says, "DST is very abrupt once sufficient shearing is done to a concentrated suspension. A small, say factor of two, increase in shear rate can lead to orders of magnitude rise in fluid viscosity. There is no intermediate state seen, which means that the fluid either displays low viscosity or high viscosity."

Several mechanisms have been proposed in the past to explain how DST occurs. Morris says, "Two possibilities are the order-disorder mechanism and hydroclustering. Order-disorder describes how a fluid moves from a low-viscosity state in a shear thinning regime to an unstable, disordered viscous state. Hydroclustering was taken directly from fluid mechanics and proposes that the thickening is due to particles clustering together in response to high shear."

Neither of these mechanisms fully explains how DST takes place. A new model has now been proposed to explain the origin of DST. One prominent factor that is extremely important in this model is friction.

THREE-DIMENSIONAL FORCE CHAIN NETWORK

Morris M. Denn, Albert Einstein Professor of Science and Engineering at The City College of New York, along with Drs. Ryohei Seto and Romain Mari, have developed a new model to explain DST that focuses on the frictional contact between particles. This model was prepared through the use of simulations that predict DST.

The numerical modeling simulations were done using Lees-Edwards boundary conditions. Cubic simulation boxes containing 512 particles and rectangular parallelepipeds were used.

Morris says, "For us, DST represented a classical fluid mechanics problem. In a hydrodynamic regime, forces are present to keep two smooth surfaces away from each other. As the surfaces get closer to each other, the film ruptures. This leads to a seizing condition on the local scale in a similar fashion to a journal bearing seizing."

In high concentrations, if one accepts that the particles must be in contact with each other, friction is generated as they rub against each other. The researchers determined how DST might occur from two aspects. Morris says, "Background on the particle interactions comes from analyzing DST, first as a fluid problem and then using ideas from the granular literature to

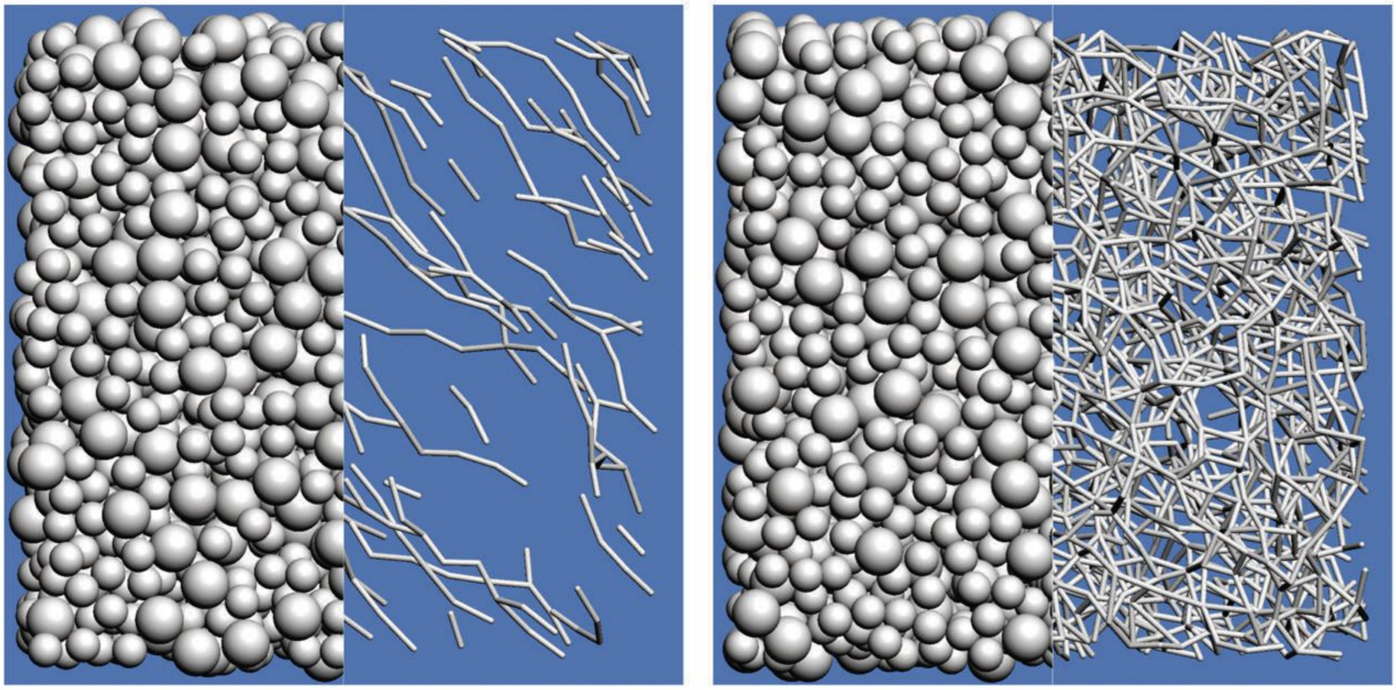

Figure 2 | **A new model for discontinuous shear thickening proposes that particles upon initial application of stress get pushed together and form force chains, as shown on the left side of the figure. Further stress leads the particles to form a three-dimensional force chain network, as shown on the right side of the figure.** *(Courtesy of The City College of New York)*

'A key ingredient of the DST model is the force chain concept derived from the granular literature. Structural transmission of forces moves from particle to particle in a manner that looks like a series of chains.'

incorporate friction. We combined these two aspects and introduced the key ideas of friction and viscosity."

Denn added, "A key ingredient of the DST model is the force chain concept derived from the granular literature. Structural transmission of forces moves from particle to particle in a manner that looks like a series of chains."

In the initial fluid state prior to the application of stress, the particles flow at a low viscosity and do not generate any friction because they do not come in contact. As stress is applied, the hydrodynamic forces push the particles together to initiate contact and friction. At this point, they start to act as a single entity. This leads to the formation of force chains that are used by the particles to transmit the stress in one direction. The left image in Figure 2 shows the stressed particles on the left side and the force chains formed as a result are on the right side.

With the increase in stress, the viscosity of the fluid radically increases, and this changes the behavior of the particles. It is not only the viscosity that increases, according to Morris. He says, "The particles want to expand and get more space."

Eventually, the particles transmit the stress not just in one direction but in all directions. Denn says, "The force developed on the particles is relieved by having chains form in three dimensions, leading to the formation of a dense network." This three-dimensional network is seen in the right side of the right image shown in Figure 2.

Another way to look at DST is by understanding the concept of shear induced jamming. Morris says, "The transition to DST is very similar to a shear jammed state in which shearing a system causes a transition to a solid that becomes so robust that it will stop fluid flow. This effect is seen in such applications as powder-injection molding where the material being forced into a mold can seize up and not move."

Future work will focus on determining the detailed structure for the three-dimensional chains and figure out how they transmit stress. Additional information can be found in a recent article[2] or by contacting Morris at **morris@ccny.cuny.edu**.

REFERENCES

1. Canter, N. (2012), "Impact-activated solidification," TLT, **68** (10), pp. 12-13.
2. Seto, R., Mari, R., Morris, J. and Denn, M. (2013), "Discontinuous Shear Thickening of Frictional Hard-Sphere Suspensions," *Physical Review Letters*, **111** (21), p. 218301.

Studying butterfly wings to reduce drag

Butterfly wings exhibit superhydrophobic and self-cleaning properties that might be applicable in real-world applications.

IN THE EFFORT TO IMPROVE THE EFFICIENCY of machinery and to look for factors causing lubrication problems, researchers have looked at Mother Nature for guidance. There are examples in nature where organisms have developed ways to reduce friction and wear to survive in their environments.

'Butterflies are fragile and must have a mechanism in place to repel water and other contaminants in order to maintain their ability to fly.'

One example was provided in a previous TLT article that described how mollusks can produce adhesive gels that enables them to adhere to moist surfaces to such an extent that the amount of force need to remove them is 200 kilopascals.[1] Key components instrumental in the performance of these adhesives are the metals iron, zinc and calcium, which are present in trace quantities.

STLE-fellow and Life-member Bharat Bhushan, Ohio Eminent Scholar and Winbigler Professor of Mechanical and Aerospace Engineering at The Ohio State University in Columbus, Ohio, discusses the properties of the lotus leaf. He says, "The Lotus Effect is attributed to this leaf displaying superhydrophobic properties that enables it to be water repellent and also exhibit the additional benefit of self-cleaning. The latter characteristic is realized due to the ability of water droplets to roll off the leaf, leading to the removal of contaminants that are mainly compatible with water."

Superhydrophobic coatings are also desirable because they can reduce the amount of drag seen in fluid flow, leading to greater efficiency. Two approaches used to develop this effect are to apply a coating to a substrate or to include roughness in the surface structure.

The shark provides an interesting example of a low drag surface through its use of riblets on its skin that reduces frictional drag as the fish moves through the water. Bhushan says, "The shark needs to move through turbulent water at a fast pace to track down its prey. The riblets on the skin lift and pin vortices that can develop in the water, which reduces cross-stream fluid motion and reduces energy loss."

The key for achieving the Lotus Effect is the use of rough, hierarchy structure combined with the presence of a waxy coating on the surface to enhance the superhydrophobic effect, and the key to the shark skin effect is to provide anisotropic riblets to reduce drag. Bharat says, "Several years ago, we came across a new species that seemed to exhibit many of the properties of lotus leaf and shark skin, enabling it to thrive in its environment. We decided to spend time studying this species to see what properties it exhibited that might be applicable for replication in real-world applications. The species is the butterfly."

GIANT BLUE MORPHO BUTTERFLY

Bhushan and his associate, Gregory Bixler, determined that on the nanoscale, butterfly wings exhibit the key combination of superhydophobicity and self-cleaning. Bhushan says, "Butterfly wings are covered with hierarchical scales that exhibit these important properties. They are needed because butterflies are fragile and must have a mechanism in place to repel water and other contaminants in order to maintain their ability to fly."

The researchers chose to study the wings from the butterfly species *Blue Morpho didius*. Bhushan says, "We selected this species because it is a relatively large butterfly with wings that are approximately three-inches long." Figure 3 shows images of the *Blue Morpho didius*.

KEY CONCEPTS

- There are several examples of Mother Nature's work that show species have developed ways to reduce friction and wear in their environments.
- One strategy used is to develop superhydrophobic coatings that can reduce the amount of drag seen in fluid flow and also are self-cleaning.
- Butterfly wings display hierarchical scales that display these superhydrophobic properties.

Replicas of the butterfly wing were produced through the use of a two-step soft lithography molding procedure. Bhushan says, "We started by using a polymer such as dental cement in preparing a negative mold. Then polydimethylsiloxane is applied and cured on the first polymer to produce a precise positive replica. A fluorinated coating is used to separate the positive copy from the mold."

The resulting replicas were characterized using scanning electron microscopy and digital camera images. Oil drag was measured by evaluating the pressure drop determined as white oil is pumped through the replicas. Measurements were taken under low-velocity and high-velocity conditions.

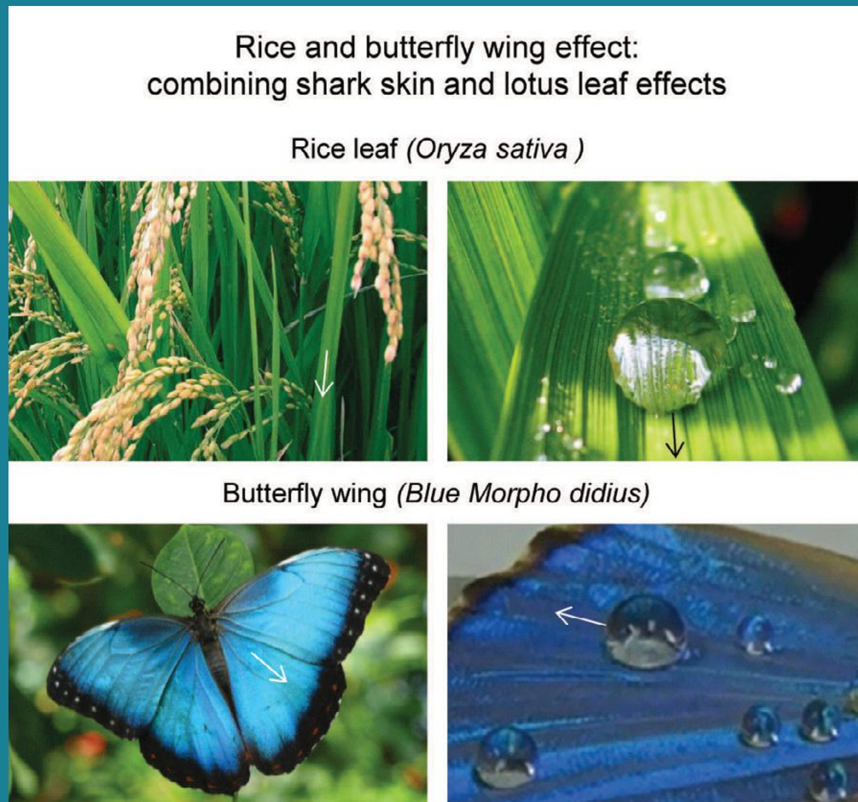

Figure 3 | **The wings of the butterfly species, *Blue Morpho didius* display superhydropobic properties, leading to reduced drag and improved efficiency.** *(Courtesy of The Ohio State University)*

> *'We found that the replicas displayed better performance under high-velocity conditions. This is anticipated because fluid flow under high-velocity conditions can be turbulent, leading to the formation of vortices.'*

Bhushan says, "We found that the replicas displayed better performance under high-velocity conditions. This is anticipated because fluid flow under high velocity conditions can be turbulent, leading to the formation of vortices. Drag reduction is seen at high-velocity due to the formation of a thin oil film on the microstructure surface of the replica." The researchers determined that the butterfly wing replica displayed a drag reduction of 6 percent.

To determine the superhydrophobicity, apparent contact angles were determined on the butterfly wings and their replicas. Differences were seen between butterfly wings and their replicas. Bhushan explains, "The reason is due to the presence of a hydrophobic wax on the butterfly wing creating the conditions for a high contact angle when exposed to water. In contrast, the untreated replicas are not nearly as hydrophobic and have much lower contact angles. This can be adjusted by applying a hydrophobic coating contacting the replicas."

Bhushan believes that the structural information obtained on the butterfly wings can be applied to real-world applications. He says, "There is potential for reducing drag in many applications including moving blood through a nano-channel, pumping crude oil through a pipeline, reducing drag on the surface of an airplane wing and improving the efficiency in which a ship's hull moves through water.

Further information can be found in a recent publication[2] or by contacting Bhushan at **bhushan.2@osu.edu.** TLT

REFERENCES

1. Canter, N. (2009), "Molluscan adhesive gels," TLT, **65** (12), pp. 14-15.
2. Bixler, G. and Bhushan, B. (2013), "Bioinspired micro-nano-structured surfaces for oil drag reduction in closed channel flow," *Soft Matter*, **9**, pp. 1620-1635.

Neil Canter heads his own consulting company, Chemical Solutions, in Willow Grove, Pa. Ideas for Tech Beat can be submitted to him at ***neilcanter@comcast.net.***

Michael Forgeron

By Karl M. Phipps / Managing Editor

The president and CEO of Analysts, Inc., discusses how future challenges in the oil analysis industry will impact end-users of commercial services.

Like father like son, Michael Forgeron, president and CEO of Analysts, Inc. *(right)* shares his expertise and knowledge in oil analysis and is passing it along to the next generation in his son, Cary *(left)*, Analysts' director of sales, who is also the youngest member to earn STLE's Certified Lubrication Specialist™ certification. Michael has another son, Eric, who manages Analysts' IT/IS operations.

(Photos courtesy of Analysts, Inc.)

Michael Forgeron
The Quick File:

Michael Forgeron is president and CEO of Los Angeles-based Analysts, Inc. Analysts operates eight laboratories in four countries, five of which are in the U.S., with the others in Mexico, Japan and China.

Michael received his bachelor's degree in business administration with a minor in marketing from California State University-Dominguez Hills and joined Analysts, Inc., in 1969. He has held several positions in customer service, sales, laboratory management and corporate management.

In addition to his duties within the parent company of Analysts, Inc., Michael is also the representative director for Japan Analysts in Tokyo, Analysts Servicios Commerciales in Monterrey, Mexico, and KYB China Analysts (KCA) in Zhenjiang, China.

Michael has been a member of STLE, ASTM International and the Technology & Maintenance Council (TMC) and participated on numerous committees involved with testing, training, education and equipment maintenance practices.

Although Analysts, Inc., is primarily a testing organization, under Forgeron's leadership and commitment to the improvement of the industry, the company developed LEM, a patented technology for the determination of soot in diesel engine oil, and quantitative spectrophotometric analysis (QSA) for varnish-related issues in various applications.

TLT: How did you get involved in the industry?

Forgeron: My father, Edward Forgeron, founded Analysts, Inc., which was the first commercial laboratory to utilize spectrographic metals analysis as a means to identify and predict abnormal component wear. When I was younger, I was always interested in my father's work and wanted to know what he did and why. I would sometimes travel with him to our first laboratory in Oakland, Calif., where he would explain the testing and how it impacted the customer's business. There really was never a question in my mind that I would join the business. I formally joined Analysts in 1969, and it has been my passion and work ever since.

TLT: How has lubricant testing changed over your career?

Forgeron: As one should expect, the industry has changed tremendously over my 43 years of involvement. In the late 1960s when I started, the laboratories didn't have the instru-

 The first day of spring in the southern hemisphere is the date of the autumnal equinox in the northern hemisphere, usually in September.

mentation or run as many different tests as we do today. Also, everything was performed manually; automation and computerization wasn't part of our process. On the customer/user side, a lot of the work we did was looked at skeptically as people couldn't understand or accept that we could accurately identify lube and component condition from the test results.

Today most of our lab processes are automated. Computerization has significantly improved the testing and allowed for direct integration into the laboratory LIMS database. Also, the level of customer awareness and knowledge about oil analysis continues to steadily improve.

As testing technology and instrumentation has improved, oil sample test regimes have evolved to become more industry and application specific. We can now test for specific areas of concern based upon the component type and use, which makes the amount of information provided and accuracy of the diagnostics much more valuable.

As testing technology and instrumentation has improved, oil sample test regimes have evolved to become more industry and application specific.

TLT: What kind of R&D is helping to promote new tests?

Forgeron: As an industry, the instrument suppliers are working on continual improvements to the existing technologies. Through the efforts of organizations such as ASTM, DIN (the German Institute for Standardization) and Japanese Industrial Standards (JIS), there is regular promotion and introduction of new technology, procedures and instrumentation.

Specifically within Analysts, Inc., we remain focused in a number of areas of continued development, including the determination of soot loading and effects in diesel engine applications, and through the company's QSA (MPC) technology the creation of varnish-related contaminates in various applications.

Labs must invest and develop in software that provides meaningful online access of oil analysis data.

TLT: What are the three biggest challenges facing the oil analysis industry today?

Forgeron: Not unlike most industries, I believe the three largest challenges the industry faces are all related to budgetary decision-making. We group the challenges as the "3 Cs"—Commoditization, Commitment and CapEx. Commoditization and commitment are user-driven, while capital expenditures are laboratory-driven.

Commoditization. Efforts toward commoditization of used oil analysis are based on desires to simply lower the price of sample testing. I don't intend to infer that cost control is a bad objective. It is positive, necessary and should be a focus for all management. But unfortunately, perhaps, due to the law of unintended consequences, decisions as to what test program is implemented based solely on cost has resulted in many industrial application programs using less than adequate test slates for the machines being sampled. This has an impact of lost or reduced benefits and savings realized from the testing.

Commitment. Companies that utilize oil analysis should insure that they manage and control their programs within their plants and facilities. Leaders are needed to champion the effort to communicate within the organization, implement and manage the sampling activities and review and follow up on the reports associated with maintenance actions. Increases in workload and reductions in workforce are resulting in fewer program leaders.

Notifications to appropriate line personnel on critical condition reports still go out, and corrective actions to the conditions continue to be initiated. However, what we see lost is the more in-depth follow up and investigation at plant sites as to root cause analysis and further proactive changes to procedures that can reduce the instances of samples with critical severities.

CapEx. Laboratories must commit to increase the scope of services provided. This includes having the appropriate instrumentation and personnel to perform the optimal testing for the machines being sampled and to accurately diagnose the condition of the samples. Labs must also invest and develop in software that provides meaningful online access of oil analysis data. Software such as our Lube Oil Analysis Management System (LOAMS) program must allow the users to efficiently and correctly manage their

Today roughly 80 percent of samples submitted for processing are considered as normal condition.

programs, with or without single appointed leaders.

Knowing that manpower levels and available time are reduced at the user level, service laboratories need to step up and fill the gaps so that benefits of the sampling activities are fully realized for the customers.

TLT: What are the three biggest myths about oil analysis?

Forgeron: People seem to forever be looking for the silver bullet, the one test or one system that will resolve all your problems and tell you everything you need to know about your sample. Lubricant technology is very complex, and the engineering that is required to manufacture today's machinery is very advanced. While there are similarities in various lubricants and equipment types, there are always going to be differences as well. Sampling that applies to the specifics of the lube and component will always be better than single-source technology.

Also, a surprisingly common misconception that we deal with daily is the belief that new oil is clean oil. Too many users continue to ignore the published literature, prevalent warnings and the training that details possibilities of contaminants, especially particulates and moisture, that can be present with new oil.

Last, the idea that a single sample can be as effective as continuous sampling and trend analysis remains in place in some segments of the market. When there is a glaring problem, this is correct. Free water, completely out of grade viscosity or extremely high values of wear metals can easily be identified as anomalies. Unfortunately, when these issues are present, much more damage has occurred versus when the problems are monitored through regular sampling and trend analysis and identified in their early stages.

TLT: What is the biggest change in oil analysis over the past decade?

Forgeron: I believe the biggest change is what and how laboratories deliver information to the users. For leading labs, testing has expanded in what legacy markets require, as well as to meet the new markets and machines and equipment that have been introduced to industry in general. Examples of this are in power generation including wind turbine and gas-fired co-generation applications.

The integration and use of computing power has significantly improved our industry. Test instrument manufacturers have leveraged this power to create new technologies that improved processing times, detection levels, accuracy and scope constituents that can be identified and measured. Instruments are now interfaced directly to laboratory LIMS systems, which reduce overall processing time and clerical errors of misreading results or transposition.

A high majority of data delivery is now done electronically via email, text messaging and online access. Online access programming such as cloud-based LOAMS provide tremendous power to users and managers of sampling programs. Trending, graphing, unique data mining, equipment management, sample labeling/barcoding and enhanced communication with the lab or co-workers are all available online today.

TLT: What will be the biggest change in oil analysis in the coming decade?

Forgeron: The coming decade should bring a large twofold change to the industry. First, on-site testing, whether by handheld units or sensors, will eventually be developed to successfully monitor certain oil properties and common contamination. This will result in a different mix of samples being submitted to laboratories. Today roughly 80 percent of samples submitted for processing are considered as normal condition. In the future, we should see a drop in this percentage with a corresponding increase in samples with abnormal conditions test results.

As sensors begin to penetrate the market, many of today's labs will need to adapt testing protocols and expand their capabilities to run more sophisticated tests. They will need to concentrate their services more on root cause analysis and recommended corrective actions. If they don't have it today, they will also need to develop expertise in order to take a more active role in assisting their client base in troubleshooting of equipment problems. A commitment to large and ongoing capital investment will be required to maintain the needed instrumentation, associated software and personnel necessary to run the tests and evaluate the results.

Second, as a result of the shift in needed instrumentation and expertise, we can expect a consolidation in the industry. Many smaller labs will not be capable of making the needed investments or will not have the required expertise to assist their customers with the in-depth testing, which will create a change in the type and number of laboratories providing the future oil analysis services.

TLT: What role will sensor technology play in oil analysis?

Forgeron: Sensors will eventually have an inclusive role in oil analysis. Whenever specific properties of an oil sample can be monitored on a real-time basis, the value of oil analysis increases. Sensors will be an enhancement to the industry.

By identifying the normal condition machines and components, more time and involvement can be spent on the equipment that needs the attention. Sensors can replace the labor required to sample normal condition equipment. They will allow monitoring of more units, particularly those units that are in remote and hard to access locations.

Additionally, we at Analysts are working on technology that will enable sensors to transmit required operating data to the laboratory, which will improve the amount and accuracy of the data received, reduce the labor needed to provide the information and allow bi-directional information back to the machine or facility from the laboratory, all in real-time.

TLT: How does oil analysis relate with other condition-based maintenance technologies?

Forgeron: Oil analysis complements other condition monitoring-based technologies such as vibration and thermography. It identifies lube and some wear conditions that the other disciplines cannot. Conversely, those disciplines identify areas oil analysis cannot. Oil analysis typically identifies issues at earlier stages and at a fraction of the cost than other technologies.

TLT: How would you sum up the oil analysis industry?

Forgeron: Oil analysis is a technical service. Its value should be determined by the return on the investment of the program, not the cost of the samples. The benefits received and ROI of the program is derived from reduced maintenance costs, increased machine uptime and productivity and longer asset life cycles. While it is a mature industry, it continues to evolve and improve—which creates value. That is a good thing.

I am proud of our work in oil analysis and proud of my career in the industry. We've come a very long way from the early days and we have an exciting road of continued advancement to follow into the future. **TLT**

You can reach Michael at **mforgeron@analystsinc.com.**

A Wafer-Scale Particle Augmented Mixed Lubrication Modeling Approach for Chemical Mechanical Polishing

Gagan Srivastava and C. Fred Higgs III (Advisor)
Department of Mechanical Engineering
Carnegie Mellon University, Pittsburgh, Pa.

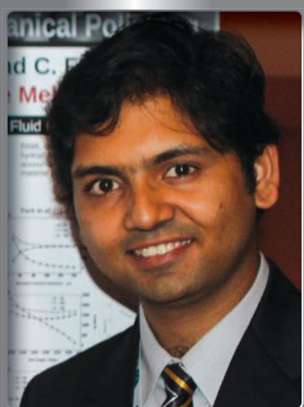

Gagan Srivastava is a doctoral student in the Particle Flow and Tribology Laboratory at Carnegie Mellon University in Pittsburgh Pa. He works in the field of mixed lubrication tribosystems under the guidance of professor C. Fred Higgs III. You can reach him at **gsrivast@andrew.cmu.edu.**

ABSTRACT

The mechanical or tribological action in CMP involves hydrodynamic lubrication, solid-solid contact and wear, primarily resulting from hard particles removing material by abrasion. Present work introduces a much faster version of the particle augmented mixed lubrication (PAML) modeling approach, previously introduced by Terrell and Higgs [1], in the form of a framework called PAML-lite. With this introduction of this model, the PAML approach can now be applied to the full-scale wafer-pad interface. Results from this work include the evolution of the hydrodynamic fluid pressure, contact stress, and finally the material removal at the local and wafer scales. Comparisons with existing CMP experiments have been made and the results are favorable.

INTRODUCTION

Chemical mechanical polishing (CMP) has been a critical process for achieving surface planarization in small scale devices and is commonly used as an intermediate fabrication step for devices such as integrated circuits and magnetic hard disk read write heads. Although CMP is a common practice in the semiconductor manufacturing industry, the physics behind the process is not completely understood due to the complex nature of the slurry flow and interaction between the wafer, pad and abrasive particles. Several models have been proposed to explain the wear action in the CMP process, ignoring one or more of the physical phenomena involved. Some of the earlier studies presented empirical models based on results from CMP experiments. Preston presented the first polishing model relating the material removal rate to the mechanical work done by the frictional force. This approach, though reasonable under certain restrictions, does not reveal insights into the wear mechanism.

Zhao and Chang [2] and Luo and Dornfeld [3] gave wear models based on the real contact area between the pad and wafer interface and the calculation of active particles. Some authors such as Sundararajan et al. [4] have approached CMP with fluid hydrodynamics to calculate wear by calculating the hydrodynamic pressure. The final approach builds up on theories of contact mechanics and fluid hydrodynamics. Shan et al. [5] presented a one-dimensional model to predict interfacial fluid pressure under the wafer by solving an average flow Reynolds Equation by introducing mixed-lubrication (the lubrication process where the load is being carried by the fluid, together with a solid-solid contact) into CMP. Higgs et al. [6] extended that work to two dimensions with a stationary wafer and determined the equilibrium orientation for calculating the hydrodynamic pressure and contact stress.

The approaches mentioned above were set up at the wafer scale and did not predict the presence of dishing, erosion and micro-scratching, defects at feature scale. Identifying a modeling approach they called PAML (Particle Augmented Mixed Lubrication), Terrell and Higgs [1] presented an asperity scale deterministic model that can overcome the shortcomings of wafer scale models. However, due to the high physical fidelity of the model, even with a small domain, the model was still computationally very expensive. The present study, similar to PAML, integrates the effect of slurry fluid flow, the mechanics of wafer and pad contact, and the abrasive wear caused by the particles during the process of polishing.

The model is presented here as a wafer scale analysis, intended to capture the wafer scale defects like inter-die polishing differences, but with sufficient computing resources, it can be scaled down to a much higher resolution to capture the asperity-scale effects such as dishing, erosion and micro-scratching.

MODELING SCHEME

The philosophy of the proposed modeling scheme is based in two parts: determining the equilibrium orientation of the wafer and calculation of wear in that orientation.

Determining the Equilibrium Orientation

The state of equilibrium in CMP is achieved when the net forces acting on the wafer and the two moments about the pivot vanish. The forces acting on the wafer during the process of CMP are hydrodynamic pressure, the contact stress and the external load applied to press the wafer against the pad. The slurry film is modeled using the polar Reynolds equation that gives the hydrodynamic pressure distribution. The particle dynamics treatment is replaced with an assumption that the particles of different sizes randomly exist in the wafer-pad interface. The particle diameters follow a known probability distribution. The contact mechanics are modeled using a Winkler elastic foundation and at each time step, the resulting hydrodynamic pressure and contact stress are used to determine the mixed-lubrication equilibrium configuration of the tribosystem by implementing a root finding algorithm that solves the load balancing equations (the second law of motion) simultaneously for the orientation variables.

Wear Calculation

At the equilibrium orientation, the number of particles participating in the wear action is calculated using the contact stress and distribution of particle sizes. The abrasive wear caused by an average-sized active particle is then calculated, which when multiplied with the number of active particles, gives the total wear.

CMP Parameters

The CMP parameters used were intended to replicate regular experiments. The speed of rotation of the pad and wafer was set at 40 RPM and 60 RPM, respectively. The wafer was loaded and pressed against the pad before beginning the simulation. The equilibrium orientation of the wafer on top of the pad was repeatedly updated over time. As the abrasive wear formulation was used for material removal, the equilibrium contact stress was used to calculate the material removed over the period of the simulation.

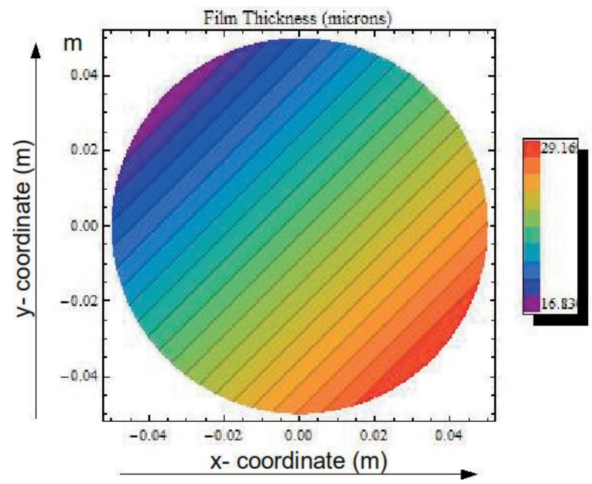

(a)

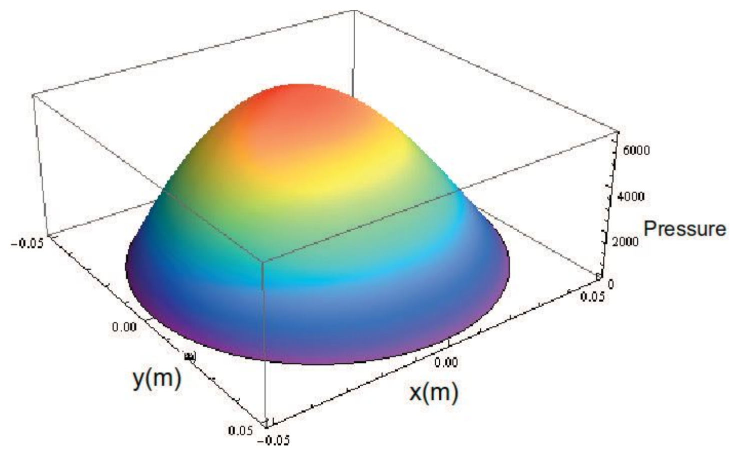

(b)

Figure 1 | **Reynolds equation solution.**

RESULTS

Equilibrium Hydrodynamic Pressure

The resulting quasi-steady state equilibrium orientation provides us the rolling angle, the pitching angle and the nominal clearance of the wafer over the pad. These orientation parameters are then used to calculate the film thickness and after solving the Reynolds equation, the hydrodynamic pressure between the wafer and the pad. Figure 1 shows the film thickness and the associated pressure field for certain values of the orientation parameters.

The solution of the Reynolds equation was quantitatively compared against the results given by Park et al. [7], who

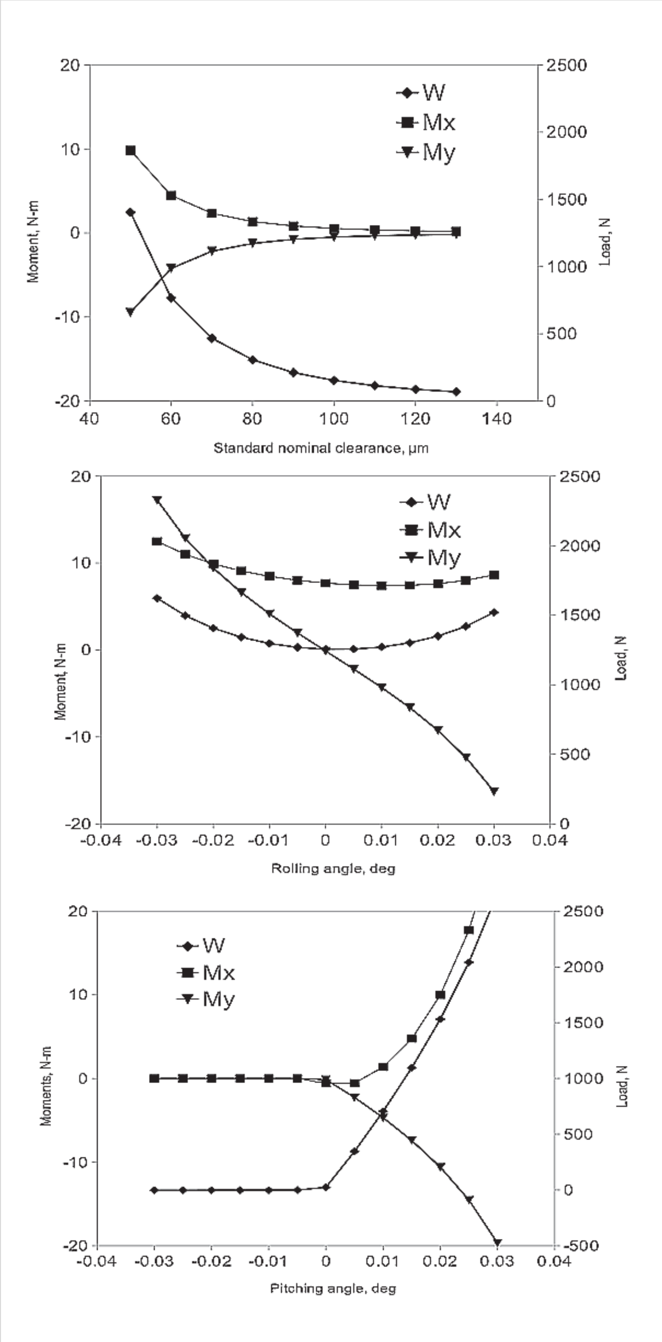

Figure 2 | **Vertical load W and horizontal moments M_x, M_y as a function of orientation parameters.**

provided the net load-carrying capacity (W) and moments in x and y direction (Mx and My, respectively) as a function of the orientation parameters by solving the Reynolds equation in their framework. Excellent match was observed between the two solutions. Figure 2 shows the predictions of the current model.

Wafer Wear

As mentioned earlier, the orientation parameters also provide us a resultant contact stress field. The contact stress is then used to calculate the material removed due to the

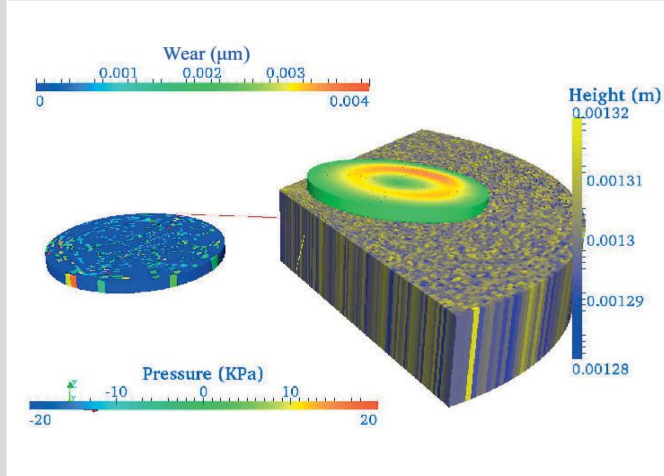

Figure 3 | ***In silico*** **polishing experiment capable of tracking interfacial fluid pressure, wear and contact stresses over time (contact stress not shown in this figure).**

abrasive wear action caused by the slurry abrasives being forced into the wafer surface. As a result, in a simulated polishing experiment, a time-evolving wafer-scale wear map can thus be constructed. Figure 3 shows a snap-shot of the *in silico* polishing experiment.

Figure 4 shows the evolution of wafer wear over time (blue represents least wear, progressing over to red showing the highest wear). The model thus gives us the capability to predict apriori, the difference in material removed across the wafer.

CONCLUSION

A new multi-physics model of PAML was developed for wafer scale analysis of CMP. The model integrated the effects of mixed lubrication and wear caused by the abrasive particles in the slurry. The hydrodynamic pressure field was calculated using the polar form of the Reynolds equation, and the resulting

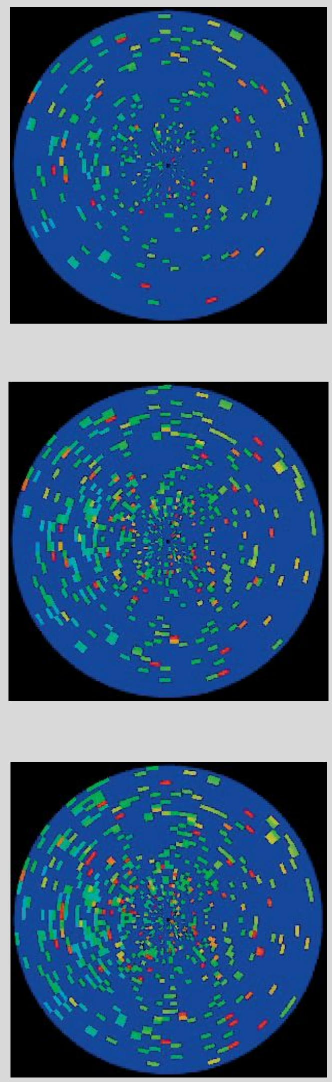

Figure 4 | **Evolution of wear on the wafer during the** ***in silico*** **experiment.**

pressure distribution agrees well with published results. Elastic foundation model was implemented to evaluate the contact stress field. The operating configuration for the wafer was determined by solving three simultaneous non-linear equations for the dynamic equilibrium, which was followed by the wear calculation. The model can thus capture wafer scale defects such as differential polishing across the wafer and edge quality deterioration.

REFERENCES

1. Terrell, E.J. and Higgs, C.F. (2009), "A Particle-Augmented Mixed Lubrication Modeling Approach to Predicting Chemical Mechanical Polishing," *Journal of Tribology*, **131** (1), p. 012201.

2. Zhao, Y. and Chang, L. (2002), "A Micro-Contact and Wear Model for Chemical–Mechanical Polishing of Silicon Wafers," *Wear*, **252** (3), pp. 220–226.

3. Luo, J. and Dornfeld, D.A. (2001), "Material Removal Mechanism in Chemical Mechanical Polishing: Theory and Modeling," Semiconductor Manufacturing, *IEEE Transactions*, **14** (2), pp. 112-133.

4. Sundararajan, S., Thakurta, D.G., Schwendeman, D.W., Murarka, S.P. and Gill, W.N. "Two-Dimensional Wafer-Scale Chemical Mechanical Planarization Models Based on Lubrication Theory and Mass Transport," *Journal of the Electrochemical Society,* **146**, pp. 761–766, Feb. 1999, WOS: 000078866400057.

5. Shan, L., Levert, J., Meade, L., Tichy, J. and Danyluk, S. (1999), "Interfacial Fluid Mechanics and Pressure Prediction in Chemical Mechanical Polishing," *Journal of Tribology*, **122**, pp. 539-543.

6. Higgs, C.F., Ng, S.H., Borucki, L., Yoon, I. and Danyluk, S. (2005), "A Mixed-Lubrication Approach to Predicting CMP Fluid Pressure Modeling and Experiments," *Journal of The Electrochemical Society,* **152** (3), p. G193.

7. Park, S.S., Cho, C.H. and Ahn, Y. "Hydrodynamic Analysis of Chemical Mechanical Polishing Process," *Tribology International*, **33**, pp. 723-730, Oct. 2000, WOS: 000165311500005.

Editor's Note: This month TLT profiles the 2013 recipients of **The E. Richard Booser Scholarship Award, Hannah Neuffer** (Auburn University) and **Anthony Chyr** (University of Utah). The Booser scholarship is awarded annually to undergraduate students who have an interest in pursuing a career in tribology. As a requirement for receiving a STLE scholarship, students are given the opportunity to participate in a tribology research project and to submit a report summarizing their research. For more information about the Booser scholarship, visit **www.stle.org.**

Hannah is a senior in polymer and fiber engineering working under the guidance of Dr. Robert Jackson in Auburn University's Samuel Ginn College of Engineering's tribology and lubrication science minor program. Her research focuses on measuring the effects of various concentrations of nanoparticles on the coefficient of friction in a ball-on-disk test machine. The results of these trials are analyzed to determine if the nanoparticles increase or decrease wear on the test unit. She is also studying the viscosity of these nanolubricants. You can reach her at **hannahneuffer@yahoo.com.**

Anthony graduated with a bachelor's of science in mechanical engineering from the University of Utah in May 2013. Currently he is a graduate student working under the guidance of Dr. Bart Raeymaekers. His major research project is design of an orthopedic knee implant friction and wear testing apparatus. You can reach him at **tony.chyr@gmail.com.**

Wear Volume Analysis Using a Nano-Lubricant for Ball-on-Disk Testing

Hannah Neuffer, Hamed Ghaednia and Robert Jackson (Advisor)
Auburn University, Department of Mechanical Engineering, Auburn, Ala.

Hannah Neuffer

ABSTRACT

The research presented in this article is a wear volume analysis of the effects of silver nanoparticles in a polyethylene-glycol lubricant (PEG). The ball-on-disk method was used to perform the tests and a surface profilometer was used to analyze the amount of wear produced by this nanolubricant. The results showed that with the addition of silver nanoparticles, the wear was reduced significantly in comparison to a control sample without any nanoparticles. This is in contrast to some of the nanoparticles which can actually increase the wear when added to a lubricant.

INTRODUCTION

What is a nanolubricant? A nanolubricant is comprised of three basic components: base oil, surfactant, and the nanoparticle. Nanoparticles are less than 100 nm and can come in a variety of shapes and materials. So why are nanolubricants important? Studies have shown that in a combustion engine, 33% of fuel energy is lost due to friction and that lubrication can improve the friction significantly[1]. Previous literature suggests that the nanoparticles as additives can induce marked effects on the lubricant properties[2]. Different combinations of nanoparticles and lubricants can result in numerous nanolubricants for different applications. Recent research has shown that nanolubricants can reduce the coefficient of friction and affect wear. This reduction of the coefficient of friction could be translated into higher fuel efficiency. However, some nanoparticles can also increase the wear. For this research, a nanolubricant containing different concentrations of silver nanoparticles was used to perform ball-on-disk friction tests to determine how nanoparticles affect wear in the mixed lubrication region of the Stribeck curve.

MATERIALS AND METHODS

The nanolubricant studied was comprised of polyethylene glycol 600 (PEG), polyvinyl pyrollidone (PVP), and concentrations of 0.15 % wt, 0.3 % wt and 0.45 % wt silver nanoparticles with average diameters of seven nanometers. In order to determine the effects of the silver nanoparticles only, the base and surfactant (PEG and PVP) was used as a control. In order to create the wear grooves, a ball-on-disk test was performed using an CETR-UMT friction testing machine with constant loads of 10 N, 30 N, and 50 N, a rotational speed of 0.5 m/s, and a total sliding distance of 2500 m, according to the ASTM standard[3]. Each test was performed three times to insure repeatability. The nanolubricant completely filled the testing reservoir and submerged the sample to insure an even distribution of lubricant during testing. After the ball-on-disk tests were complete, the resulting wear grooves were analyzed by using a stylus profilometer with a vertical resolution of less than one nanometer. Using a numerical scheme, the surface scans were stitched together to produce a 3D surface image of the wear groove, as seen in Figure 1.

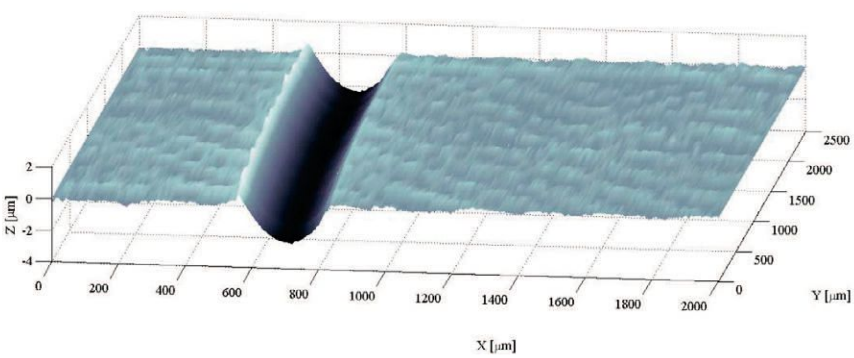

Figure 1 | **3D Wear Groove of one the samples.**

In order to determine the wear track width, the 3D surface plot was used to pin-point where the groove edges began. An average diameter measurement was then used to calculate wear volume from Eq.1 [3], which assumes that the groove's cross section is an enclosed arc and that it travels in around the circumference of the disk at a radius, R

$$Wear\ Volume = 2\pi R\left[r^2 \sin^{-1}\frac{d}{2r} - \frac{d}{4}(4r^2 - d^2)^{\frac{1}{2}}\right] \quad (1)$$

R = wear track radius
d = wear track width
r = sphere radius

RESULTS AND DISCUSSION

The effects of the nanoparticle concentration on wear volume can be seen in Figure 2. The results indicate that the addition of silver nanoparticles reduces the amount of wear when compared to that of the control lubricant. The coefficient of friction (COF) was also monitored throughout the ball-on-disk tests, and it was discovered that the COF is reduced by approximately 20% at the nanoparticle concentration of 45 mM and normal load of 30 N in comparison to the control sample. Previous research has suggested that the mechanism present to reduce friction between two surfaces is by reducing the real area of contact as the particles prevent the surfaces asperities from coming into contact as frequently[4,5]. However, other mechanisms may also be at work.

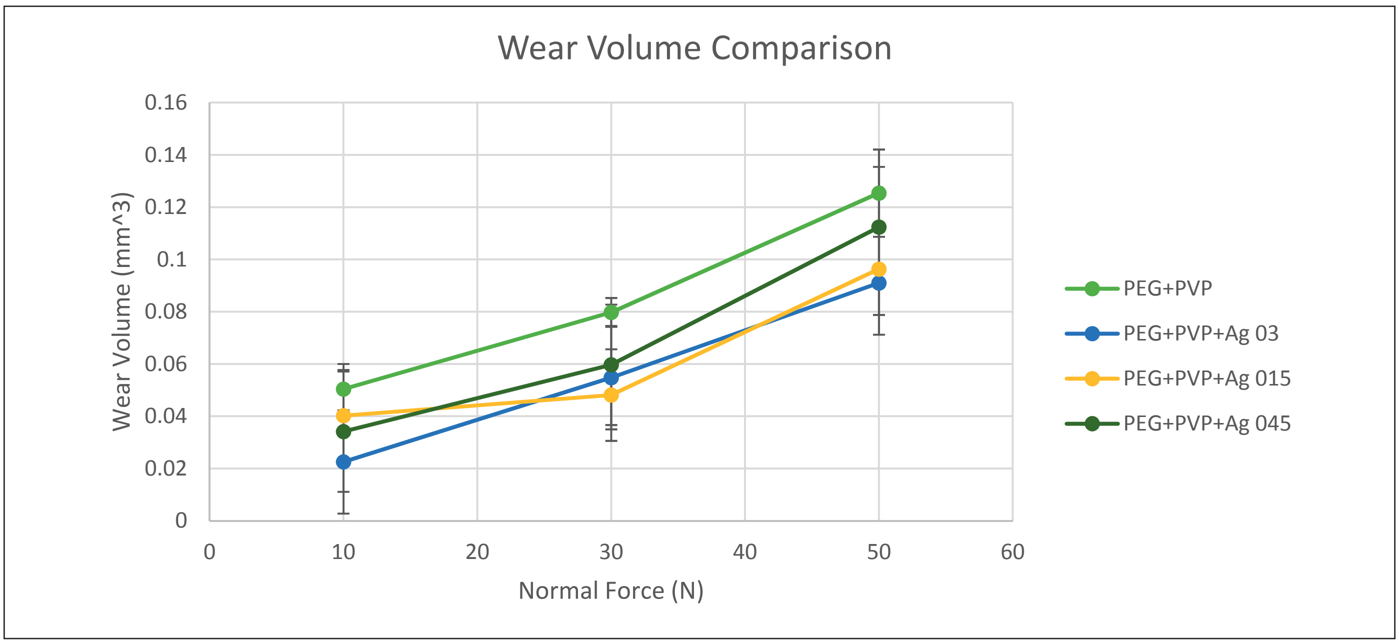

Figure 2 | **Wear volume analysis results of PEG+PVP+Ag nanolubricant at different loads.**

CONCLUSION

When the wear volume of each nanolubricant concentration was compared to the base lubricant, the results show that there is a definite reduction of wear. This may be due to the relatively soft silver particles protecting the tested surfaces like a cushion, or they could be improving the load-carrying capacity of the lubricant itself. Further research looking at the wear reduction mechanisms needs to be pursued.

ACKNOWLEDGMENTS

I would like to thank STLE for awarding me the 2013 E. Richard Booser Scholarship. Having industry support is crucial to cultivating the next-generation of young tribologists and STLE is at the forefront of providing that support. I would also like to thank Dr. Robert Jackson (associate professor in the department of mechanical engineering at Auburn University) and Hamed Ghaednia (PhD candidate in the department of mechanical engineering at Auburn University) for their support and assistance throughout the research process.

REFERENCES

1. Holmberg, K., Andersson, P., and Erdemir, A. (2012), "Global Energy Consumption Due to Friction in Passenger Cars," *Tribology International*, **47**, pp. 221-234.

2. Martin, J.M., and Ohmae, N. (2008), *Nanolubricants,* Tribology Series, John Wiley & Sons Ltd., England.

3. 2010 Annual Book of ASTM Standards (Section Three): Metals Test Methods and Analytical Procedures, Vol. **03.02**: Corrosion of Metals; Wear and Erosion.

4. Ghaednia, H., Jackson, R.L., and Khodadadi, J.M. (2013), "Experimental Analysis of Stable Cuo Nanoparticle Enhanced Lubricants," *Journal of Experimental Nanoscience*, pp. 1-18.

5. Ghaednia, H., and Jackson, R.L. (2013), "The Effect of Nanoparticles on the Real Area of Contact, Friction and Wear," *Journal of Tribology,* **135**(4):041603-041603-10.

Patterned microtexture to reduce friction in prosthetic hip joints

Anthony Chyr and Bart Raeymaekers (Advisor)
Department of Mechanical Engineering, University of Utah, Salt Lake City, Utah

ABSTRACT

Approximately 285,000 total hip replacement (THR) surgeries are performed in the U.S. each year. Most prosthetic hip joints consist of a cobalt-chromium (CoCr) femoral head that articulates against a polyethylene liner (usually ultra-high molecular weight polyethylene (UHMWPE)), lubricated by joint fluid. The statistical survivorship of these metal-on-polyethylene prosthetic hip joints declines significantly after 15 years of use, primarily due to wear and wear debris incited disease. The current engineering paradigm aims to increase the longevity of prosthetic hip joints by manufacturing ultra-smooth articulating surfaces. In contrast, we aim to increase the longevity of prosthetic hip joints by adding a patterned microtexture to the ultra-smooth CoCr femoral head. The patterned microtexture increases the lubricant film thickness between the articulating surfaces, thereby reducing friction and wear. We have numerically optimized the microtexture geometry to maximize the lubricant film thickness between the articulating surfaces of the prosthetic joint, and experimentally demonstrate reduced friction for the microtextured compared to the smooth articulating surfaces lubricated with joint fluid.

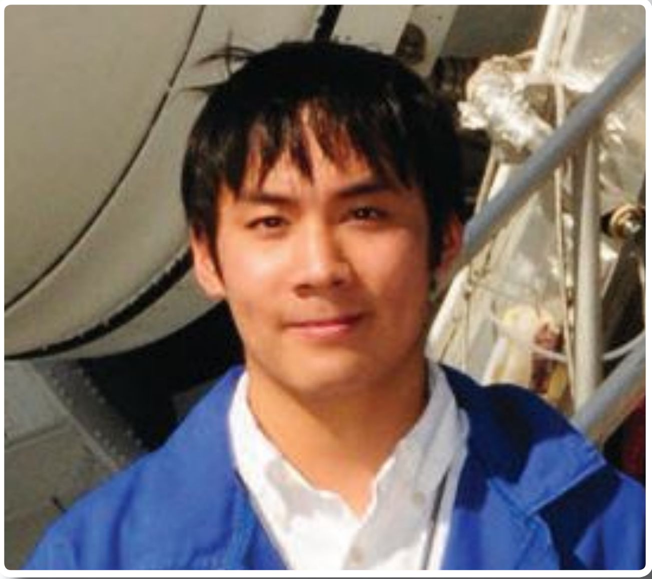

Anthony Chyr

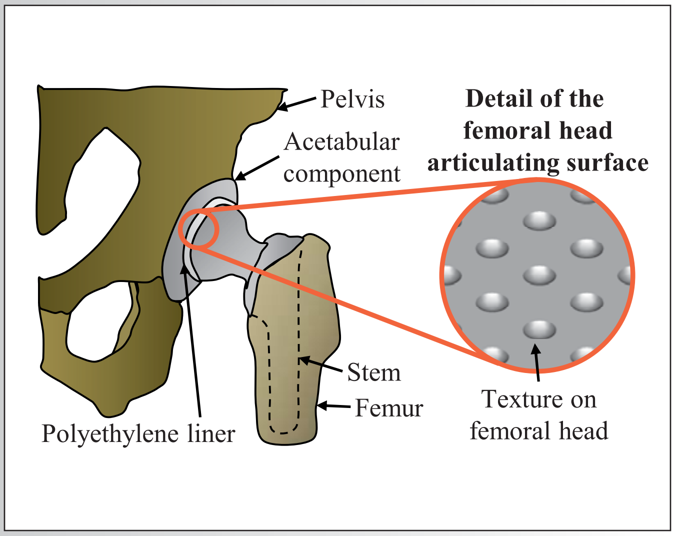

Figure 1 | **Metal-on-polyethylene (MOP) prosthetic hip joint with a patterned microtexture on the CoCr femoral head[6].**

INTRODUCTION

More than 285,000 total hip replacement (THR) surgeries are performed in the U.S. each year. The statistical survivorship of these prosthetic hip joints declines significantly after 15 years of use[1], primarily because adverse biological reaction to indigestible wear debris leads to osteolysis, instability and loosening of the implant[2]. This lack of durability has unacceptable effects such as riskier revision surgery[3,4] and surgery postponement with its attendant pain and disability. This research focuses on metal-on-polyethylene (MOP) prosthetic hip joints, which are the most common in the U.S. The current engineering paradigm for combating implant wear is to manufacture smoother sliding surfaces[5]. In contrast, we attempt to reduce friction and wear by adding a patterned microtexture to the ultra-smooth femoral head, as illustrated in Figure 1.

A few researchers have attempted to improve the durability of MOP prosthetic hip joints by applying a surface texture

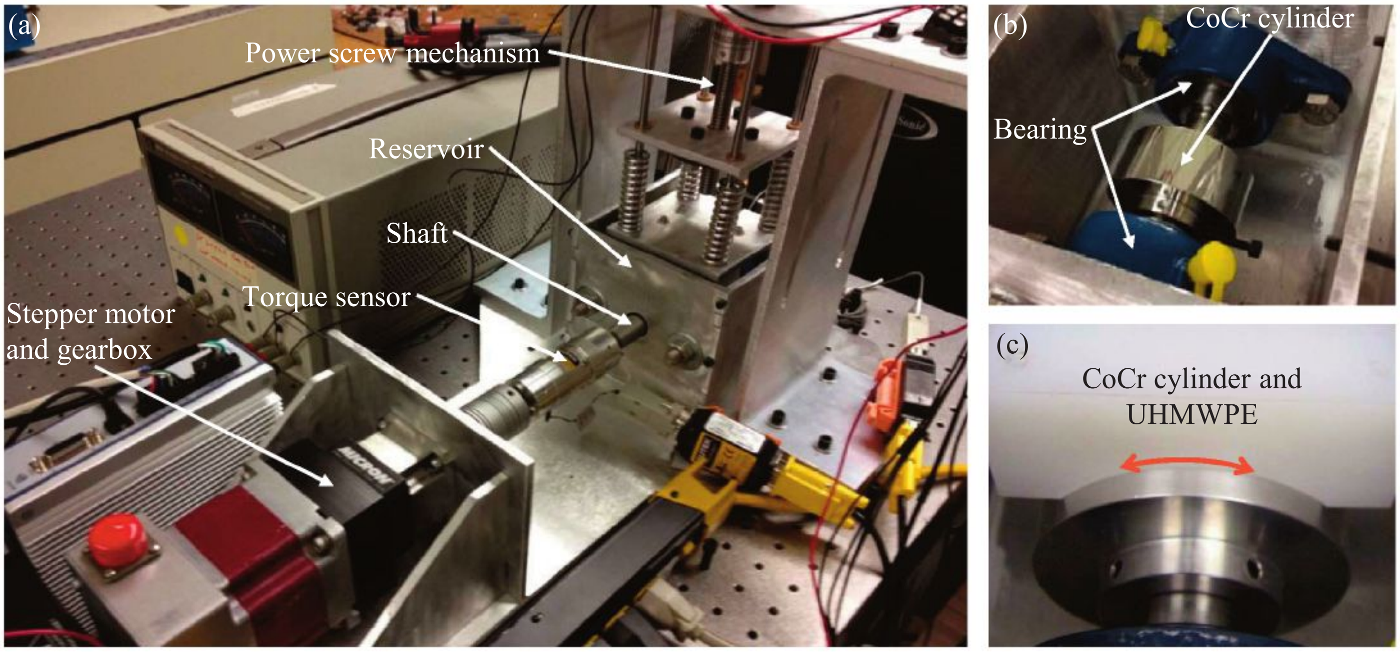

Figure 2 | **Experimental apparatus (a) overview picture, (b) detail of a CoCr specimen mounted on the reciprocating shaft in the reservoir, and (c) detail of interacting CoCr and UHMWPE bearing surfaces[10].**

or increasing the surface roughness of the femoral head in order to trap wear debris or store and dispense joint fluid. Ito et al.[7] observed a 17% reduction in friction and a 36% reduction in polyethylene wear after creating circular texture features into the smooth femoral head. Sawano et al.[8] observed a modest reduction in wear after manufacturing channels into the smooth femoral head running perpendicular to the direction of articulation. Zhou et al.[9] observed that surface microtexturing did not improve lubrication after adding concave texture features via a diamond spherical indenter into the smooth femoral head. Tall ridges were observed around the contour of the texture features, which may have resulted in increased friction.

In contrast to the current engineering paradigm and earlier research, the objective of this work is to increase the durability of MOP prosthetic hip joints by creating a patterned microtexture that reduces friction in the prosthetic hip joint by increasing the lubricant film thickness. We have used a lubrication model to optimize the microtexture geometry in terms of maximum load-carrying capacity (or, equivalently, maximum lubricant film thickness for a constant load) of the prosthetic joint. We experimentally demonstrate that a surrogate MOP prosthetic hip joint with a patterned microtexture on the CoCr specimen reduces the friction coefficient when compared to a traditional smooth CoCr specimen tested under realistic hip operating conditions[6].

EXPERIMENT APPARATUS

Figure 2 shows the friction apparatus that we have built and used. It is more realistic than a pin-on-disk (POD) apparatus but less complex than a hip simulator[10], and it creates the axial loading and flexion/extension rotation experienced during hip gait between the articulating CoCr and UHMWPE specimens. Figure 2(a) depicts the mechanical assembly of the apparatus. A cylindrical CoCr cylinder specimen is mounted on the shaft in the lubricant reservoir (Figure 2(b)) and a concave UHMWPE specimen is loaded against the convex CoCr specimen (Figure 2(c)) using a power screw mechanism. The loading mechanism is designed to self-align the UHMWPE specimen with the CoCr specimen. A geared stepper motor creates a reciprocal motion between the CoCr and UHMWPE specimens, while the torque and normal load between both specimens are continuously measured. This allows the friction coefficient to be computed as a function of time. The articulating surfaces are submerged in bovine serum with a protein concentration of 20 mg/ml[11].

SPECIMENS

A traditional lubrication model is used to optimize the geometry of the microtexture in terms of maximizing the load-carrying capacity of the lubricant film between the CoCr specimen and the UHMWPE specimen[6]. The microtexture geometry is determined by the texture density S_p, defined as the area covered by the texture divided by total bearing area, and the texture aspect ratio ε, defined as the ratio of the depth and diameter of a texture feature. Four different microtexture designs are selected, based on load-carrying capacity, from the modeling results. These microtexture patterns are manufactured on polished CoCr (ASTM F1537-08) cylinders of diameter 50 mm and average surface roughness R_a < 50 nm using laser surface texturing (LST) with a solid-state laser. The characteristic radius of the spherical texture

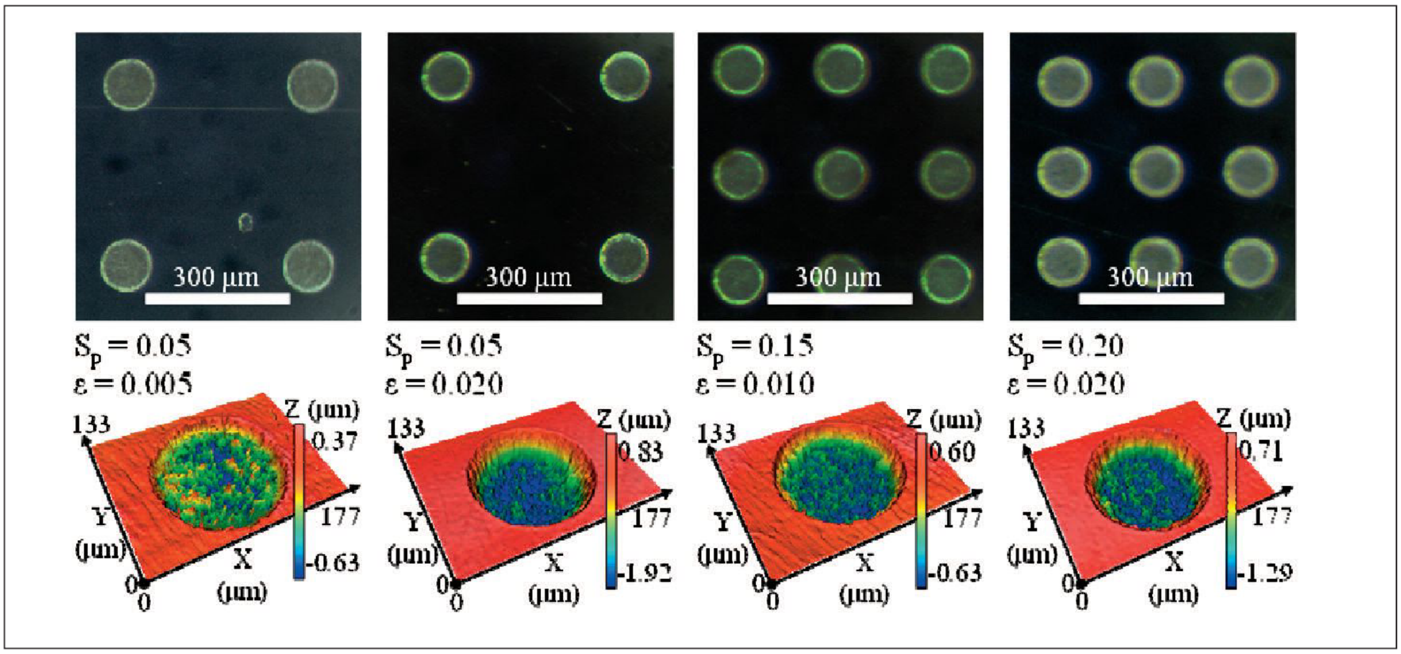

Figure 3 | Optical microscope and white light interferometer images of each of the four microtexture patterns manufactured on cylindrical CoCr specimens (ASTM F1537-08) showing the results of the LST process. The radius of the dimples, r_p = 50 μm[6].

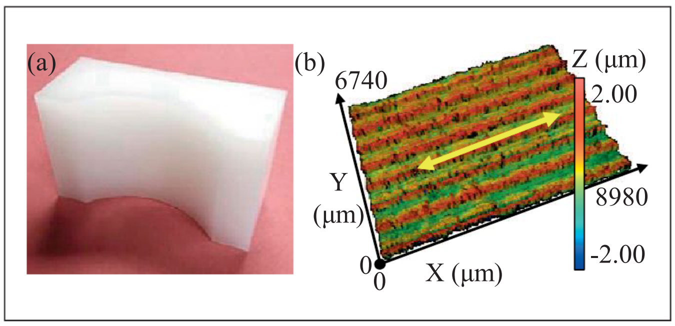

Figure 4 | UHMWPE specimen (a) photograph and (b) white light interferometer image of the articulating surface. The yellow arrow indicates the direction of articulation[6].

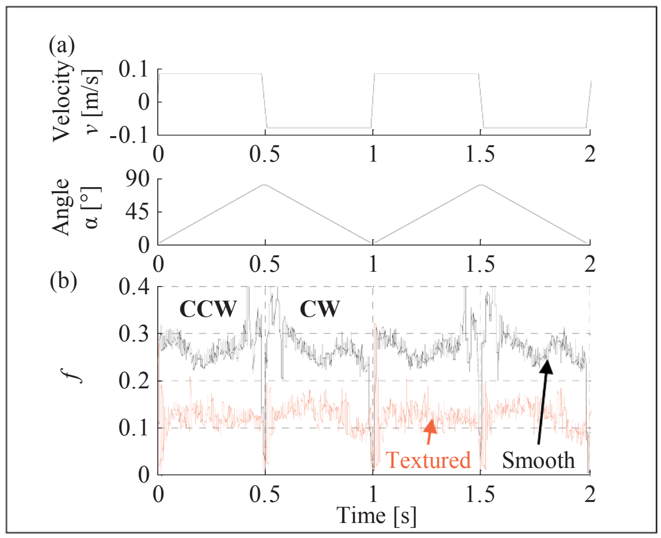

Figure 5 | (a) Kinematic cycle of the CoCr specimen articulating with the UHMWPE specimen and (b) Friction coefficient as a function of time for the microtextured (red) specimen (S_p = 0.05, ε = 0.005) and the smooth (black) specimen articulating with the UHMWPE specimen under a contact pressure of 0.90 MPa showing that the microtextured specimen outperforms the smooth specimen over almost the entire kinematic cycle[6].

features is r_p = 50 μm. Figure 3 shows optical microscopy and white light interferometry images of each of the four microtexture patterns implemented on CoCr cylinders. Minimal material deposition resulting from the laser texturing process is observed around the contour of each dimple. A concave UHMWPE (ASTM F648) specimen conformal with the convex CoCr specimens over a span of 90 degrees acts as the surrogate polyethylene liner and is shown in Figure 4. The average surface roughness of the articulating UHMWPE surface is R_a < 800 nm. Both the CoCr and UHMWPE specimens are manufactured and finished to identical specifications as commercial MOP prosthetic hip joints.

RESULTS AND DISCUSSION

Figure 5 shows two seconds of typical results extracted from a longer duration experiment performed in our experimental apparatus. Figure 5(a) shows the kinematic cycle including velocity and angular position of the CoCr specimen with respect to the UHMWPE counterface as a function of time. The kinematic cycle is designed to maximize the portion during which a constant velocity is maintained to best approach the

Table 1 | **Different microtexture designs, showing the percentage of the 1 Hz kinematic cycle during which the microtextured CoCr specimen outperforms the smooth CoCr specimen for different values of constant bearing contact pressure[6].**

Texture design	Texture parameters	Max contact pressure [MPa]			
300 µm	S_p, ε	0.57	0.71	0.90	1.13
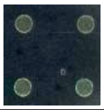	$S_p = 0.05$, $\varepsilon = 0.005$	98%	98%	94%	24%
	$S_p = 0.05$, $\varepsilon = 0.020$	88%	67%	58%	19%
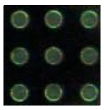	$S_p = 0.15$, $\varepsilon = 0.010$	94%	96%	91%	22%
	$S_p = 0.20$, $\varepsilon = 0.020$	93%	90%	83%	15%

steady-state lubrication model used to optimize the microtexture geometry. The frequency of the kinematic cycle is 1.0 Hz [12] (ISO 14242-1), which is similar to walking gait. Figure 5(b) shows the friction coefficient as a function of time for a microtextured (S_p = 0.05, ε = 0.005) and smooth CoCr specimen, articulating against the UHMWPE specimen with a contact pressure of 0.90 MPa, realistic for hip joints.

We observe that the friction coefficient is periodic with reversals between clockwise (CW) and counter-clockwise (CCW) rotations. The magnitude of the friction coefficient is maximal surrounding the starts and stops, and it is minimal throughout the middle of each cycle when the sliding velocity at the surface of the cylinder is constant (0.1 m/s). The microtextured CoCr specimen outperforms the smooth specimen in two ways. First, the friction coefficient is lower for the microtextured compared to the smooth cylinder over almost the entire kinematic cycle (for this particular texture geometry, kinematic cycle, and loading example), indicating that friction is reduced significantly. Second, the friction coefficient for the microtextured CoCr specimen experiences a sharp drop surrounding direction reversals (at t = 0.5, 1.0, 1.5). In contrast, the friction coefficient for the smooth CoCr specimen decreases slowly after direction reversals. This indicates that solid-on-solid contact between the CoCr and UHMWPE surfaces is reduced for the textured versus the smooth surfaces. This could lead to reduced wear and, correspondingly, increased longevity.

To evaluate and compare the performance of the four microtexture geometry designs, we have quantified the portion of the kinematic cycle during which each of the microtextured CoCr specimens displays a lower friction coefficient than the smooth CoCr specimen. Table 1 summarizes the results and shows the percentage of the kinematic cycle during which the microtextured CoCr specimen outperforms the smooth one. Each microtexture geometry design outperforms the traditional smooth surface design over at least part of the kinematic cycle. These results confirm the hypothesis that friction can be reduced at low sliding velocities in a surrogate MOP prosthetic hip joint by means of a patterned microtexture on the surface of the femoral head.

CONCLUSION

We find that the friction coefficient between the surrogate convex CoCr and the concave UHMWPE specimens is lower for textured CoCr specimens than for the benchmark smooth CoCr specimen. This demonstrates that the patterned microtexture reduces friction by reducing contact between the articulating surfaces. A reduced friction coefficient between the articulating bearing surfaces promises reduced wear and increased longevity of a prosthetic hip joint. Also, in contrast with the smooth surrogate CoCr femoral head, the friction coefficient decreases very quickly after sliding direction reversals for the microtextured surrogate femoral heads. Daily human joint activity includes frequent starts and stops, and it is during these periods of high-friction boundary lubrication that the most wear occurs. Thus, the microtexture reduces friction and wear precisely at instants where it is needed most.

REFERENCES

1. American Academy of Orthopaedic Surgeons, "Total Hip Replacement," December 2011. [Online]. Available: **http://orthoinfo.aaos.org/topic.cfm?topic=A00377.** [Accessed August, 13, 2013].
2. Jacobs, J., Hallab, N., Urban, R. and Wimmer, M. (2006), "Wear Particles," *J. Bone Joint Surg. Am.*, **88** (2), p. 99.
3. Kurtz, S., Mowat, F., Ong, K., Chan, N., Lau, E. and Halpern, M. (2005), "Prevalence of Primary and Revision Total Hip and Knee Arthroplasty in the United States from 1990 through 2002," *J. Bone Joint. Surg. Am.*, **87** (7), pp. 1487–1497.
4. Ong, K., Lau, E., Suggs, J., Kurtz, S. and Manley, M. (2010), "Risk of Subsequent Revision after Primary and Revision Total Joint Arthroplasty," *Clin. Orthop. Rel. Res.*, **468** (11), pp. 3070–3076.

5. Sychterz, C.J. Engh Jr., C.A., Young, A.M., Hopper Jr., R.H. and Engh, C.A. (2000), "Comparison of In Vivo Wear Between Polyethylene Liners Articulating with Ceramic and Cobalt-Chrome Femoral Heads," *J. Bone Joint Surg.* B., **82** (7,) pp. 948-951.

6. Chyr, A., Qiu, M., Speltz, J., Jacobsen, R.L., Sanders, A.P. and Raeymaekers, B. "A Patterned Microtexture to Reduce Friction and Increase Longevity of Prosthetic Hip Joints," *Submitted for publication.*

7. Ito, H., Kaneda, K., Yuhta, T., Nishimura, I., Yasuda, K. and Matsuno, T. (2000) "Reduction of Polyethylene Wear by Concave Dimples on the Frictional Surface in Artificial Hip Joints," *J. Arthroplasty,* **15** (3), pp. 332-338.

8. Sawano, H., Warisawa, S.I. and Ishihara, S. (2009), "Study on Long Life of Artificial Joints by Investigating Optimal Sliding Surface Geometry for Improvement in Wear Resistance," *Prec. Eng.,* **33** (4), pp. 492–498.

9. Zhou, X., Galvin, A.L., Jin, Z., Yan, X. and Fisher, J. (2011), "The Influence of Concave Dimples on the Metallic Counterface on the Wear of Ultra-High Molecular Weight Polyethylene," *Proc. Inst. Mech. Eng. Part J-J. Eng.,* **226** (6), pp. 455-462.

10. Chyr, A., Sanders, A. and Raeymaekers, B. (2013), "A Hybrid Apparatus for Friction and Accelerated Wear Testing of Orthopedic Total Knee Replacement Bearing Materials," *Wear,* **308**, (1-2), pp. 54-60.

11. Liao, Y.S., Benya, P.D. and McKellop, H.A. (1999), "Effect of Protein Lubrication on the Wear Properties of Materials for Prosthetic Joints," *J. Biomed. Mater. Res.,* **48** (4), pp. 465-473.

12. Murray, M.P., Drought, A.B. and Kory, R.C. (1964), "Walking Patterns of Normal Men," *J. Bone Joint Surg.,* **46** (2), pp. 335-360.

PUBLICATIONS RESULTING FROM THIS WORK

Journal Publications

1. Chyr, A., Sanders, A. and Raeymaekers, B. (2013), "A Hybrid Apparatus for Friction and Accelerated Wear Testing of Orthopedic Total Knee Replacement Bearing Materials," *Wear*, **308** (1-2), pp. 54-60.

2. Chyr, A., Qiu, M., Speltz, J., Jacobsen, R.L., Sanders, A.P. and Raeymaekers, B. "A Patterned Microtexture to Reduce Friction and Increase Longevity of Prosthetic Hip Joints," Submitted for publication.

Conference Proceedings

1. Chyr, A., Sanders, A. and Raeymaekers, B. "Improving Durability of Metal-on-Polyethylene Hip Joints using Surface Microtexturing," STLE 68th Annual Meeting & Exhibition, Detroit, Michigan (USA), May 5-9, 2013.

Raymond Thibault, CLS, OMA I&II, MLT I&II, MLA II&III

Use of ASTM tests in the evaluation and selection of industrial lubricants

Review the various testing methods and their correlation to field performance before deciding which lubricant to use.

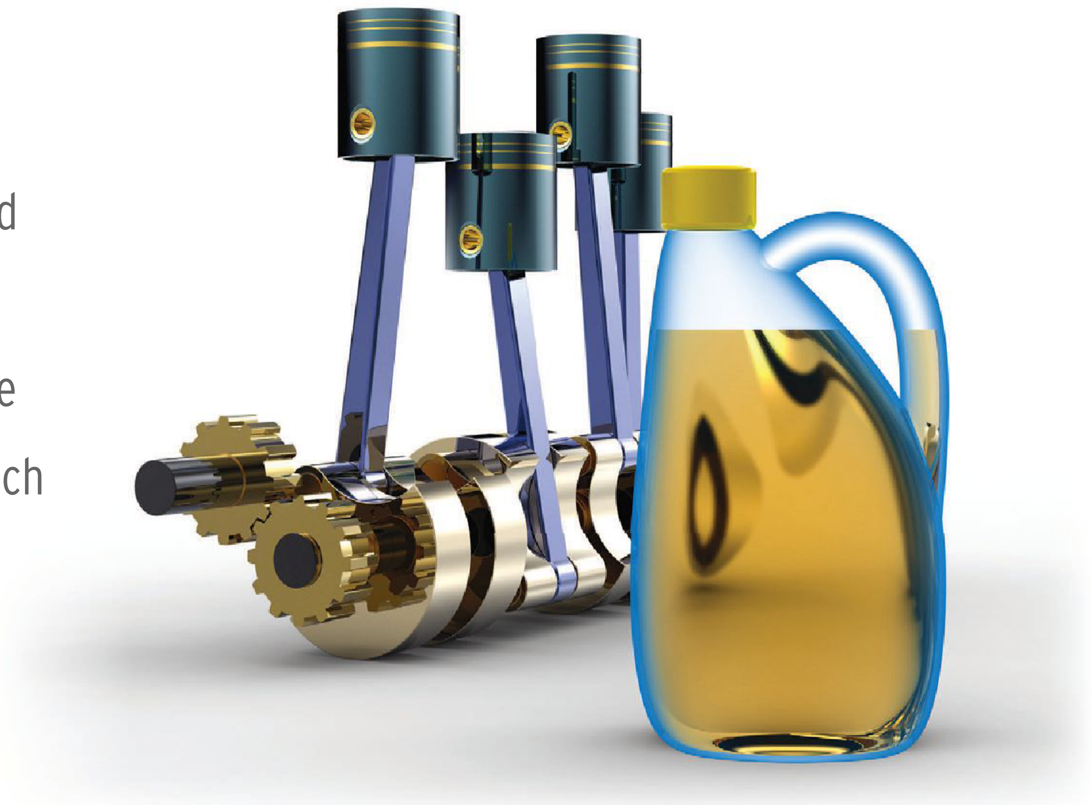

KEY CONCEPTS

- ASTM International offers standardized tests used to evaluate lubricant performance.
- Lubricant testing is classified into two major categories: physical/chemical and performance.
- Additive and finished lubricant manufacturers utilize ASTM tests to help with developing new products.

PREDICTING HOW LUBRICANTS will perform requires the use of standardized tests. The organization supplying these standards is ASTM International, formerly known as the American Society of Testing and Materials. This organization defines how a test should be performed and the precision of the result. The use of standardized tests is utilized by three major groups:

1. Additive manufacturers and finished lubricants producers utilize these tests in development of new products.
2. OEMs utilize these tests to set minimum performance standards on lubricants used on their equipment.
3. End-users utilize these tests to help them in the selection of the optimum lubricant for their equipment.

The best test in the selection of the proper lubricant for a particular application is an actual field test or experience with this lubricant in a similar application. Uses of ASTM tests are the first step in the selection of the proper lubricant. These tests provide a level playing field when comparing lubricants from different suppliers if they are conducted according to the ASTM procedures and provide an indication on how they will perform in the field.

This article will examine the most common tests utilized for turbine, hydraulic and gear oils.

MEET THE PRESENTER

This article is based on Webinars originally presented by STLE University. "Lubricant Testing Methods" is available at **www.stle.org:** $39 to STLE members, $59 for all others.

Ray Thibault is the owner of Lubrication Training & Consulting in Houston. Previously, he spent 31 years working for ExxonMobil. He has several years of experience in conducting extensive training and consulting for numerous lubricant companies. He also served as contributing editor for *Lubrication Management & Technology* magazine and authored a bimonthly column on lubrication for nine years. In addition, Ray has presented several papers and conducted lubrication courses at various industry conferences such STLE, MARTS and IMC. He also holds STLE's Certified Lubrication Specialist™ and Oil Monitoring Analyst™ (I&II) certifications, as well as Machinery Lubrication Technician (Levels I&II) and Machinery Lubrication Analyst (Levels II&III). You can reach Ray at **rlthibault@msn.com.**

Ray Thibault

OVERVIEW

Lubricant tests are divided into two major categories: physical/chemical and performance.

Physical/Chemical Tests:

- Viscosity
- Viscosity index
- Flash point
- Pour point
- Neutralization number

Performance Tests:

- Rust prevention
- Copper strip corrosion
- Turbine oil stability
- Dry turbine oil stability
- Rotary pressure vessel oxidation
- Extreme pressure oil oxidation
- Foaming sequence
- Air release
- Water separability
- Demulsibility characteristics of lubricating oils
- Four-square gear oil tester
- Timken extreme pressure
- Four-ball EP
- Four-ball wear
- Hydrolytic stability
- Accelerated hydraulic pump fluid test

COMMON INDUSTRIAL LUBRICANTS TESTS

Tables 1-3 illustrate the most common tests for turbine, hydraulic and gear oils.

Table 1 | **Typical Turbine Oil Specification Tests**

Test Method	Expressed Value	ASTM #
Viscosity @ 40 C and 100 C	Centistokes (cSt)	D445
Viscosity index	Number with no units	D2270
Flash point	F & C	D92
Pour point	F & C	D5950
Neutralization number	Milligrams of KOH/gram of sample	D974
Rust prevention test	Pass/Fail	D665 A/B
Copper strip corrosion	1-4	D130
Turbine oil stability test	Hours	D943
Rotary pressure vessel Oxidation Test	Minutes	D2272
Foaming sequence I/II/III	Milliliters of foam	D892
Air release	Minutes	D3427
Water separability	Milliliters of oil/water/emulsion	D1401
Four square gear oil tester	Highest stage (1-13) achieved	D5182

Table 2 | **Typical Hydraulic Oil Specification Tests**

Test Method	Expressed Value	ASTM #
Viscosity @ 40 C and 100 C	Centistokes (cSt)	D445
Viscosity index	Number with no units	D2270
Flash point	F & C	D92
Pour point	F & C	D5950
Neutralization number	Milligrams of KOH/gram of sample	D974
Rust prevention test	Pass/Fail	D665 A/B
Copper strip corrosion	1-4	D130
Turbine oil stability test	Hours	D943
Rotary pressure vessel oxidation test	Minutes	D2272
Foaming sequence I/II/III	Milliliters of foam	D892
Air release	Minutes	D3427
Water separability	Milliliters of oil/water/emulsion	D1401
Four square gear oil tester	Highest stage (1-13) achieved	D5182
Hydrolytic stability	Acid # and mass loss of Cu in mg	D2619
Accelerated hydraulic fluid pump test	Weight loss in mg.	D2882

operating temperature should be at least 20 F above its pour point.

Table 3 | **Typical Gear Oil Specification Tests**

Test Method	Expressed Value	ASTM #
Viscosity @ 40 C and 100 C	Centistokes (cSt)	D445
Viscosity index	Number with no units	D2270
Flash point	F & C	D92
Pour point	F & C	D5950
Neutralization number	Milligrams of KOH/gram of sample	D974
Rust prevention test	Pass/Fail	D665 A/B
Copper strip corrosion	1-4	D130
Extreme pressure oil oxidation	% Viscosity increase at 100 C	D2893
Foaming sequence I/II/III	Milliliters of foam	D892
Demulsibility characteristics of lubricating oils	Milliliters of free water and emulsion Percent water in clean oil	D2711
Timken extreme pressure	Maximum load in lbs	D2782
Four ball EP	Load carrying capacity in kilograms	D2783
Four ball wear	Scar diameter in millimeters	D2266
Four square gear oil tester	Highest load stage (1-13) achieved	D5182

ASTM SPECIFICATION TESTS

Viscosity (D445). Defined as resistance to flow of a fluid, which is the most important property of a lubricant. Kinematic viscosity is determined by the time it takes in seconds for a fixed volume of fluid to flow through a calibrated capillary tube. The test is run at 40 C for industrial oils and 100 C for engine oils. The units are usually expressed as centistokes (cSt) or millimeters^2/second, which are equivalent. When selecting a lubricant for an application, viscosity, which is indicative of a lubricant's film thickness, is the most important consideration.

Viscosity index (VI) (D2270). Expresses the rate of change in viscosity as oil is heated. It can be determined by comparing the viscosity of the oil to two reference oils at 40 C and 100 C. The low VI oil is arbitrarily set at 0 and the high VI oil is called 100. A mathematical relationship comparing the viscosities of the three oils is used to determine the VI, a unitless number of the unknown oil. When plotting the viscosity of an oil at 40 C and 100 C, the steeper the slope of the line, the lower the VI. In the past, most industrial oils had VIs <100 but today, with the emergence of Group II oils, VIs exceed 100. Many synthetics such as polyalphaolefins have VIs well over 100. High-VI oils give better protection with a thicker film than low-VI oils of the same ISO viscosity grade at higher temperatures.

Flash point (D95). A measure of the evaporative losses of oil as it is heated. The test for new oils is conducted in an open cup by heating test oils at a rate of 10 F/minute and passing a flame over the fluid at 5 F increments. When the fluid ignites with a flash, that temperature is recorded as the flash point. The fire point is determined by continuing to heat the fluid until it burns for five seconds. Lower quality oils with more volatiles have a lower flash point. As you proceed from Group I-III, the flash point goes up because the molecular structures of the oils are more uniform. Comparisons of flash points of various oils should be made at the same viscosity. Synthetics have higher flash points than mineral oils because they have more compactness in their hydrocarbon molecular structures.

Pour point (D5950). An indicator of the low temperature behavior of lubricants. It is conducted by cooling a fluid at 5 F increments in a test chamber. The fluid is tilted at each point until no movement occurs. The pour point is the last temperature where fluid movement was observed. A lubricant's operating temperature should be at least 20 F above its pour point.

Neutralization number (D974). Determined by titrating the fluid with KOH until it is neutralized. This determines the acid number of the lubricant and is expressed as milligrams of KOH/gram of sample to neutralize the fluid. It is based mainly on the acidity of the additives. Lubricants with higher additive concentrations usually have a higher acid number. Turbine oils, which have low additive concentrations, have acid numbers around 0.05-0.1 while gear oils are 0.5-0.8. The acid number is very useful in used oil analysis. As used oil is oxidized, it creates weak acids. By comparing the new oil acid number to the used oil acid number, the oxidation of the used oil is indicated. New oil acid numbers should be updated yearly by providing new oil to the oil analysis laboratory so a new oil reference can be updated. Don't use the product data sheet acid number as the reference for used oil analysis.

ASTM performance tests have a degree of variability, which is defined as the precision of the tests. Precision is the variability of the results of the test with a 95 percent statistical confidence level, which is one value out of 20 exceeding the precision limits. Repeatability is defined as the difference in results run by the same operator with the same equipment under the same conditions. Reproducibility is comparing results run by different laboratories on the same sample under the same conditions. Reproducibility variability is higher than repeatability. ASTM has established precision limits for each of their tests. This is expressed as percent of mean value.

Rust prevention test (ASTM D665 A/B). Predicts how well lubricants prevent rusting of ferrous equipment components. This test predicts field performance very well. It is conducted with 300 mL of the test oil put in a beaker and 30 mL of distilled (A) or synthetic seawater (B) is added during stirring and brought to a temperature of 140 F. A freshly polished steel rod is immersed in the mixture for


HANZHOU SUNGATE
杭州盛材
Supply high quality China-made lubricant additives
Honesty, Responsibility, Reliability and Cooperation
Pay special attention to every detail
If you want to find a professional and reliable Chinese lubricant additives supplier, we are your choice
Import outstanding additives and their raw materials from overseas
Good experience in matching and supplying the corresponding equivalent additives with good quality made in China
Add me, Stronger!
Anti Wear and Extreme Pressure
SungateLube TPPT, S-349, S-232,S-211
Antioxidant
Antioxidant L135, Di Nonyl Diphenylamine
Corrosion Inhibitor
Sungate BSB,729, BSN, L190
Detergent and Dispersant
Alkyl Salicylates,Alkyl Phenates
ZDDPs
Zinc Dioctyl Dithio Phosphate
VISIT US AT BOOTH #321 IN STLE 2014
Web:http://www.sungatechem.com Tel:0086-571-87040747 Fax:0086-571-87040749 E-mail:ericchen@sungatechem.com
Add:2008,Fengqi Business Building,129Dongqing Road,Hangzhou,China PC.:310003

typically four hours and then removed and visually observed. Any rust on the rod constitutes a fail on the test. This test has also been run for 24 hours.

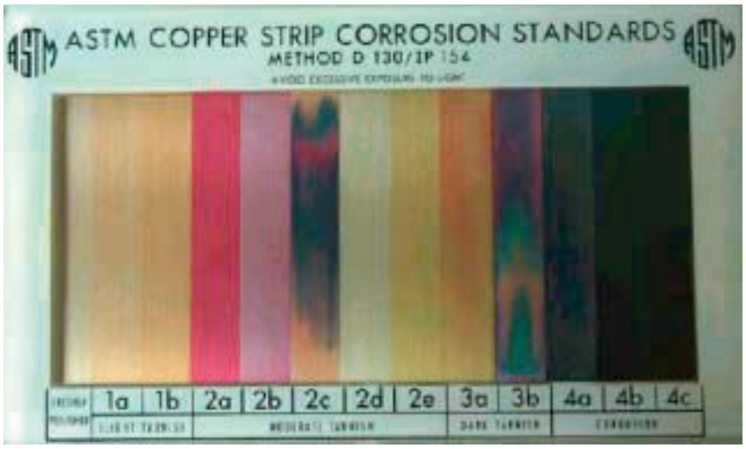

Figure 1 | **Copper strip corrosion test.**

Copper strip corrosion test (ASTM D130). Sulfur components in lubricant base stocks and additives can cause tarnishing and corrosion of yellow metals by the fluid. This test measures the corrosivity of the lubricant on copper and its alloys. A freshly polished copper strip is immersed in a test tube containing 30 mL of the test fluid and heated in a bath for three hours at 212 F. The strip is removed, wiped off and compared with the ASTM Copper Strip Corrosion Standard illustrated in Figure 1.

The scale ranges from 1-4. Level 1 is slight tarnish (1a&1b) and increases in tarnishing up to Level 4, which is corrosion. Most OEMs will not approve a lubricant above 1b.

Turbine oil stability test (ASTM D943). This is the most popular test to measure the oxidation life of turbine, hydraulic and R&O circulating oils. The test is conducted by adding 300 mL of the lubricant along with 60 mL of water to an oxidation test cell, which has a catalyst of iron and copper. The water and catalyst help promote oxidation in the test. The fluid is heated in a bath at 95 C and three liters/hour of oxygen is bubbled continuously through the sample. At predetermined intervals, a sample is extracted and an acid number is run to determine the level of oxidation.

When the acid number reaches 2.0, the test is terminated and the result reported in the number of hours of runtime. The test cannot exceed 10,000 hours if only one cell is run because the sample level in the cell at that time is below the catalyst. In the past, results were reported for Group II oils in excess of 10,000 hours because multiple cells were used. As fluid was depleted in one cell, it was then taken from another cell. One lubricant company reported numbers for one of their turbine oils in excess of 30,000 hours. Today most lubricant companies report 10,000+ hours as the highest level. Typical Group I turbine oils range from 4,000-8,000 hours, while Group II turbine are in excess of 10,000 hours. This test is useful in comparing the relative oxidative life of various lubricants.

Rotary pressure vessel oxidation test (ASTM D2272). This test previously was called the Rotary Bomb Oxidation Test (RBOT), as the name was changed over 10 years ago. This is a rapid test which measures the oxidative life of oils with similar formulations. It is primarily used to measure depletion of additives in used turbine oils by comparing the percent drop in life of the used oil compared to the new oil. A 25 percent remaining life in the used oil requires changing or conditioning of the turbine oil. This test should not be used to compare new turbine oils from different suppliers. GE no longer has RPVOT as a performance requirement for new turbine oils. Because Group II oils have a much better response to additives than Group I oils, their RPVOT values for new oils are much higher than Group I oils and range from 1,000-3,000 minutes. An oil sample of 50 grams along with 5 milliliters of water is introduced in a glass vessel containing copper wire as a catalyst. This is then immersed in a pressurized oxidation cell containing 90 psi of oxygen at 77 F. The cell is placed in a preheated bath at 150 C and rotated at an angle. This is illustrated in Figure 2. Once the pressure reaches 192 psi in the pressurized vessel, readings are taken at predetermined intervals and the drop in pressure is recoded.

When the pressure drops by 25 psi, which indicates full oxidation of the oil, the test is terminated and the time is reported in minutes. The repeatability and reproducibility on this test, as reported by ASTM, based on round-robin testing on seven different turbine oils ranging from 30-1,000 minutes, was 12 and 22 percent of the mean value, respectively. The variance is greater for Group II oils, which have RPVOT values >1,000 minutes. Reproducibility values run on Group II oils reported a variability of 39 percent of mean value.

Dry turbine oil stability test (TBN). This test was recently approved by

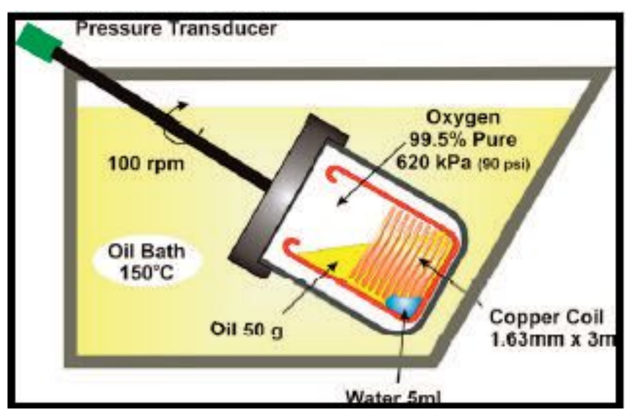

Figure 2 | **Rotary pressure vessel oxidation test (ASTM D2272).** *(Courtesy of Fluitec)*

ASTM and will be given a number designation in the spring of 2014. With deposit formation and varnishing being a big issue with gas turbine oils, a test was developed by Mitsubishi Heavy Industries (MHI) to measure deposit formation during oxidation of turbine oils. The test is run in equipment similar to TOST D943 test. The turbine oil has no water added to it in the test cell and the temperature in the bath is maintained at 120 C. The test is run a minimum of 500 hours. At predetermined time intervals, an RPVOT value is run on the sample. Once the RPVOT reaches 25 percent of the new oil value, the test is terminated and the deposits in the oxidation cell are weighed. The deposits are reported as mg/kg. A value >100 mg/kg is a failure on the test. This test is designed primarily to evaluate Group II oils and is difficult to pass. It has been shown that turbine oils with high RPVOT may not pass the test.

Extreme pressure oil oxidation test (ASTM D2893). This test is designed to measure the high temperature stability of EP gear oils. A 300 mL sample of the gear oil is placed in a 600 mm specialized test tube and immersed in a bath. Previously the bath temperature was 95 C but with new OEM requirements, the temperature has been increased to 121 C (250 F). Ten liters/hour of dry air is passed through the sample for 312 hours. At the end of the test, the kinematic viscosity at 100 C is measured and compared to the viscosity of the new oil. Gear oils must not exceed 6 percent to meet the AGMA 9005 requirement. This test is a good field predictor of the relative oxidative life of new EP gear oils.

Foaming characteristics of lubricating oils (ASTM D892). This test is a good field predictor of foaming tendencies of lubricating oils. A 190 mL sample of fluid is placed in a 1000 mL graduated cylinder and air is blown in the sample for five minutes. A reading is taken of the foam height in mL. The sample is allowed to settle for 10 minutes and a reading is taken. This test is run in three different sequences:

- Sequence I: 75 F
- Sequence II: New fluid run at 200 F
- Sequence III: Sequence II fluid cooled to 75 F.

The results are reported as x/y for each sequence. The top number is the initial reading and illustrates the tendency of the fluid to foam. The bottom number, which is the most important, measures the stability of the foam after 10 minutes of settling. For example, GE's requirement for turbine oils is a maximum of 50/0 for all three sequences. This test is also used to evaluate used fluids for loss of defoamant.

Air release properties of petroleum oils (ASTM D3427). Air entrainment can affect lubricant performance by causing sponginess, lack of control and micro-dieseling in turbine and hydraulic oils. As reservoirs are built smaller, the oil has less residence time and must release entrained air in a shorter period of time. The test is conducted by adding 180 mL of the fluid to a specially fitted glass container. The test is run at 50 C for viscosities up to 90 cSt and at 75 C for viscosities >90 cSt. The density of the fluid is measured by attaching a sinker to a balance beam and recording the density of the fluid. Air is then bubbled through the fluid for 7 minutes. The sinker is immersed in the fluid and the density is recorded. Readings are taken until the density of the fluid reaches 99.8 percent of the initial value. The time is then recorded in minutes. Most OEMs require no more than 5 minutes for ISO 32 oils, 7 minutes for ISO 46 and 10 minutes for ISO 68.

Water separability of petroleum oils (ASTM D1401). This test is a good predictor of field performance and is also used to test in-service steam turbine oils to measure the loss in water separability. Figure 3 illustrates the test apparatus. Forty milliliters of lubricant and distilled water at 54 C are mixed for 5 minutes at 1500 rpm in the apparatus. The amount of oil water and emulsion is recorded in 5-minute intervals. The test is terminated in 30 minutes. Results are recorded as oil/water/emulsion. For example, a reading of 40/40/0 (15) indicates that the oil had complete separation in 15 minutes, which is excellent water separability. To pass the test, no more than three milliliters of emulsion remain after 30 minutes. Most lubricant suppliers with good water separability report the three-number code on their product data sheets. The test is run normally on oils with a maximum viscosity of 90 cSt. Higher viscosity oils are run at 82 C.

Demulsibility characteristics of lubricating oils (ASTM D2711). This test is designed to determine the demulsibility characteristics of oils experiencing high water contamination under turbulent conditions. The test for EP gear oils is conducted by adding 90 mL of distilled water to 360 mL of the test fluid in a special graduated separatory funnel and stirring at 2500 rpm for 5 minutes at 82 C. After mixing, the fluid is allowed to separate for five hours at the test temperature. The amount of free water is drained and measured. The amount of water remaining in the oil and emulsion phases is determined by centrifuging the oil and emul-

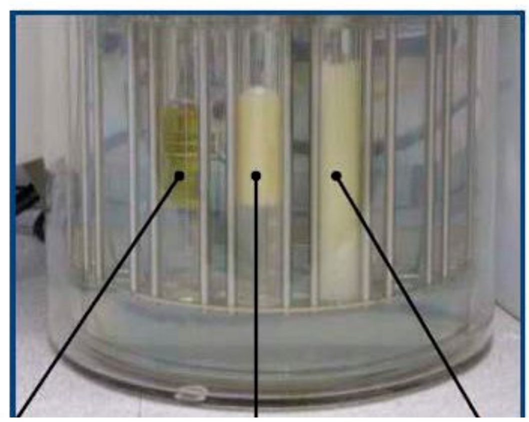

Figure 3 | **Test apparatus of the water separability of petroleum oils.**

sion phases. The amount of water after centrifuging is added to the total free water. Also recorded is the amount of emulsion remaining and the amount of water in the centrifuged oils. Gear oils with good demulsibility properties should separate a minimum of 80 mL of water. The test is also run on non-EP oils where 405 mL of test oil is mixed with 45 mL of distilled water. In this test, oils with good demulsibility characteristics will separate 36-45 mL.

Timken extreme pressure test (ASTM D2782). This is a rapid and old test for determining the load-carrying capacity of lubricants. It has poor repeatability at 30 percent of mean value and very poor reproducibility at 74 percent of mean value. It has been replaced by other tests, but it is still reported on product data sheets for gear oils and greases. AGMA 9005 no longer includes Timken for new oil specifications.

The test reservoir is filled with three quarts of test oil at 100 F. A test cup is on a spindle, and the test block is on a special holder. The test cup is flooded with lubricant and the spindle is run at 800 rpm. The test is run for 10 minutes at increasing loads measured in pounds. After each stage, the test block is examined for scoring and welding. Once scoring is observed, the last stage with no scoring is reported as the Timken OK value. Scoring is defined by the appearance of a wide scar on the test block. This test is subjective based on the observations of the analyst. Typical EP gear oils achieve 60 pounds on the test.

Four-ball EP test (ASTM D2783). This test determines the load-carrying capacity of a lubricant. This test is used primarily for EP gear oils. Three immovable balls are placed in a test pot containing the tested lubricant. A fourth ball rotates against the three lower balls. A series of 10 second runs at 1760 rpm are made at increasing loads until welding of the four balls occurs. The load is measured in kilograms. The test can be run up to 800 kilograms. Most test results reported for gear oils are at 250 kg, which meets the OEM requirements. This is a popular test and is reported on many gear oil product data sheets. The repeatability is 17 percent of mean value and the reproducibility is 44 percent of mean value. Figure 4 illustrates the tester

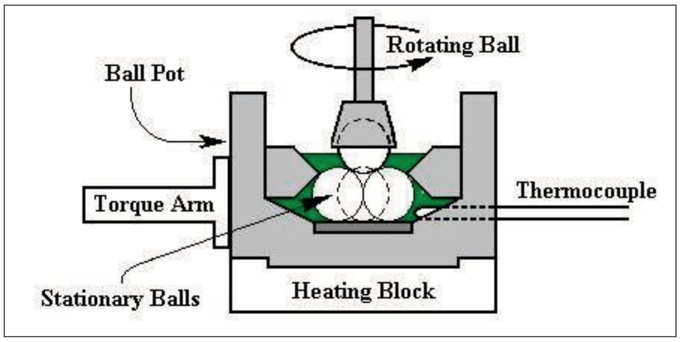

Figure 4 | **Four-ball EP test.**

Four-ball wear test (ASTM D2266 modified). This test is a good field predictor afforded by a lubricant at different loads. The original ASTM test was D4172 but has been replaced by D2266 modified, which conforms to U.S. Steel Method S-205. The test apparatus is illustrated in Figure 4. A 10 mL sample is put in the ball pot and heated to 130 F. Three immovable balls are placed in the test cup. A fourth ball rotates at 1800 rpm against the three lower balls at a constant load of 40 kg for one hour. At the end of the test, the average scar diameter of the three lower balls is recorded. This test is used primarily for gear and hydraulic oils to measure lubricant wear protection. Gear oils should have a scar diameter not exceeding 0.35 mm, while hydraulic oils should fall between 0.50-0.80 mm.

Four-square gear oil test (ASTM D5182 (FZG Procedure)). This test evaluates the scuffing tendencies of lubricants containing EP or antiwear additives and is used to meet OEM specifications for industrial gear oils, hydraulic fluids, automatic transmission fluids and turbine oils. For example, GE requires a minimum FZG of 8 for geared turbines. The test rig, which is illustrated in Figure 5, consists of two gearsets arranged in a four square configuration driven by an electric motor at a speed of 1450 rpm. The test fluid is added to bring the oil level to the centerline of the gear shafts and the fluid temperature is maintained at 194 F. The test is run for 15 minutes at increasing load stages.

After each stage, the pinion test gear is inspected for damage. The visual method examines the gears without disassembly and records a failure if the sum total width of scuffing or scoring on all the gear teeth exceeds the total width of one gear tooth, which is normally 20 mm. The other method for failure determination weighs the

Figure 5 | **Four-square gear oil test rig** pinion at each stage and a 10 mg or more loss is a failure. The FZG rating is recorded as the load stage before the failure occurred. The test goes to 13 stages and some tests have gone as high as 14 stages. Fluids with high levels off EP generally exceed the limits of the test. Hydraulic oils will usually reach Stage 10.

Hydrolytic stability test (ASTM D2619). This test is used to evaluate the hydrolytic stability of hydraulic fluids in contact with water to measure the instability of the additives, especially ZDDP. Additive decomposition can create insoluble inorganic salts, which can block filters and tiny orifices in valves. The test is conducted by placing 75 grams of sample and 25 grams of water in a six-ounce beverage bottle, which contains a weighed copper strip. The bottle is placed in a rotating device and heated to 98.3 C in an oven for 48 hours. The following fluid measurements are made:

- Acid number of water phase
- Viscosity change of oil phase
- Weight loss of Cu strip.

Acceptable hydraulic fluids should have an acid number <4.0 mg KOH/gram of sample and <0.2 mg/cm^3 of weight loss.

Accelerated hydraulic fluid pump test (ASTM D2882). Most hydraulic pump manufacturers have their own in-house tests to qualify hydraulic fluids because of the diversity of pump speeds and pressures encountered. ASTM has developed a severe test, which is applicable to all hydraulic fluids except 95/5 high water base. A test pump, where the cartridge ring, vanes and bushings have been individually weighed, is placed in a test stand. A 10-gallon sample is added and run at 1000 psi until the temperature reaches 150 F. The pressure is then reset to 1900 psi and run for 100 hours. The pump parts are cleaned and weighed. A typical weight loss for the cartridge components should not exceed 30 mg for an antiwear mineral hydraulic oil.

OEM SPECIFICATION REQUIREMENTS

Table 4 | **General Electric Specification for ISO 32 Turbine Oil**

Test Method	GEK10194a	GEK107395a CC
Viscosity @ 40 C	32	32
Viscosity index	95	98
Flash point	420 F min.	420°F min.
Pour point	10 F max.	10°F max
Neutralization number	0.20	0.20
Rust prevention test	Pass	Pass
Copper strip corrosion	1b	1b
Turbine oil stability test	3000 min.	3000 min.
Rotary pressure vessel oxidation test	500 min.*	1000 min*
Foaming sequence I/II/III	50/0 all sequences	50/0 all sequences
Air release	5.0 max.	5,0 max

*RPVOT no longer a GE new turbine oil specification

Table 5 | **Typical EP Gear Oil Specification Tests**

Test Method	AISE 224	AGMA 9005-E02
Rust prevention test	Pass	Pass
Copper strip corrosion	1b	1b
Extreme pressure oil oxidation	6.0% max. viscosity increase	6.0% max.viscosity increase
Foaming sequence I/II/III		75/10 all stages
Demulsibility characteristics of lubricating oils	80 mL free water 2.0% oil in water max. 1.0% emulsion max.	80 mL free water 2.0% oil in water max. 1.0% emulsion max.
Timken extreme pressure	60	
Four ball EP	250 kg	
Four ball wear	0.35 mm	
Four square gear oil tester	11	12

CONCLUSION

Why are ASTM specification tests used and who utilizes them? Additive and finished lubricant manufacturers utilize ASTM tests to aid in the development of new products. These laboratory tests can be run rapidly and give a general indication of field performance. Once a new product has been developed, more extensive tests are run both in the laboratory and the field to demonstrate actual performance. The use of ASTM tests is the first step in evaluating the performance of a lubricant.

OEMs utilize ASTM specification tests to set minimum standards for a lubricant to be used in their equipment. This is the initial step in eliminating inferior products and the end-user may void his warranty if the specified products are not used. Lubricants need to be compared on a level playing field. That is why ASTM tests are used, and they must be run under specified conditions to make meaningful comparisons between different lubricants.

End-users are faced with selecting the best lubricant from a large number of suppliers, which can be a difficult task. The true performance test is to run a highly controlled field test but before this happens, different lubricants need to be screened before a field test is conducted. This is accomplished by setting minimum specifications based on ASTM tests and having the lubricant suppliers adhere to these minimum standards.

There are many people who read product data sheets that have limited knowledge on how the tests were run and their significance to field performance. However, the more educated end-users and lubricant sales representatives are about these tests, the better off they will be in selecting the correct lubricant for a particular application. TLT

FEATURE ARTICLE

Jeanna Van Rensselar / Contributing Editor

Tribological Bearing Testing

KEY CONCEPTS

- With modern improvements in manufacturing, testing technology and care, bearing life has been extended 400 fold since the 1940s.
- The bearing fatigue limit incorporated into ISO Standard 281: 2007 is not universally accepted.
- Of the three bearing test categories, no one test is ideal.

Modern technology has improved (but not perfected) our ability to predict failure for these critically important components.

THE WORLD'S SMALLEST BEARINGS have an inner diameter of 0.5 mm, an outer diameter of 1.5 mm and a width of 0.65 mm (about the size of a pinhead). They are used in devices that require extreme precision on a nano scale, such as miniaturized medical devices and micro-motors.

At the other extreme, some bearings measure 18 meters on their outer diameter and weigh more than 15 tons. These are used in giant tunnel-boring machines.

In between are a multitude of machines that rely on the accuracy and durability of their bearings.

A space shuttle is propelled into orbit by two solid rocket motors and three liquid-fed main engines. After the solid motors fall away, the shuttle engines continue to run for eight minutes. During this time, low- and high-pressure turbo pumps inject the engines with fuel. A critical component of the turbo pump is the main shaft, which supports the drive turbine, pump inducer and impeller. During rotation, rolling element bearings hold the shaft in place. If the bearings were to fail, the shaft would move out of position, creating physical contact between the turbo pump components in a fuel-rich environment. The result could be catastrophic.[1]

According to STLE-fellow Erwin V. Zaretsky, P.E., Consulting Engineer, Distinguished Research Associate, NASA Glenn Research Center in Cleveland, Adjunct Professor of Engineering, Case Western Reserve University (one of the top practitioners in the field), the design and development of the space shuttle turbo pump bearings evolved over several decades. They were based on computer analysis, laboratory rig testing and static ground testing of the shuttle turbo pumps under simulated flight conditions. The bearing computer analysis alone could not predict with reasonable engineering certainty the endurance and failure characteristics of these bearings.

The most thorough test (application simulation) is too time-consuming and costly for most bearing manufacturers and OEMs. And some experts question the validity of computer simulation and bench tests that analyze bearings in isolation.

The condition that most often limits bearing function and longevity is rolling element fatigue and the most common predictability calculation of failure is L_{10} bearing life. This method was first proposed in 1924 by Swedish researcher Arvid Palmgren. The L_{10} bearing life (the point in hours or bearing inner-ring revolutions at or before, which 10 percent of the bearings in a group will have failed by rolling element fatigue), is based on Palmgren's observation that no bearings in a group run under the same conditions or fail at the same time.[2] In other words, bearing life is probabilistic or distributive, not deterministic.

Rolling element fatigue is a spall manifesting itself across the width of the running track and through to the depth of the maximum shearing stress beneath the contact surface. A spall can begin as a crack from a subsurface inclusion, defect or void below the contacting surface or from a crack emanating from a surface defect or a debris dent that spreads into a network of cracks.

L_{10} BEARING LIFE CALCULATION

The L_{10} rating life of a group of identical roller bearings is the number of revolutions that 90 percent of bearings in a group will complete or exceed before the first evidence of fatigue (the point at which exactly 10 percent of the bearings are showing signs of fatigue). L_{10} is calculated in terms of millions of revolutions or in terms of hours.

[1] **http://ntrs.nasa.gov/archive/nasa/casi.ntrs.nasa.gov/20100023061_2010023664.pdf.**

[2] Per E.V. Zaretsky, more specifically, the L_{10} life, in millions of inner-race revolutions, is the theoretical life that 90 percent of a bearing population should reach or exceed without failure at its operating load.

Ordinary Partnering	***Afton Partnering***
Interested	***Passionate***
Sharing	***Giving***
Cooperative	***Flexible***
Considerate	***Caring***
Understanding	***Collaborative***
Working together	***Embedded***
Connected	***Embracing***
Innovative	***Mold breaking***
Answers	***Solutions***

Rob Shama
President, Afton Chemical Corporation

Afton® CHEMICAL
Passion for Solutions®

For 90 to 95 percent of machine design applications, the recommendations in bearing manufacturers' catalogs lead to safe and reliable functioning. Remaining applications require specialized knowledge and analysis.[3]

Rolling element fatigue occurs in both bearing races and rolling elements. It is extremely variable but statistically predictable depending on such life factors as:

- Operating conditions
- The method of steel processing
- The method of bearing manufacture (including the heat treatment)
- The steel type
- The lubricant.

Fatigue failures that originate below the contacting surface (classic rolling element fatigue) are an inevitable result of age. But most bearings are removed for other reasons before this happens.

Failures other than those caused by age (rolling element fatigue) can be avoided as long as the bearing is not overloaded and is correctly designed, installed, lubricated and not subject to harsh operating conditions. With improvements in manufacturing, today's testing technology and care, bearing life has been extended appreciably.

The term *basic bearing life* refers to the L_{10} life without dependent life factors such as those listed above. Because the vast majority of undamaged bearings are removed from service for reasons other than the end of their calculated L_{10} life, it is cost-effective to inspect and place back into service those undamaged bearings that were removed before reaching their L_{10} life.

Per Zaretsky, probable causes for rolling element bearing removal and the approximate percent of failures include:

- Fatigue (surface and subsurface) (3 percent)
- Cage wear (3 percent)
- Wear (6 percent)
- Handling damage (7 percent)
- Dimensional discrepancies (17 percent)
- Debris denting/contamination (20 percent)
- Corrosion pitting (27 percent)
- Other (17 percent).

Other causes include true and false brinelling, misalignment, bearing overload, excessive thrust lubrication, roller-edge stress, electric arc discharge and cage element or ring fracture. While these causes can be mitigated, they can never be completely eliminated. This makes understanding and determining bearing life even more important.

BEARING TESTS

There are three basic types of bearing tests: application simulation, computer simulation and individual bearing tests in the lab. Each method has its pros and cons. Design engineers tasked with bearing acceptance testing need to determine which test(s) best satisfies their specific situation.

STLE-member Joe Braza, senior scientist for Lancer Systems in Allentown, Pa., explains, "For plain bearings, there are straightforward service life equations that can be used to predict the life of a bearing. These equations depend on a number of factors such as load, speed, lubrication, temperature, dimension (i.e., radial clearance) and material, including understanding the effect of contamination or seal design. In developing new plain bearing materials, these factors are not yet defined; therefore, bearing testing needs to occur before any type of bearing life formulas can be used."

Let's examine the three bearing-test categories.

Application Simulation. For some OEMs, there is no substitute for actual application simulation testing. During this type of analysis, bearings are tested in either a prototype or the actual assembly where they operate. For complex simulations, the bearing manufacturer and OEM may need to develop a formal test plan together. In some less-critical machinery, one way around application simulation is for the bearing manufacturer to supply bearings in mounted assemblies.

Application simulation tests ensure that the bearings will perform as specified in actual application operating conditions. While this is true, application simulation is very expensive in terms of time and dollars and yields comparatively paltry statistics.

Actual application testing is more important in some bearing applications than others—especially where there is no room for failure. Examples

ISO 281:2007

ISO 281:2007 specifies methods of calculating the basic dynamic load rating of roller bearings manufactured from high-quality hardened bearing steel. It also specifies the methods of calculating the basic rating life (L_{10}). In addition, ISO 281:2007 specifies methods of calculating the modified rating life; where lubrication condition, lubricant contamination, fatigue load of the bearing and other factors are taken into account. It does *not* cover the effects of wear, corrosion and electrical erosion on bearing life. ISO 281:2007 does not apply to designs where the rolling elements operate directly on a shaft or housing surface, unless that surface is equivalent in all respects to the bearing ring (or washer) raceway it replaces.

[3] Per E.V. Zaretsky, many engineers don't understand that the life they are calculating is not based on the point just before no failures will statistically occur but on the point at which 10 percent of the bearings are statistically expected to fail. This mistake can result in warranty and product liability claims for the OEM.

are wind turbines, where post-installation repairs are extremely costly; spacecraft, where repairs are either costly or impossible; and CT scanners where a noisy bearing makes the machine effectively unusable. Application testing makes sense just about any place where bearings are key to the proper functioning of critical equipment.

Actual bearing performance can stray from computer simulation predictions because of unknown load and mounting effects (incomplete input data) and variations in tolerances. While bearing inspections verify physical characteristics, they don't provide any information about performance characteristics like torque and effective operating tolerances. Application testing resolves these issues.

"Optimal testing should replicate the application as closely as possible in terms of load, speed, temperature, lubrication and environment," Braza says. "Besides closely simulating the application, the bearing tester should be designed with fixture flexibility to accommodate various test coupons, force transducers or measuring devices (load cells, thermocouples, speed sensors and accelerometers) and data acquisition system to provide information about the bearing performance—particularly in real-time."

Braza adds, "One word of caution. The majority of the time researchers design accelerated tests to speed up the process of obtaining bearing information quickly. The downfall of accelerated testing is that the bearing may fail by a different mechanism and not be representative of the actual service condition."

Computer Simulation. If performed carefully, computer simulation provides the answers to real-world functionality. It is a good alternative to bearing tests and application simulations where those costs would be prohibitive or the scale would be unwieldy or the logistics just too complex. Another good reason to opt for computer simulation is security.

But the accuracy of computer simulations depends on the validity of the simulation models and the consistency of the results. The simulation model should provide the same (or nearly the same) result for each execution. The process is much easier if the equations for simulation are already in place. Accurate calibration, verification and validation of simulation models are the keys to success. Tribologists are advised to understand these three factors.

1. Calibration. The base model's parameters should be specified and calibrated so that the model matches the ultimate application as closely as possible. Of the three types of errors that can affect calibration (input error, model error and parameter error), input error and parameter error can be remedied by the user. But since model error is rooted in the methodology, it requires more to fix. Another consideration is that simulation models can produce conflicting results if they are based on different modeling theories.

2. Verification. Once calibrated, the model must be verified to ensure that it is operating as expected based on the statistical input. Verification is achieved by comparing initial output data with what is expected from the input data. Basically it is an analysis of the output to see if it is reasonable. For example, in bearing simulation, the type and level of damage can be verified to ensure that it is reasonably close to what the researcher would expect, given the parameters.

3. Validation. Once the model has been verified, the final step is to validate it by statistically comparing the outputs to existing historical data. This establishes the model's ability to replicate reality. The process of validation highlights the importance of careful planning, thoroughness and accuracy during calibration and verification.

Computer simulations can be time- and money-saving substitutes for bearing tests and lab simulations, but in order to be relevant they must accurately model the intended use. Unless these techniques are employed, the accuracy of the model will always be open to question.

"No matter how good the bearing computer analysis is, the successful operation of the system is dependent on the boundary conditions and assumptions that are inserted into the computer analysis," Zaretsky says. "The difference in performance between the predicted and the experimental results can mean the difference between a successful product and a financial disaster."

'The downfall of accelerated testing is that the bearing may fail by a different mechanism and not be representative of the actual service condition.'

He continues, "In the last four decades, bearing modeling and analysis based on theoretical analysis has become very sophisticated and reasonably accurate in predicting bearing performance, life and reliability based on classical rolling element fatigue. There are 26 variables that can affect rolling element fatigue.[4] However, some of these variables are not necessarily susceptible to accurate analysis. As a result, testing rather than computer analysis may be a condition precedent for reliable bearing operation for some critical applications."

Bearing Tests in the Lab. STLE-member Harvey Nixon, senior technologist, bearings, for Meritor Heavy Vehicle Systems in Troy, Mich., says, "Laboratory testing plays a rather large role in determining the design and manufacturing capability of the supplier. Such testing is done at both the component level (individual bearings) and in the intended application positions."

Napoleon Engineering Services (NES) in St. Olean, N.Y., operates the largest independent bearing test facility in the U.S. Its bearing test lab programs focus on three main aspects of testing: life (dynamic), environmental and impact/static testing.

Life (dynamic)Testing. For OEMs, laboratory bearing life testing is performed as a means of comparing the performance of multiple suppliers. The most cost-effective method is via the standard bearing test (SBT) for validation of bearing design, material quality, manufacturing capability and overall workmanship quality. An SBT is performed without significant input on application conditions.

Considerations include application loads, speeds and lubricant conditions, but the test is accelerated to shorten overall test time—with considerable effort to maintain a failure mode common to the application. The tester runs the bearings to the point of failure, using classical or sudden-death testing methods. This yields relatively large quantities of data.

The lab generates a Weibull plot from the failure times (or failure and suspension times), and the result is an empirically derived supplier reliability metric. The addition of upper and lower confidence boundaries establishes the anticipated variability within a supplier's population. When results between suppliers are compared, they provide a valuable understanding of relative performance differences. Lab testing of a baseline bearing supplier with known application experience allows an OEM to predict expected bearing life in an application from a new supplier.

Although SBT is the most common and cost-effective bearing test, it is also possible to perform theoretical application simulation (TAS) in the lab. The difference between TAS and SBT is that TAS test conditions are application-driven. Bearing loads and speeds are representative of how a bearing will perform within a particular application. Duty-cycle testing falls into this category. As a result, TAS tests often take longer to reach failure or are run only to a suspension point. The testing benefit to the OEM is the knowledge and confidence that they have tested the bearing under simulated real-life performance conditions. However, results are based on a smaller data subset.

Dynamic lab testing can have the added benefit of yielding additional test results without significantly influencing a test budget and lead time. Examples include:

- Supplier life adjustment factors
- Catalog load rating validation
- Bearing efficiency comparison – torque and temperature
- Weakest link failure mode – due to design or quality of workmanship
- Model correlation
- Material/process validation.

Environmental Testing. When primary bearing failure is due to external contamination (rather than pure fatigue failure), the ability of the seal to withstand contamination intrusion becomes paramount. Environmental lab tests that use mud slurry, water spray and fine particle dust are the tests of choice because of their relatively short runtimes and ability to replicate harsh operating environments. The end re-

[4] Articulated the book that Zaretsky co-authored and edited, *Life Factors for Rolling Bearings, 2nd Edition*, STLE (1997).

sult is significant time savings over application-style field testing for comparing seal efficiency.[5]

Impact/Static Load Testing. Due to the increase in the global supply of through-hardened bearing materials, over case-carburized steel in tapered roller bearings (TRB) and mast guide bearings, impact and static load lab testing is on the rise. Such testing provides information on cone rib flange resistance to fracture on TRBs and true-brinelling indentation depth for mast guide bearings. Simple test fixtures can create extreme load and impact conditions without requirements for full application accessories to create the failure condition.

By using test rigs and test parameters with relatively short test times and lower costs, standard bearing testing examines operational differences between suppliers or designs. But it does not take intended application conditions into consideration.

Nixon explains, "Bench testing of the individual bearings is used most often for validation after the bearing samples have met all the initial scrutiny in the multistep evaluation process. Bench testing can be less expensive than full-scale application testing, and more bearing samples can be evaluated in less time. The more test data, the better the reliability of the conclusions about the performance capability of the bearing products. By necessity, the loading is higher in order to accelerate the testing. It is then important to compare the results to the life performance prediction model and compare it to a known validated supplier performance baseline (the existing production supply base, i.e., comparative testing of two suppliers).

WHEN TO TEST

Bearing tests are necessary when the proper functioning of a critical or costly machine depends on the bearing. While catalog data is sufficient for the majority of applications, it only describes the estimated performance characteristics of bearings. In reality, the performance strays from catalogue stats for reasons that include operating conditions like load, tolerance and mounting configuration. It's difficult to predict exactly how a bearing will perform until it is assembled and mounted. Testing determines key performance characteristics and whether the bearing can even meet application requirements. Testing makes sense when:

- The equipment must be reliable
- In-service repair is extremely difficult or impossible
- The equipment is expensive
- The equipment is critical to operations
- Equipment failure could result in injury or death
- Certification is required; for example to maintain the warranty.

"At Lancer Systems, we developed a ceramic matrix composite material to replace silicon carbide bearings for fluid film plain bearings," Braza says. "During the development, it was im-

THE WEIBULL PLOT[6]

The Weibull plot is a graphical technique for determining if a dataset comes from a population that would work with a 2-parameter Weibull distribution (one of the most widely used lifetime distributions in reliability engineering). The Weibull Plot has scales that are designed so that the points will be linear (or nearly linear) as long as the dataset follows a Weibull distribution.

The least squares fit of this line yields estimates for the shape and scale parameters of the Weibull distribution. The shape parameter is the reciprocal of the slope of the fitted line and the scale parameter is the exponent of the intercept of the fitted line.

The Weibull distribution also has the property that the scale parameter falls at the 63.2 percent point regardless of the shape parameter value. The plot shows a horizontal line at this 63.2 percent point and a vertical line where the horizontal line intersects the least squares fitted line. This vertical line shows the value of scale parameter.

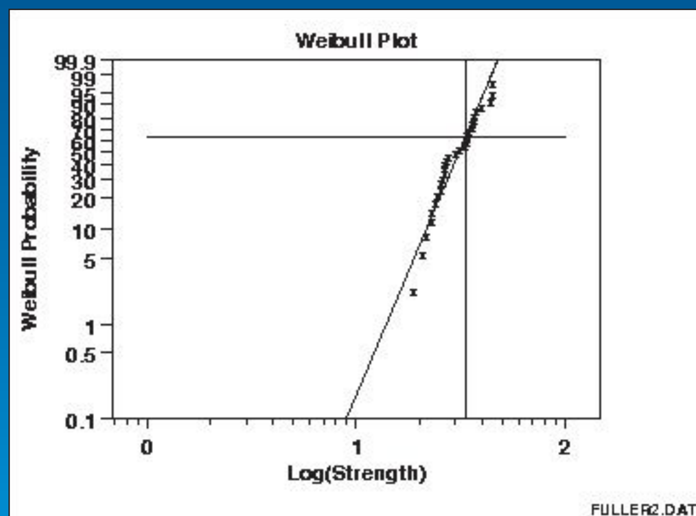

[5] Most environmental testing is performed in an A-B comparison format.

[6] **http://www.itl.nist.gov/div898/handbook/eda/section3/weibplot.htm.**

perative to generate technical data regarding the performance of the material as fluid film bearing in order to convince our customers to use this material in their pumps. The pump design engineers needed an understanding of the material as a bearing, particularly its pressure velocity limitation, chemical resistance and dry-run capabilities."

TESTING VS. ISO 281 L_{10}

Bearing tests and standards have been the source of confusion and controversy for decades. Rolling element bearing fatigue life calculations for most industrial and machine applications are dictated in the U.S. by ANSI/ABMA Standard 9 for ball bearings and ANSI/ABMA Standard 11 for roller bearings.

Outside of the U.S., both ball and roller bearing fatigue life is dictated by ISO Standard 281: 2007, which incorporates a fatigue limit into its L_{10} bearing life calculation. It is hotly disputed by bearing experts that include Zaretsky. He and others are certain that no true fatigue limit for a bearing has ever been established and that existing data does not support the establishment of a fatigue limit.

Zaretsky explains, "What can happen when using the ISO Standard 281: 2007 is that the life of a rolling element bearing can be over-predicted for a specific application. Since the bearing life that is predicted is greater than that which may be required, the bearing size is reduced as well as the bearing acquisition cost. This can result in an undersized bearing for the application and early bearing failure. Then there is the matter of warranty and liability issues when the bearing or bearings do not perform as predicted for the application."

He continues, "It's important to distinguish between the rolling element bearing's service life and the bearing's L_{10} fatigue life. Bearing service life can be defined as the time a bearing is removed from service for any cause. The bearing's theoretical life analysis is based, for the most part, on the L_{10} fatigue life. It is my opinion that, with some exceptions, bearing (L_{10}) fatigue life analysis is no longer theoretical but experimentally established with reasonable engineering and statistical certainty."

Zaretsky adds that rolling element bearing (service) life, whether based on fatigue or other failure mode, is probabilistic and not deterministic. It is not a calculation of the absolute value of a bearing's operating time but, rather, the probability that a specific bearing operating under well-defined conditions will equal or exceed a calculated operating time based upon a defined failure mode.

If performed carefully, computer simulation provides the answers to real-world functionality.

"There is a conundrum associated with bearing fatigue life calculations and bearing service life," Zaretsky says. "If a bearing is properly designed, installed, lubricated and maintained, it should theoretically fail by classical rolling element fatigue. However, probably less than 5 percent of bearings removed from service are removed because of rolling element fatigue. This means that the probable cause for bearing removal for most applications is not rolling element fatigue (which is the basis for the ANSI/ABMA and ISO standards). The cause for removal and thus the bearing service life depends on the bearing application."

Zaretsky concludes that ISO 281:2007 does not provide a valid representation of actual bearing life in real-world application conditions.

Nixon adds, "ISO and ABMA standards rely on the assumption that proper bearing quality steels and adequate internal geometric design have been incorporated to give the standard catalog performance-rating placed on the product. But improper internal geometry and inadequate steel performance can negate the load rating established by the rating equations."

IN THE END

"Any company that purchases and uses bearings in their equipment should do adequate testing to validate the bearing supplier's products," Nixon says. "It is, however, just as important to validate the supplier's capability to produce the product to the same specifications on an ongoing basis. Most suppliers can provide acceptable prototype samples but may not be able to maintain specifications in series production. Therefore, scrutiny of the supplier's quality systems and their manufacturing processes along with supply base is just as important."

Reliable bearings are essential for many applications, including space development. For example, satellites have a flywheel to maintain them in the correct position and orientation. Some satellites, along with their flywheels' ultra-high-precision bearings, have been operating seamlessly in space for more than 15 years.

The accuracy of any bearing-equipped machinery is determined by the accuracy of its bearings' revolution. For example, the deflection from the central axis of a computer's hard disk drive (which uses ultra-high precision bearings) is less than 100 nanometers (100 billionths of a meter).

This points not only to the necessity for performing tests but choosing the correct test and carefully analyzing the data. While bearing tests have improved markedly during the past 60 years, the challenge to improve bearing life through testing remains. TLT

Jeanna Van Rensselar heads her own communications firm, Smart PR Communications, in Naperville, Ill. You can reach her at ***jeanna@smartprcommunications.com.***

 Despite the term vernal equinox, the day when there are 12 equal hours of daylight and darkness usually happens before the first day of spring.

PEER-REVIEWED

Cage Friction in High-Speed Spindle Bearings

Christian Brecher, Alexander Hassis, and Jens Rossaint
Laboratory for Machine Tools and Production Engineering (WZL) of RWTH Aachen University
52074 Aachen, Germany

Manuscript received Jan. 14, 2013
Manuscript accepted Sept. 5, 2013
Review led by Vasilios Bakolas

Editor's Note: The introduction of the bearing greatly reduced the amount of energy lost due to friction in rotating components. Over time, better design and better lubricants have continued to improve efficiency; however friction-induced heat remains a limiting factor in high-speed applications. This month's Editor's Choice paper highlights the importance in factoring the influence of the cage friction when estimating the overall bearing friction. Deriving a better calculation model will aid design improvement, resulting in a further reduction in friction to allow for use in a wider range of applications.

Evan Zabawski, CLS
Editor

KEYWORDS

Cage Friction; Spindle Bearings; High Speed Bearings; Friction Calculation; Cage Optimization

ABSTRACT

Friction-induced heat is one of the main reasons for the upper speed limit of high-speed angular contact ball bearings (spindle bearings). One source of friction inside the bearing is the cage. In this article, it is shown through experimental results that the frictional losses due to the cage are of significant magnitude. Based on measurements, a new, simple calculation model is proposed to estimate the cage induced frictional losses in spindle bearings under high rotational speed with minimal lubrication. The cage is assumed to rotate eccentrically around the bearing's axis and to be in contact with the outer ring at just one position. One single ball at the same position is assumed to drive the cage. Thereby, the friction between the cage and the outer ring is transformed in a breaking torque for the inner ring and the shaft. Both the cage outer ring contact and the ball cage contact are handled according to Coulomb's law of friction. Despite its simplicity, this model shows a close correlation with experimental results. Consideration of the centrifugal and thermal expansion provides insight into the relation between cage clearance and cage friction and hence allows for the development of new cage designs. Finally, the design and experimental results of optimized cages made of polyether ether ketone (PEEK) are presented.

INTRODUCTION

Angular contact ball bearings (spindle bearings) that are used in machine tool main spindles play a key role in determining the spindle performance. In high-speed applications, friction-induced heating of the bearings is one of the main factors limiting the operational speeds. According to Townsend, et al. *(1)* and Harris and Kotzalas *(2)* there are five major sources of friction in high-speed angular contact ball bearings: Spinning torque between the balls and the raceway is the result of the tilted rolling axis of the balls. Due to the curvature of the raceways, the contact area is divided into three segments: One of them is characterized by backward sliding and two by forward sliding, resulting in rolling friction. Houpert *(3)*, *(4)* points out that these hydrodynamic rolling losses may not be neglected in ball bearings because they are a contribution to friction that does not occur in bearings featuring line contact between the rollers and the raceway. Houpert *(3)* described how the size and location of the three different zones can be calcu-

Nomenclature

ax	= Axial
c	= Correction factor for centrifugal expansion of weakened ring
D	= Ball diameter
d	= Diameter
d_m	= Bearing pitch diameter
E	= Young modulus
F	= Force
F_{ax}	= Axial bearing load
F_c	= Centrifugal force
F_f	= Friction force between two bodies
F_n	= Normal force between two bodies
l	= Length
m	= Mass
n	= Rotational speed
T	= Overall torque
T_B	= Ball-induced friction torque
T_C	= Cage-induced friction torque
Z	= Number of balls
α	= Thermal expansion coefficient
ε	= Relative cage eccentricity
$\Delta\vartheta$	= Change in absolute temperature
μ	= Coulomb friction coefficient
ν	= Poisson's rate
ρ	= Density
ω	= Angular velocity

Subscripts and Superscripts

B	= Ball
C	= Cage
CP	= Cage pocket
$guide$	= Guiding land
IR	= Inner ring
i	= Inner
OR	= Outer ring
o	= Outer
$therm$	= Thermal
$\ldots'$	= Value under operating condition
0	= Nominal value
1, 2	= Counting index

lated. Additionally, Biboulet and Houpert *(5)*, *(6)* show that the hydrodynamic rolling friction depends on the lubrication regime in the lubrication gap and that the transition between these regimes and the shape, size, and possible truncation of the contact zones are major difficulties in calculating this friction. In particular, for nearly round point contacts found in lightly loaded ball bearings, Poiseuille currents in the lubricant gap vertical to the rolling direction account for a not negligible part of the overall hydrodynamic rolling losses (Biboulet and Houpert *(6)*). The elastic deformation of the balls and the raceways causes hysteresis losses, which are usually very small compared to other losses (Houpert *(3)*). Squeeze out of lubricant from the raceways by the rolling balls causes churning friction. Last, the interaction of the cage with the rolling elements, the outer ring, and the lubricant contributes to the overall bearing friction. For bearings operating under high speeds, churning losses due to the friction between rotating bearing elements and the lubricant air flow in the bearing might be substantial.

Brecher, et al. *(7)* introduced a new method for calculating the overall frictional losses in high-speed spindle bearings due to relative motions in the contact ellipses (i.e., spinning and rolling friction). By assuming that the balls have 6 degrees of freedom, the equilibrium of torques and forces acting on the balls can be calculated. The zones of the Hertzian contacts between the balls and the raceways are divided into a discrete number of rectangles. With the contact forces provided by the force and torque equilibriums and the calculation of local friction coefficients, the overall frictional forces on every ball can be obtained. Two major challenges using this model are the determination of the exact kinematic conditions of the balls under high rotational speeds and the local coefficients of friction.

Another difficulty associated with the evaluation of frictional losses in spindle bearings is the calculation of the cage friction. The cage is designed to maintain a certain radial clearance between its guiding land and the outer ring to prevent jamming under thermal and centrifugal expansion. This causes an eccentric run-out of the cage regarding the bearing's axis.

In general, there are several theories about cage friction in bearings. One approach, mostly used for standard oil-lubricated bearings, is to assume that the radial space between the cage and the outer ring is completely filled with oil. Thus, the cage outer ring friction can be calculated using hydrodynamic short bearing theory (Harris and Kotzalas *(2)*). For high-speed spindle bearings running under minimum quantity lubrication, cage friction is often considered to be negligible (Steinert *(8)*).

In more sophisticated approaches, Houpert *(9)*, for example, uses advanced computational methods to calculate the forces between the cage and the rollers under consideration of the tribological conditions to determine the cage behavior. Brown and Foster *(10)*, *(11)* use the ADORE (Advanced Dynamics of Rolling Elements) package to simulate all forces inside a bearing in order to investigate the effects of different cage materials on the cage and bearing behavior.

In the field of cage design, Pederson, et al. *(12)* use a cage model consisting of lumped masses connected by springs and dampers to simulate the effects of ball-to-cage pocket clearance and cage stiffness on the operational behavior of ball guided steel cages. By various experiments, Sathyan, et al. *(13)* showed that the size and shape of the cage pocket geometry as well as the design of the cage guiding land can have a significant influence on the cage frictional moment and the stable operation of the cage.

As shown in this article, neglecting the cage friction would lead to underestimations of the overall frictional losses un-

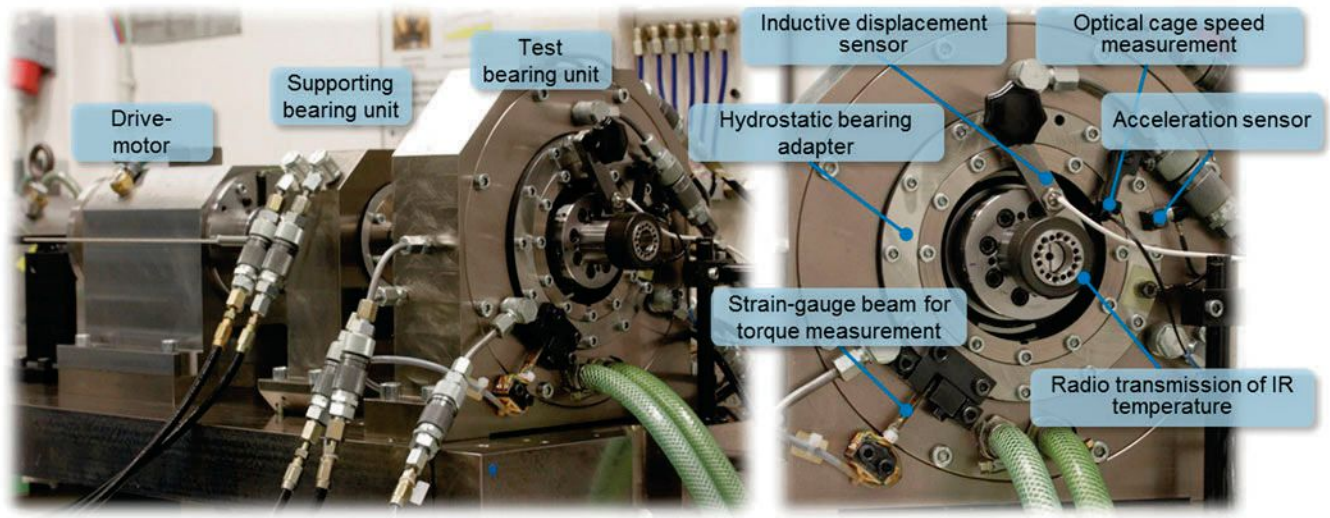

Figure 1 | **Hydrostatic bearing test rig with sensor equipment.**

der high rotational speeds. In contrast, it is obvious that the assumption of a fully flooded cage outer ring contact zone is not valid for spindle bearings running under minimum quantity lubrication (i.e., oil and air/grease lubrication). For basic estimations of cage friction, multibody simulations and other highly advanced simulation techniques are unsuitable due to their high modeling and calculation efforts.

One major goal in the development of spindle bearings is the realization of higher rotational speeds. Because the friction-induced heating will increase considerably with the rotational speed, efforts are necessary to reduce frictional losses. The first step toward the reduction of the overall friction of a bearing is the identification and quantification of the different sources of friction. As described above, the existing methods to determine cage-induced friction in spindle bearings do not yield satisfying results with reasonable efforts. It is therefore the aim of this article to measure cage friction in spindle bearings under high rotational speeds and introduce a simple calculation model. The proposed model considers the frictional forces between the cage and the outer ring due to the centrifugal forces arising from the eccentric rotation of the cage. In this model, the balls are incorporated as a source of friction in the cage pockets. Additionally, they transform the cage outer ring friction force into a breaking torque for the inner ring and thereby into a part of the overall frictional torque of the bearing. Experiments with several standard cages and new cages with a polygonal outer surface are presented.

MATERIAL AND METHODS

To evaluate the influence of cage friction on total bearing friction, two hybrid spindle bearings with six different cages were investigated on a high-speed spindle bearing test rig.

The spindle bearing test rig shown in Figure 1 features a synchronous servo motor driving the main spindle. The main spindle is supported by a smaller support bearing and a test bearing in a back-to-back arrangement. The support bearing acts as the floating bearing. Via its outer ring, an adjustable, precisely controlled axial preload is induced into the system. Due to the separate housings for the support bearing and the test bearing, the thermal interference between the two bearings is minimized. The test bearing's outer ring is mounted in the bushing of an axial and radial hydrostatic bearing. This ensures an almost frictionless and yet stiff and accurate support of the bearing. A strain-gauge beam is used as the only torque support for the bushing. Thereby, the frictional torque of the test bearing can be determined. In addition to the torque measurements, the test rig features measurements of the inner and outer ring temperature of the test bearing as well as its axial displacement of the inner ring relative to the outer ring. Additionally, sensors for the determination of the cage speed and the measurement of vibrations can be applied.

TABLE 1—TEST BEARINGS

	SB1	SB2
Contact angle[a] (%)	21	23
Osculation IR (%)	9	9.3
Osculation OR (%)	6	4.7
Ball diameter (mm)	9.525	12.7
Number of balls	24	18

[a]Values in mounted condition.

As shown in Table 1, the test bearings (SB1, SB2) are two different hybrid bearings with ball diameters of 9.525 and 12.7 mm, respectively, and nominal contact angles of 21 and 23° in a mounted condition. The cages summarized in Table 2 are made from polyether ether ketone (PEEK) and fiber-reinforced phenol formaldehyde resin (PH resin), respectively.

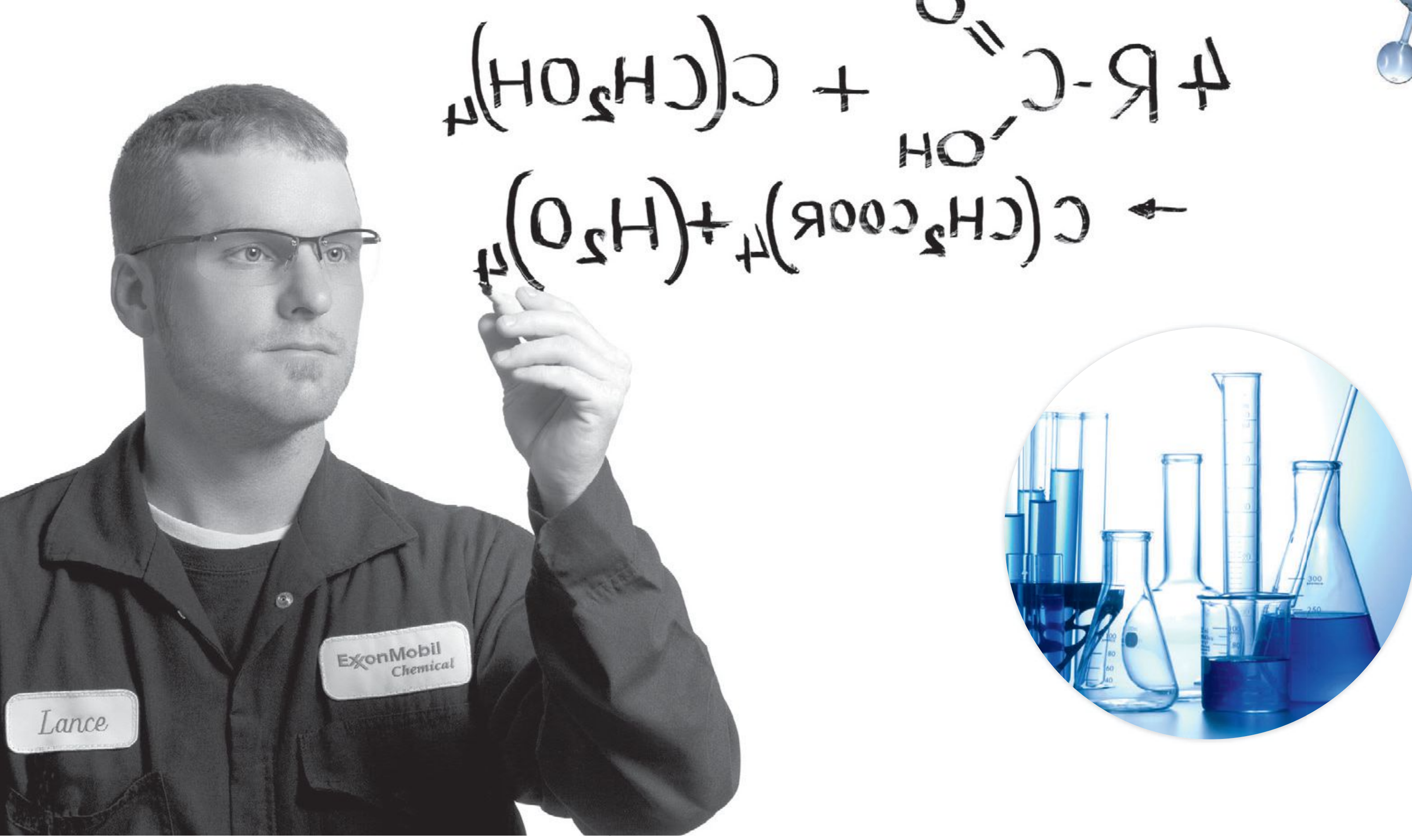

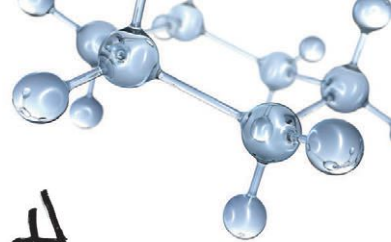

supplying the world with innovation

It starts with our people—with the leading research and development teams in the field. At ExxonMobil Chemical, it comes down to our tireless commitment to innovation that drives us to do more for our customers. That's why we've developed a diverse portfolio of low- and high-viscosity polyalphaolefins (PAOs), metallocene-polyalphaolefins (mPAOs), alkylated naphthalenes and esters that open the door to a broad range of solutions. Whether it's working to help solve your latest formulation challenge or meeting changing specifications, everything we do is part of our ongoing investment to supply the world with innovation. Start your next formulation with the global leaders of synthetic lubricant base stocks. Talk to our people, and find out how we can help make your next formulation a success.

Synesstic™ AN

Esterex™ Esters

SpectraSyn Elite™

SpectraSyn™

exxonmobilsynthetics.com

ADVANCED SYNTHETIC BASE STOCKS | *Innovative lubricants start here*

ExxonMobil Chemical

TABLE 2—MATERIAL AND DIMENSIONS OF THE TEST CAGES

	1Std1	2Std1	2Std2	2Std3	2Mod1	2Mod2	2Mod3
Designed for bearing	SB1	SB2	SB2	SB2	SB2	SB2	SB2
Material	PEEK	PEEK	PEEK	PH resin	PEEK	PEEK	PEEK
Radial bord clearance (20°C) (mm)	0.5	0.6	0.275	0.6	0.55	0.35	0.25
Bord form	Cylindrical	Cylindrical	Cylindrical	Cylindrical	Polygon	Polygon	Polygon
Pocket clearance (mm)	0.475	0.35	0.35	0.5	0.35	0.35	0.35
Pocket form	Spherical	Spherical	Spherical	Cylindrical	Spherical	Spherical	Spherical

The cage pockets are either of cylindrical or spherical shape. Cages with different outer diameters were used to investigate the influence of the radial clearance between the cage and the outer ring on cage friction.

To prevent jamming of the cage due to its thermal and centrifugal expansion at high rotational speeds and to allow for the design of small radial clearances at the same time, the cage expansion has to be reduced. For this purpose, a newly designed cage concept as shown in Figure 2 and described in

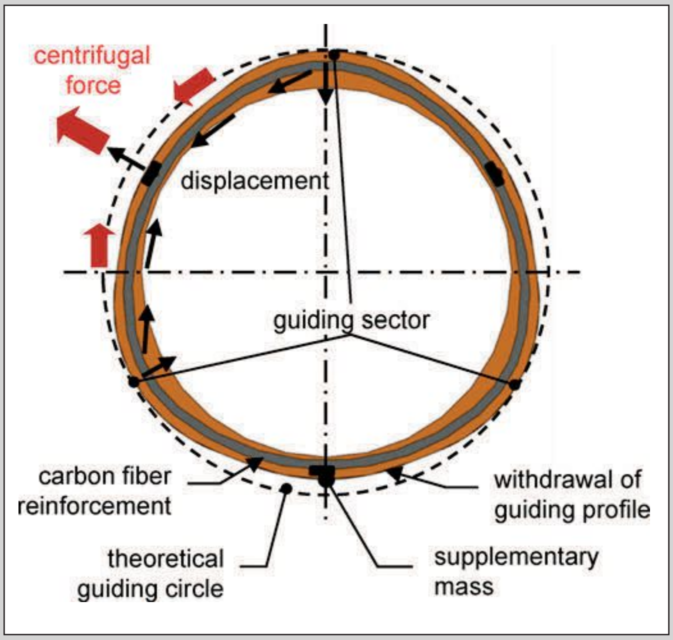

Figure 2 | **Concept of cage with expansion compensation.**

Rossaint *(14)* was invented. For most of the circumference, the outer surface is withdrawn from its original diameter. In three equally distributed areas, the outer diameter remains unaltered. These guiding sectors are the areas were the cage can come into contact with the outer ring guiding land. At higher rotational speeds, additional weights located centered between the guiding sectors will be drawn further to the outside than the pure PEEK areas due to centrifugal forces. The carbon fibers in the circumferential groove cause a tension and tangential movement between two guiding sectors. This movement draws the guiding sectors inwards. Thus, at high rotational speeds the outer surface of the cage deforms toward the shape of a circle. Furthermore, the carbon fiber reinforcement reduces the overall centrifugal and thermal expansion of the PEEK cage. Due to the smaller or even prevented radial expansion of the cage's guiding sectors, smaller radial clearances than in standard cages can be realized without facing the danger of jamming. As it will be shown in the following, this is supposed to have positive effects on the cage-induced friction. Three different prototypes (2Mod1, 2Mod2, 2Mod3) were manufactured from PEEK with spherical cage pockets as described in Table 2.

To determine the load- and speed-dependent bearing friction, torque runs were performed on SB1. While the rotational speed remains constant, the axial load is increased from 350 to 2,750 N. This procedure is automatically performed for different rotational speeds, which yields the operational behavior of the bearing over the total load-speed range. To evaluate the influence of the cage design on resulting bearing friction and hence inner and outer ring temperatures in continuous operation, step runs were executed with SB2, equipped with six different cages, under identical conditions. During these runs the rotational speed of the bearing is increased stepwise every 30 min up to 30,000 rpm while the axial preload remains constant at 1,250 N. All tests were carried out using oil and air lubrication with 120 μl/h of a synthetic ISOVG 68 oil.

In order to determine the cage friction from measurements of the total torque, the following assumptions are made: The total bearing friction T is assumed to consist of a cage-induced T_C and a ball-induced T_B part. The cage friction is assumed to be independent of the number of balls Z and the axial bearing load F_{ax}. The ball-induced friction is the sum of the friction values of the single balls. For pure axial load and therefore equal load distribution among the balls, every ball contributes the same share of friction, which mainly depends on the load per ball and the rotational speed n. With these assumptions, Eq. [1] can be established:

$$T(F_{ax}, n) = T_C(n) + Z \cdot T_B\left(\frac{F_{ax}}{Z}, n\right). \quad [1]$$

From two measurements with a different number of balls and the same load per ball, a set of values for Z and T according to Eq. [1] can be used to determine T_C and T_B. This means that the operating conditions for a single ball remain

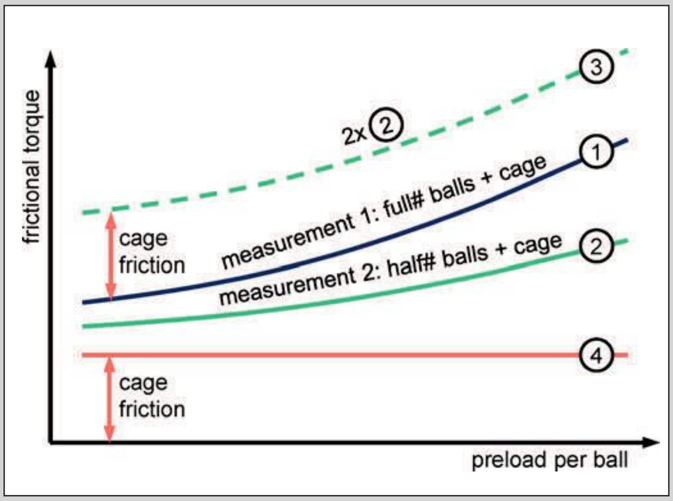

Figure 3 | **Experimental cage friction identification.**

the same in both measurements and hence the ball-induced torque per ball. As long as the cage's and the ball's contributions to total torque are independent of each other, it is not necessary to know the exact influences on ball and cage torque because these influences are the same in both measurements. The measured cage torque is a result of a relative comparison between two measurements under the same conditions for the cage and each single ball.

This procedure is illustrated in Figure 3 for two torque runs, one with the full number of balls (curve 1) and one with half of the balls and half the preload to keep the load per ball constant (curve 2). Subtracting curve 1 from two times curve 2 (curve 3) yields the cage friction (curve 4).

Figure 4 shows the overall frictional torque of the test bearing SB1 with the full number of balls (24) as an example. The same measurements have been done for this bearing

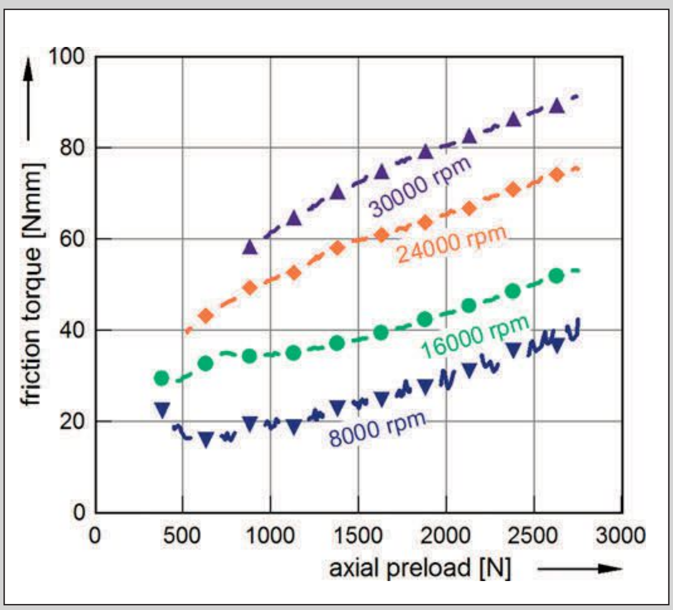

Figure 4 | **Total bearing friction at various loads and speeds.**

with half the number of balls (12) and half the axial preload range. By comparing the measurement curves, the cage friction can be determined for the different speeds and also for different loads per ball. According to the assumptions made, the latter should not have any influence on cage torque.

THEORY AND CALCULATIONS

In general, cages for spindle bearings are designed as outer ring land guided cages. To allow for an analytical solution, the following theory applies to cages with outer ring guidance only. However, under certain operating conditions, partial ball guidance regimes may occur that can only be described using multi-body simulation tools.

As displayed in Figure 5, the cage is thought to contact the outer ring at one single spot. To simplify the analytical calculation, it is assumed that just one ball is in contact with the cage and thereby transfers forces between the cage and the inner and outer ring. This ball is imaginarily located at the angular position were the cage contacts the outer ring. The cage rotates about the bearing axis with its center being eccentrically dislocated from the bearing axis. The maximum eccentricity can be obtained from the difference between the cage outer diameter and the outer ring guiding land inner

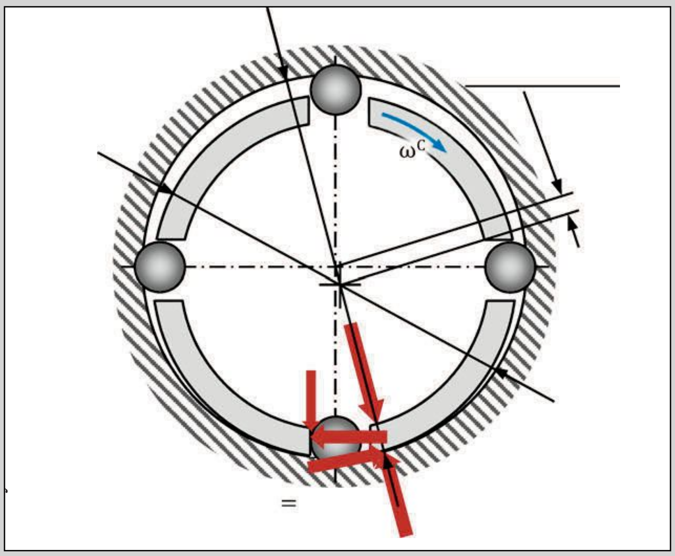

Figure 5 | **Geometrical relations and forces between ball, cage, and outer ring.**

diameter. By the introduction of the eccentricity parameter ε, ranging from 0 to 1, a possible oil film between the cage and the outer ring is considered as a factor reducing the effective eccentricity. Due to the cage's mass, eccentricity, and rotational speed it is pressed against the outer ring guiding land with the centrifugal force F_c^C (Eq. [2]). According to Coulomb's law of friction, the resulting friction force $F_f^{C\text{–}OR}$ can be calculated with the friction coefficient $\mu^{C\text{–}OR}$ (Eq. [3]). This force is equal by magnitude to the normal force $F_n^{B\text{–}CP}$ in the contact between the cage pocket and the ball driving the cage.

$$F_c^C = \frac{d_{guide}^{OR'} - d_{guide}^{C'}}{2} \cdot \varepsilon \cdot \omega^{C)2} \cdot m^C \quad [2]$$

$$F_f^{C-OR} = F_n^{C-OR} \cdot \mu^{C-OR}. \quad [3]$$

Considering the contribution of the friction force in the cage pocket F_f^{B-CP} and its self-reinforcing effect, the contact force between the cage and the outer ring can be calculated from Eq. [4]:

$$F_n^{C-OR} = F_c^C + F_f^{B-CP} = F_c^C + F_n^{B-CP} \cdot \mu^{B-CP}. \quad [4]$$

In steady-state operating conditions the cage speed remains the same. Thus, the sum of torques acting on the cage has to be zero. From this formulation in Eq. [5] the normal force between the ball and cage pocket F_n^{B-CP} can be obtained from Eq. [6] using Eqs. [2]–[4].

$$\sum T_{ax}^C = 0 = F_f^{C-OR} \cdot \frac{d_{guide}^{OR'}}{2} - F_n^{B-CP} \cdot \frac{\mathrm{d}_m}{2} + F_f^{B-CP} \cdot \frac{\mathrm{D}}{2} \quad [5]$$

$$F_n^{B-CP} = F_c^C \cdot \frac{\mu^{C-OR} \cdot d_{guide}^{OR'}}{\mathrm{d}_m - \mu^{C-OR} \cdot \mu^{B-CP} \cdot d_{guide}^{OR'} - \mu^{B-CP} \cdot D}. \quad [6]$$

Figure 6 shows the forces and torques acting on the ball as well as the bearing inner geometry. The cage-induced normal force F_n^{B-CP}, acting on the ball, has to be counterbalanced by the frictional forces between the ball and the inner and outer raceway (Eq. [7]).

Additionally, the sum of torques acting on the ball driving the cage in the direction of the bearings axis has to be zero, which is expressed through Eq. [7]. The same is valid for the sum of forces in the rolling direction (Eq. [8]).

$$\sum F^B = 0 = -F_{f,C}^{B-OR} + F_n^{B-CP} - F_{f,C}^{B-IR} \quad [7]$$

$$\sum T_{ax}^B = 0 = -F_{f,C}^{B-OR} \cdot l_1 + F_{f,C}^{B-IR} \cdot l_2 - F_f^{B-CP} \cdot \frac{\mathrm{D}}{2}. \quad [8]$$

Under common operating conditions, the distances $l1$ and $l2$ are about the same size. Assuming that $l_1 \approx l_2 \approx \frac{D}{2}$, the friction force acting on the inner ring due to cage friction can be obtained from Eqs. [7] and [8], resulting in Eq. [9]. This friction force causes the total bearing friction rise as defined by Eq. [10].

$$F_{f,C}^{B-IR} = F_n^{B-CP} \cdot \frac{(1 + \mu^{B-CP})}{2} \quad [9]$$

$$T_{f,C}^{IR} = F_{f,C}^{B-IR} \cdot \left(\frac{\mathrm{d}_m}{2} + \frac{\mathrm{D}}{2}\right). \quad [10]$$

The same results would be obtained by calculating the outer ring torque.

Changes in the cage and outer ring diameter caused by thermal and/or centrifugal effects have a nonnegligible effect on the cage eccentricity and are taken into account by Eqs. [11] and [12].

$$d_{guide}^{C'} = d_{guide}^C + \cdot \Delta d_{therm}^C + \cdot \Delta d_c^C \quad [11]$$

$$d_{guide}^{OR'} = d_{guide}^{OR} + \cdot \Delta d_{therm}^{OR}. \quad [12]$$

According to Beitz and Küttner *(15)*, the expansion of a ring due to centrifugal forces can be calculated using Eq. [13]. The correction factor *c* takes into account the weakening of the cage due to the pockets. Finite element simulations returned a radial expansion of the cage that is approximately 50% larger than that of a narrower ring, representing the width of the unweakened circumferential areas of the cage. Equation [14] yields the thermal expansion for both the cage and the outer ring.

$$\Delta d_c = \frac{\rho \cdot c \cdot \omega^2}{E} \cdot \frac{d_{o,0}}{2} \left(\frac{3+\nu}{4} \cdot \left(\frac{d_{i,0}}{2}\right)^2 + \frac{1-\nu}{4} \cdot \left(\frac{d_{o,0}}{2}\right)^2 \right)$$

$$\text{with} \quad c \approx 1.5 \quad [13]$$

$$\Delta d_{therm} = d_0 \cdot \Delta\vartheta \cdot \alpha. \quad [14]$$

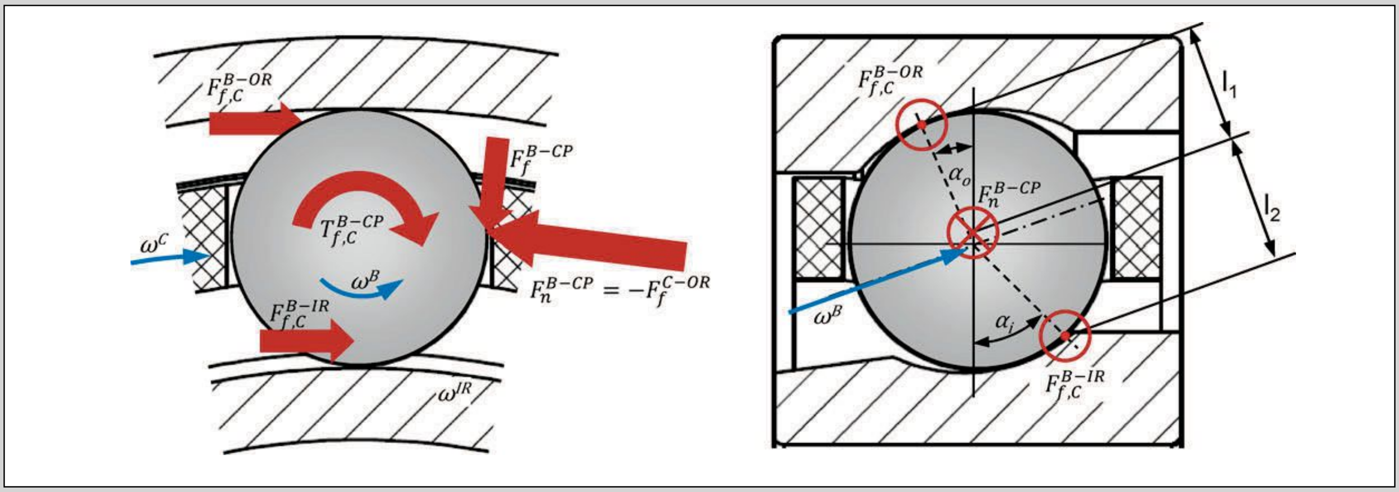

Figure 6 | **Forces acting on the ball driving the cage.**

The considerations concerning cage friction show that a reduced clearance between the cage and the outer ring will result in a lower possible eccentricity of the cage and thereby reduce the normal contact forces in the cage ring contact and thus the frictional forces. However, the thermal and centrifugal expansion makes cages with small radial clearances more prone to bearing failure due to the cage contacting the outer ring at the whole circumference and thereby being blocked and destroyed. This led to the development of the above-described cage with expansion compensation.

EXPERIMENTAL RESULTS

Using the method described above, the effective cage friction of SB1 with the PEEK cage and spherical cage pockets was determined according to Eq. [1] by carrying out two torque runs with the full and half number of balls, respectively. The results of these measurements, shown in Figure 7, confirm the assumption that the cage friction is mostly independent of the applied load per ball. Some decrease in cage friction with an increasing load per ball (i.e., an increasing axial preload) may be explained by the more stable running behavior of the cage at higher preloads.

By averaging the effective cage friction torque over the whole range of the specific ball preload for each speed step, the cage friction torque can be displayed as a function of rotational speed only, as shown in Figure 8.

Additionally, the overall friction torque of the standard bearing SB1 over the rotational speed is plotted for low and high preloads. As generally expected, the friction torque increases with the bearing load and the rotational speed. These measurements confirm that the influence of the cage on the overall bearing friction is not negligible, especially at higher rotational speeds and low loads.

For the same bearing, Figure 9 shows a comparison between the measured friction torque and the calculated friction torque with regard to the rotational speed. The bearing temperature is assumed to increase linearly with the rotational speed. For a considered friction coefficient of $\mu = 0.25$, which is a similar magnitude as measured by Boesinger and Warner *(16)*, the calculation yields good correlation with the measurements, especially at medium and high speeds. It has to be mentioned that due to the experimental setup and the calculations conducted above, possible churning losses due to the interaction between rotating elements and the oil and air lubricant flow cannot be considered separately. If they occur, they will be part of the measured cage friction. In addition to the roughness of the outer ring board, which is higher than that of the raceway, this might be a possible explanation for the friction coefficient, which is considerably large. The calculated results show that at low to medium speeds the effect of the quadratic increase in the centrifugal forces with rotational speed dominates the development of cage friction. For high rotational speeds, the expansion of the cage and therefore the reduction of eccentricity become more significant, which leads to a decreasing slope of the cage friction over rotational speed. In reality there are several other effects that influence the slope of the cage friction curve, which are not covered in this simple cage friction model. Therefore, the results have to be interpreted carefully.

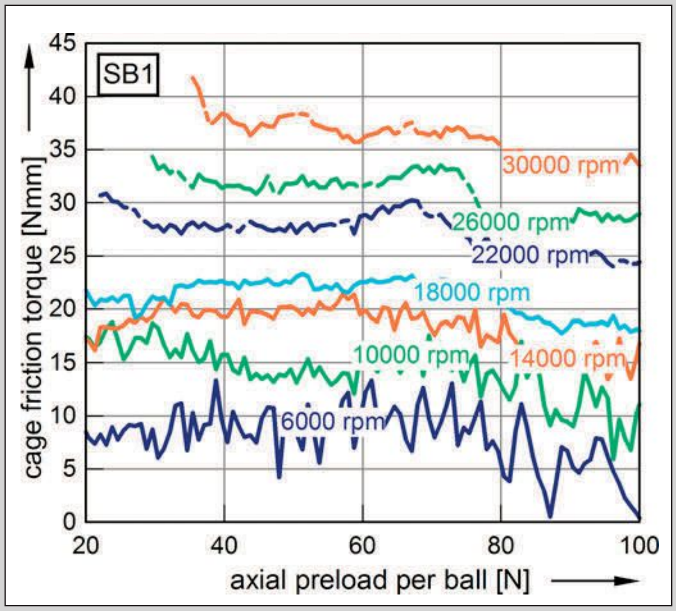

Figure 7 | **Measured effective cage friction.**

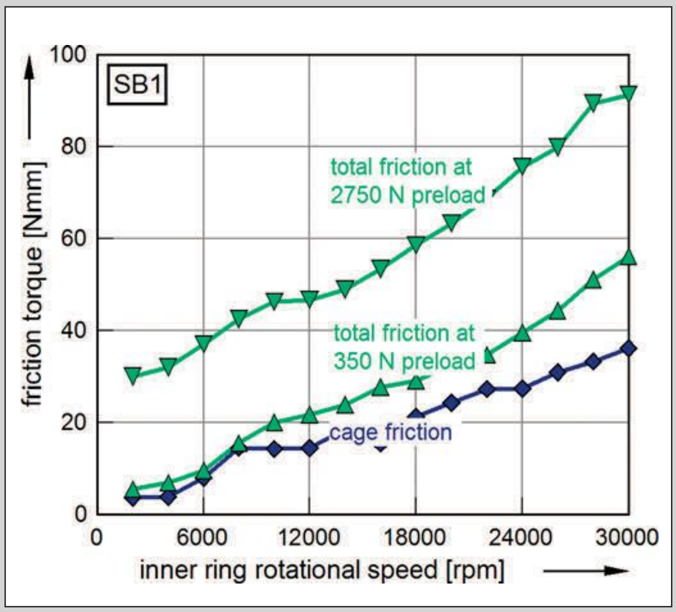

Figure 8 | **Measured effective cage and total bearing friction.**

Figure 10 shows the inner and outer ring temperatures measured during step runs using the same bearing (SB2) with different cages. The ring temperatures are a valid representation for the friction torque because the friction losses are converted into heat. Thus, higher temperatures directly correlate with higher friction torque, which is solely caused by the differences in the cages.

Cages 2Std1 and 2Std2 are both made from PEEK but fea-

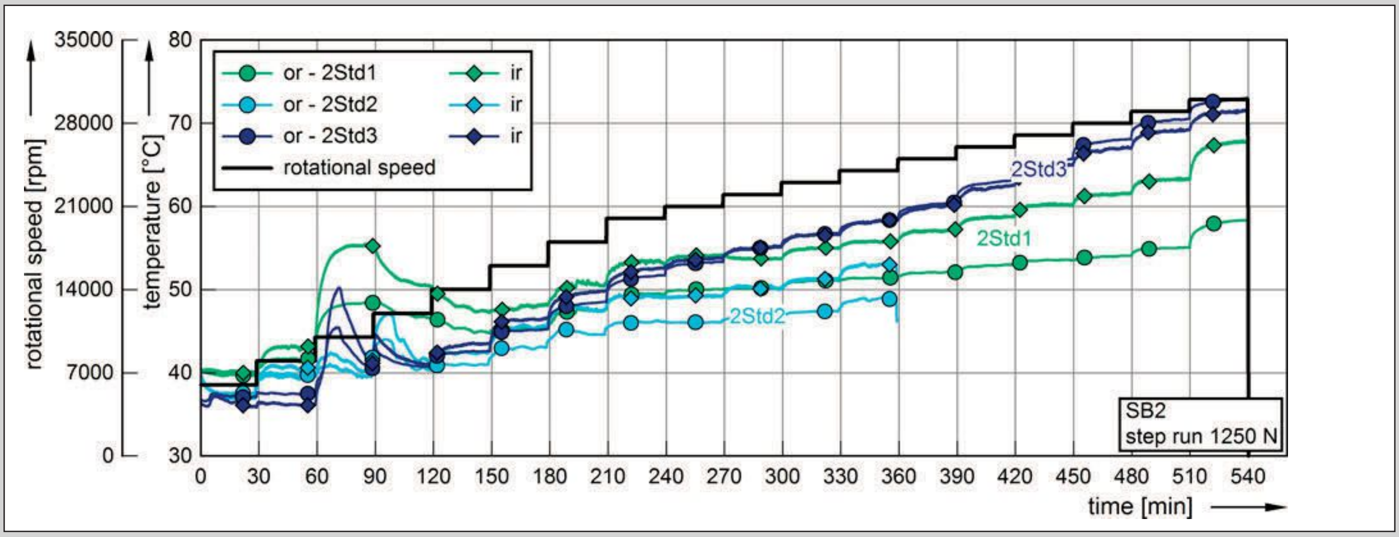

Figure 10 | **Inner and outer ring temperatures for different board clearances and cage materials.**

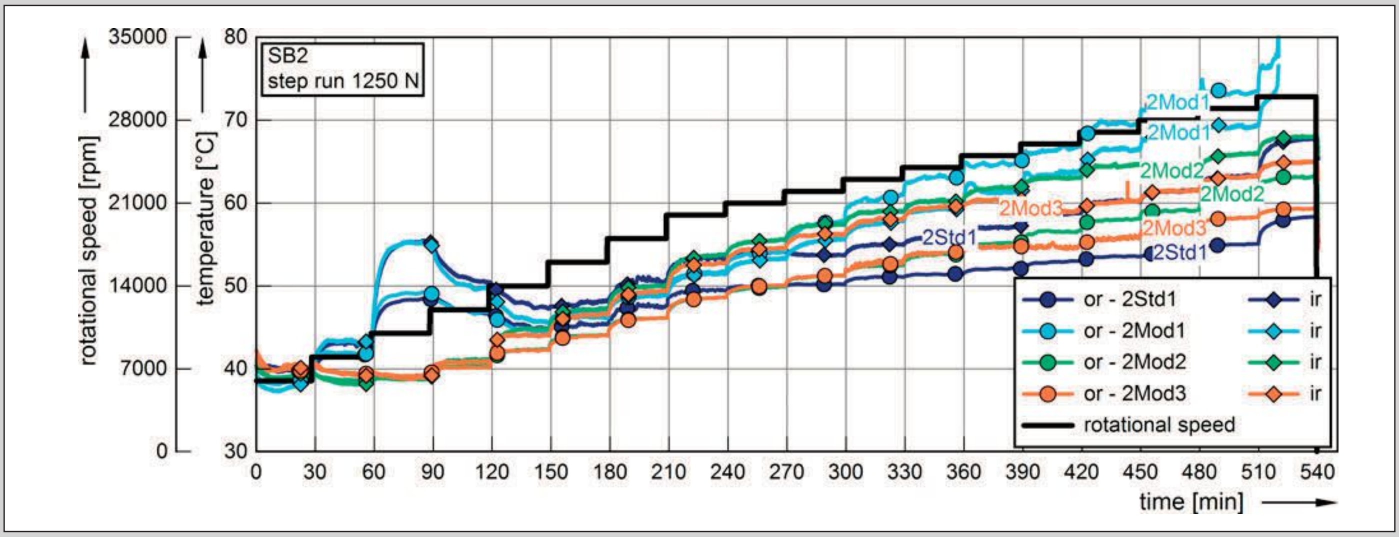

Figure 11 | **Inner and outer ring temperatures for cages with modified geometries.**

ture different board clearances of 0.6 mm (2Std1) and 0.275 mm (2Std2). It can be seen that the cage with the smaller board clearance shows lower temperatures (i.e., lower frictional torque). In addition to those advantages, the tests with the clearance-reduced cage had to be terminated at a speed of 24,000 rpm because at higher rotational speeds the thermal and centrifugal expansion would completely compensate for the cage clearance and hence cause jamming and destruction of the cage.

Cages 2Std1 and 2Std3 differ in cage material and cage pocket design. Both cages feature enough board clearance to allow for the high radial expansion at maximum speed. However, the PH resin cage shows considerably higher ring temperatures. One possible reason for this behavior is the higher Young's modulus of the PH resin and its lower thermal expansion coefficient compared to PEEK. This results in a lower radial expansion at high rotational speeds. Hence, the eccentricity and the centrifugal forces of the PH resin are higher, resulting in higher cage friction. For a detailed analysis, additional effects like different tribological properties, damping behaviors, and densities of the cages have to be taken into account.

Analogous to Figure 10, Figure 11 shows the bearing ring temperatures for modified PEEK cages in the same bearing (SB2). The cages feature the expansion compensation shown in Figure 2 in combination with different nominal board clearances ranging from 0.55 mm (2Mod1) to over 0.35 mm (2Mod2) to 0.25 mm (2Mod3). As with the cylindrical cages, for the polygonal cages there is a clear correlation between board clearance and ring temperature (i.e., cage friction). Because a regular cage with a board clearance of 0.25 mm is expected to jam at about 22,000 to 24,000 rpm, the fact that even the cage with the smallest clearance reaches the maximum speed is clear proof of the positive effects of the expansion reduction measures. However, it should be mentioned that, regarding temperatures and friction, none of the modified cages reaches the friction performance of the standard cage at high speeds. For low rotational speeds, the expansion-compensated cage with reduced radial clearance exhibited a more stable running behavior than the standard cage.

DISCUSSION

On the one hand, the experiments described above show that, especially at low to medium loads and high rotational speeds, cage friction is not negligible regarding the overall bearing friction. On the other hand, the description of the dynamic transient behavior of the cage is a complex problem. Within the bearing, the cage can interact with the outer ring at constantly changing positions. In addition, the positions and number of balls the cage is in contact with vary. Although lubricant quantity is very low in spindle bearings, the cage lubricant interaction can play a significant role. To consider all effects, a detailed model would have to incorporate elaborate multibody simulations of the whole bearing.

Nevertheless, the simple analytical calculations proposed here seem to yield satisfying estimations of the order of magnitude and the development of the cage friction in spindle bearings. In addition to the general goodness of fit, it is especially helpful with the estimation of the effects of differences in board clearance. Because the model takes the thermal and centrifugal expansion into account, it points at the vital role that board clearance plays in spindle bearings. With smaller board clearances, the possible eccentricity of the cage and thereby the friction forces due to centrifugal forces are reduced. Due to the expansion effects, such cages are more prone to a complete loss of board clearance, which leads to a sudden bearing failure.

Standard cages are designed to feature an optimal board clearance at high rotational speeds but yield a relatively large board clearance at low rotational speeds. Thus, the cages with a polygonal outer surface and expansion compensation do not show any advantages regarding friction at high speeds. Nevertheless, such cages may be beneficial in other cases: Expansion-compensated cages are fail-safe regarding possible use in speed regimes beyond those the bearing was originally designed for. The withdrawn areas of the guiding profile may be beneficial for the flow of lubricant into the bearing. Furthermore, these cages feature a low board clearance along the whole speed range, which has proved to be beneficial for stable running behavior at lower speeds. However, it should be mentioned that cage behavior is a highly dynamic phenomena and multibody simulations will be necessary to further investigate the possible advantages of optimized cages.

CONCLUSION

The experiments show that neglecting the cage friction in high-speed angular contact ball bearings results in a considerable underestimation of the overall bearing friction.

A calculation model for cage friction considering all aspects of the transient cage behavior would require the incorporation of multibody simulations. By making several assumptions, in the simplified analytical approach presented here, the complexity of the system is reduced considerably. The experiments show a decent correlation between the developed formula and measurement results. By taking into account the thermal and centrifugal expansion of the cage and/or the outer ring, the calculation allows for an estimation of the effects of radial clearance on the cage friction.

Investigations of a cage with integrated expansion compensation prove the general functionality of the concept. This allows for the design of cages with low radial board clearances along the whole range of operational speeds. However, the first prototype cages did not show advantages regarding cage friction at high rotational speeds.

ACKNOWLEDGEMENTS

The authors thank Deutsche Forschungsgemeinschaft (DFG) for providing financial support for the experiments under registration number BR 2905/14–2, "Gestaltungsvarianten für Spindellager zur Steigerung der erreichbaren Drehzahlen."

REFERENCES

(1) Townsend, D. P., Allen, C. W., and Zaretsky, E. V. (1973), "Friction Losses in a Lubricated Thrust-Loaded Cageless Angular-Contact Bearing," **NASA Technical Note (TN D-7356)**.

(2) Harris, T. A. and Kotzalas, M. N. (2007), *Advanced Concepts of Bearing Technology,* 5th ed., CRC Press: Boca Raton, FL.

(3) Houpert, L. (1999), "Numerical and Analytical Calculations in Ball Bearings," *Proceedings of the 8th European Space Mechanism and Tribology Symposium,* Toulouse, France, September 29.

(4) Houpert, L. (2002), "Ball Bearing and Tapered Roller Bearing Torque: Analytical, Numerical and Experimental Results," *Tribology Transactions*, **45**(3), pp 345–353.

(5) Biboulet, N. and Houpert, L. (2010), "Hydrodynamic Force and Moment in Pure Rolling Lubricated Contacts. Part 1: Line Contacts," *Proceedings of the Institution of Mechanical Engineers - Part J: Journal of Engineering Tribology,* **224**(8), pp 765–775.

(6) Biboulet, N. and Houpert, L. (2010), "Hydrodynamic Force and Moment in Pure Rolling Lubricated Contacts. Part 2: Point Contacts," *Proceedings of the Institution of Mechanical Engineers - Part J: Journal of Engineering Tribology,* **224**(8), pp 777–787.

(7) Brecher, C., Bäumler, S., and Rossaint, J. (2013), "Calculation of Kinematics and Friction of a Spindle Bearing Using a Local EHD-Friction Model," *Tribology Transactions,* **56**(2), 245–254.

(8) Steinert, T. (1995), *Das Reibmoment von Kugellagern mit Bordgef¨uhrtem K¨afig [Frictional Torque of Ball Bearings with Outer Ring Guided Cages]*, Doctoral Thesis, University Aachen, Germany.

(9) Houpert, L. (2010), "CAGEDYN: A Contribution to Roller Bearing Dynamic Calculations Part I: Basic Tribology Concepts," *Tribology Transactions*, **53**(1), pp 1–9.

(10) Brown, J. R. and Foster, N. H. (2002), "Numerical Investigation of the Effect of Carbon–Carbon Composite Cages on High-Speed Bearing Operating Temperatures," *Tribology Transactions*, **45**(3), pp 411–417.

(11) Brown, J. R. and Forster, N. H. (2003), "Carbon–Phenolic Cages for High-Speed Bearings Part III—Development of Numerical Models for Heat Generation and Temperature Prediction in Lightly Lubricated Bearings," **AFRL-PR-WP-TR-2003–2033**.

(12) Pederson, B. M., Sadeghi, F., and Wassgren, C. (2006), "The Effects of Cage Flexibility on Ball-to-Cage Pocket Contact Forces and Cage Instability in Deep Groove Ball Bearings," **SAE Technical Paper No. 2006-01-0358**.

(13) Sathyan, K., Gopinath, K., Lee, S. H., and Hsu, H. Y. (2012), "Bearing Retainer Designs and Retainer Instability Failures in Spacecraft Moving Mechanical Systems," *Tribology Transactions,* **55**(4), pp 503–511.

(14) Rossaint, J. (2012), "Lagerkäfig mit Reduzierter Aufweitung für hohe Drehzahlen [Bearing Cage with Reduced Expansion for High Rotational Speeds]," **German Patent Application DE 10 2011 014 078 A1**.

(15) Beitz,W. and Küttner, K.-H. (1994), *Dubbel Handbook of-Mechanical Engineering,* Springer: New York.

(16) Boesinger, E. andWarner, M. (1991), "Spin Bearing Retainer Design Optimization," **NASA Conf. Publ. 3113**.

TOP STORIES

NANO MECH BUILDS NEW GLOBAL CAMPUS

Springdale, Ark.-based, **NanoMech** announces the company will build an adjoining state-of-the-art facility to the company's existing factory, located east of its headquarters.

The new factory will incorporate cutting-edge assembly lines, laboratories and the latest in security, environmental and safety systems for handling advanced manufacturing, military and strategic projects.

"The new factory and expanded headquarters will provide for approximately 25-50 new jobs for world-class scientists and support staff. The space will also allow us to meet current demand for our products while advancing ongoing research and development efforts," says Jim Phillips, CEO of NanoMech.

The new factory and headquarters is expected to be fully operational by the summer of 2014.

BASF ANNOUNCES PLANT EXPANSION IN CHINA

BASF announces the company will build a new production plant to manufacture specialty amines at its existing wholly-owned site in the Nanjing Chemical Industry Park in China.

The plant will have dimethylaminopropylamine (DMAPA) and polyetheramines (PEA) as the main products, complementing existing DMAPA and PEA facilities in Germany and the U.S.

"BASF is a leading supplier of DMAPA and PEA globally, and this investment reflects our continued commitment to meeting the growing market demand in Asia Pacific," says Sanjeev Gandhi, president of BASF's intermediates division. "Our ability to produce these products within the region will strengthen our supply reliability and better serve our customers with shorter lead times."

DMAPA is used in various applications including dye-stuff intermediates, lubricant additives, electroplating, coupling agents for rubber and others.

PEA is an intermediate chemical for epoxy curing agents used in the production of plastics, polyurea coatings, adhesives, reaction injection molding and wind blade composites.

EXXONMOBIL STARTS NATURAL GAS PRODUCTION IN MAYALYSIA

ExxonMobil Corp. announces the company will start natural gas production at the Damar field off the east coast of Peninsular Malaysia.

According to ExxonMobil, the Damar field has a projected capacity of 200 million cubic feet of gas per day. ExxonMobil and joint-venture partner Petronas Carigali Sdn. Bhd. have planned a total of 16 development wells for the platform.

"Damar will help meet increasing natural gas demand in Malaysia," says Neil W. Duffin, president of ExxonMobil Development Co. "It also represents one of several projects that will add to ExxonMobil's global production in the coming years as we remain focused on delivering profitable volumes over the long term."

Damar was developed under a gas production sharing contract between ExxonMobil, Petronas Carigali and Petronas. ExxonMobil is the operator of the Damar field and Petronas Carigali holds a 50 percent interest.

PIONEER SOLUTIONS AMERICAS INKS ARCHWAY SALES AS DISTRIBUTOR

El Monte, Calif.-based, **Pioneer Solutions Americas** has selected St. Louis-based **Archway Sales, Inc.** to represent the company's solid acrylic resin line. Archway will represent Pioneer Solutions in all states east of the Rocky Mountains. Representation in the states of Indiana, Michigan and Ohio will be shared with current distributor Aal Chem LLC.

"The quality of Pioneer Solutions Americas products and the opportunity to partner with a company geared for growth supports Archway's goal of bringing the best possible products to our customers," says David Baumstark, president of Archway Sales.

Pioneer Solutions products are marketed under the PChem brand.

We are excited to partner with Archway Sales. Their geographic reach and technical sales capabilities make a good fit for our expansion efforts," says D.B. Jiang, president of Pioneer Chemicals.

PROMOTIONS & TRANSITIONS

SPECTRO INC. ADDS TWO VPs TO SENIOR MANAGEMENT TEAM

Chelmsford, Mass.-based, **Spectro Inc.** has named **Mark Spillane** and **Bob Wopperer** as vice of president of operations and vice president of business development, respectively.

Spillane most recently served as director of manufacturing at Ambient Corp., where he was responsible for global activities that included materials management, purchasing, supply chain, testing, quality and NPI program support. Prior to Ambient, he was the senior director of operations at Ahura Scientific, before and after its acquisition by Thermo Fisher Scientific. At Ahura, he was responsible for all operational activities while managing a team of 90 employees. Spillane assumes all purchasing, supply chain management and manufacturing responsibilities for Spectro.

Mark Spillane

Bob Wopperer

Wopperer previously worked for Thermo Fisher Scientific's portable analytical instrument division, where he was senior director of marketing and business development and part of a senior leadership team that grew the business's revenues greater than 300 percent over a five-year period. Prior to joining Thermo Fisher, he handled a variety of marketing, sales and business development roles with Oxford Instruments. Wopperer oversees Spectro's marketing, product management and applications functions, where he is responsible for identifying and executing a wide set of initiatives in current and new vertical market applications.

SEA-LAND CHEMICAL APPOINTS BOARD CHAIRMAN

Don Smith

Westlake, Ohio-based **Sea-Land Chemical Co.** has named **Don Smith** as chairman of the company's board of directors. Smith succeeds **Jim Hanesworth**, who retired after more than 30 years but remains on the board as a director.

"Everyone associated with Sea-Land Chemical is appreciative of Jim's efforts throughout his chairmanship," says Joseph Clayton, president of Sea-Land Chemical. "He has been instrumental in putting essential corporate governances in place, as well as leading the executive and compensation committees."

Clayton adds, "Don brings many years of experience and a very inquisitive nature to the role. His probing questions will assist management as they make decisions and will be a benefit as he leads the board."

SHARE YOUR STLE 2014 PRESENTATIONS WITH SUBMISSION OF AN EXTENDED ABSTRACT!

With over 400 technical-paper presentations to choose from at STLE's 2014 Annual Meeting & Exhibition, May 18-22 at Disney's Contemporary Resort in Lake Buena Vista, Florida, a major concern for attendees is scheduling conflicts, as they might miss presentations that they would like to hear or cannot share the contents with their colleagues that are unable to attend the meeting.

In an effort to provide attendees with the opportunity of not missing a presentation, we encourage speakers to submit a 2-3 page **Extended Abstract,** which may also include handout materials of your presentation. Both abstracts and handouts must be converted as PDFs before submission.

We suggest that speakers submit their abstracts and handouts before **Wednesday, April 30** that way we can make presentations available to attendees prior to the meeting. We realize speakers might still be working on their presentations before they arrive, so abstracts and handouts may also be submitted anytime after **April 30,** as well as during and immediately following the annual meeting to allow more of your colleagues to benefit from your presentations.

For further information and instructions on submitting extended abstracts, visit **www.stle.org** or please contact Karl Phipps, (847) 825-5536, **kphipps@stle.org.**

Want to be recognized in TLT?

TLT is interested in hearing from our readers. Let us know what's happening in your company. If you have news about a new employee or if someone in your company has been recognized with an award or any other interesting items, let us know. Please send us your news releases and photos for publication in Newsmakers to TLT Magazine, Attn: Karl Phipps, 840 Busse Highway, Park Ridge, IL 60068, **kphipps@stle.org.**

HIGH-PERFORMANCE PRODUCTION HYDROFORMING PRESS

Interlaken Technology, a manufacturer of production press equipment for hydroforming, elevated temperature forming and hot stamping systems, introduces a new four-column **Hydroforming Press System** for running high-volume production while reducing cycle time. Hydroformed parts are stronger and weigh less due to structural integrity and fewer welds or add-on pieces. In addition, costs are reduced and time is saved by eliminating secondary operations, reducing scrap, lowering material and manufacturing costs and increasing design flexibility. With superior control over forces and motions, the Interlaken Hydroforming Press System provides a greater overall quality of formed parts. The multichannel, closed-loop control system is easily programmed to handle various sizes and materials. It also offers dynamic mode switching, which enables users to switch between a variety of feedbacks such as force, position, internal pressure and other system variables.

Interlaken Technology
Chaska, Minn.
(952) 856-4210
www.interlaken.com

SHELL'S HEAVY-DUTY ENGINE OIL APPROVED FOR MAN EURO 6 ENGINES

Shell Rimula R6 LME, the latest heavy-duty diesel engine oil in the Shell Rimula premium synthetic range, has been approved by MAN to meet the MAN M 3677 oil specification, suitable for their Euro 6 engines. Shell Rimula R6 LME is a 5W-30 viscosity grade oil designed to provide all the benefits of the Shell Rimula R6 technology alongside proven fuel economy benefits. According to Shell, it has been independently proven to deliver up to 2.0 percent fuel savings over 100,000-km-oil-drain interval compared with a typical 10W-40 oil. Shell Rimula R6 LME offers Shell's optimal engine protection and efficiency through a three-fold approach: synthetic base oil technology, advanced additive technology and a unique antiwear booster system. These three elements combine to help deliver strong performance, long drain intervals and fuel saving capability without compromising durability. Shell Rimula R6 LME is formulated with reduced levels of ash and sulphur to help control diesel particulate filter (DPF) blocking and maintain the efficiency of the latest and future vehicle technologies. It delivers exceptional wear protection and engine piston cleanliness in the latest engines and has been tested to help ensure long engine life and protection throughout the oil maintenance interval. For more information, visit **www.shell.com.**

CHEVRON ORONITE INTRODUCES LOW-TEMPERATURE VISCOSTY MODIFIER

Chevron Oronite introduces **PARATONE® 8900E**, an enhanced viscosity modifier that offers excellent low-temperature performance, superior thickening efficiency and extended shear stability. PARATONE 8900E is designed for use in formulating passenger car and heavy-duty engine oils, other multigrade crankcase oils, power transmission fluids and industrial engine oils.

"Our polymer scientists took a fresh look at the building blocks of PARATONE 8900E and its detailed molecular structure, and how each of its key attributes influence the overall performance of finished lubricants," says Bill Paschal, global product manager, viscosity index improvers, Chevron Oronite. "After several years of research and testing, we have identified and implemented small, precise adjustments in the polymer molecule, resulting in a product that delivers robust low-temperature performance while providing the excellent thickening efficiency and extended shear stability our customers have come to expect and rely upon with PARATONE 8900E."

According to Chevron Oronite, PARATONE 8900E works well with numerous pour-point depressants and provides improved formulating flexibility for lubricant designers.

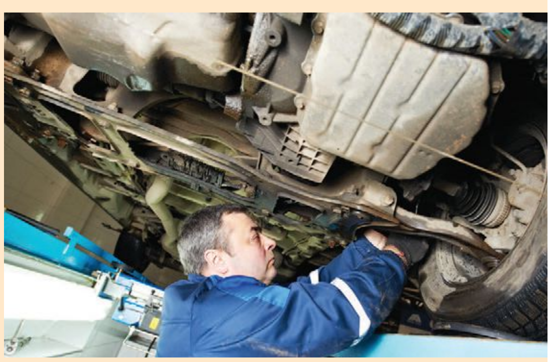

Chevron Oronite Co. LLC
San Ramon, Calif.
(877) 512-7200
www.oronite.com


NLGI
Serving the grease industry since 1933
Ocean's '14:
Staying Ahead in the Grease Game
A wave of Education, Science & Profitable Partnerships
NLGI 81st Annual Meeting
June 14-17, 2014
Palm Beach Gardens, FL

Send us your new product news with color photos to: TLT Magazine, Attn: Karl Phipps, 840 Busse Highway, Park Ridge, IL 60068, kphipps@stle.org

VEGETABLE-BASED WATER-SOLUBLE LUBRICANT FOR STEEL APPLICATIONS

QualiChem, Inc., introduces **EQO-PURE 452,** a new vegetable-based water-soluble lubricant for severe hardened steel and stainless steel machining applications. EQO-PURE 452 is a heavy-duty, vegetable-derived, micro-emulsion fluid with extreme pressure additives formulated to improve tool life and part quality while eliminating foaming and staining. EQO-PURE 452 is designed for use in many applications that previously used straight oil, including boring, deep-hole drilling, gun drilling, reaming, roll forming, tapping and threading. EQO-PURE 452 is formulated for use on ferrous or non-ferrous metals where high levels of boundary and extreme-pressure lubrication are required. It provides excellent corrosion control for ferrous metals and machine tools. Its bioresistant qualities result in long fluid life in both central systems and individual sumps without biocides.

QualiChem, Inc.
Salem, Va.
(540) 375-6700
www.qualichem.com

STARTER LEAK DETECTION KIT FOR OIL-BASED SYSTEMS

Spectronics Corp. introduces the **OPK-441 Industrial Leak Detection Kit,** a new starter kit designed to effectively pinpoint the exact source of all leaks in hydraulic equipment, compressors, engines, gearboxes and fuel systems. The kit features the OPTIMAX™ 400 violet-light LED flashlight, a compact, high-intensity unit that quickly reveals all leaks in small- to medium-sized industrial systems—even in cramped areas that are inaccessible to larger lamps. Included is an 8 oz. (237 ml) twin-neck bottle of patented OIL-GLO™ 44 concentrated fluorescent oil dye, which is compatible with all synthetic and petroleum-based fluids. When a leaking system is scanned with the OPTIMAX™ 400 flashlight, the dye glows a bright yellow/green at all leak sources to reveal the precise location of each and every leak. The kit also includes an 8 oz. (237 ml) spray bottle of GLO-AWAY™ dye cleaner, dye treatment tags and fluorescence-enhancing glasses.

Spectronics Corp.
Westbury, N.Y.
(800) 274-8888
www.spectroline.com

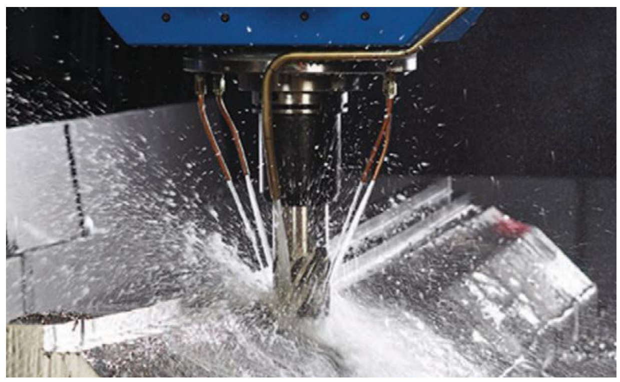

HIGH-PERFORMANCE MACHINING FLUIDS

5ME introduces the company's **CYCLO COOL® 900 series synthetic metal machining fluids**, which utilize a unique, near-neutral pH formula developed to meet heavy-duty, high-heat machining requirements at a lower cost than semisynthetics and soluble oils. The additive-free, low-foaming fluids are specially formulated for machining titanium, Inconel®, beryllium cooper, hardened steels, stainless steels and other exotic alloys. The cationic-based synthetic coolants contain specialized boundary lubricants that penetrate the cut zone heat barrier, even at lower fluid pressures (300 to 400 psi), to absorb heat from the tool and the part, minimizing tool-tip work hardening and premature wear. Free of biocides/fungicides and aggressive pH adjusters, they provide increased sump life and environmental friendliness when replacing high-maintenance, chlorinated, semisynthetics and soluble oils in all metal-removal operations.

5ME
Cincinnati, Ohio
(513) 719-1600
www.5ME.com

Describe the most challenging bearing testing problem your company faced and your solution.

Bearings are virtually everywhere, as are the problems and challenges incurred during their application and use. TLT readers have certainly seen their share of problems, based on their answers to this month's survey questions. In some cases where problems occurred, an improper grease was specified. In others, it was poor lubrication practices such as over lubricating the bearing. One reader cited the challenges faced in changing from one bearing supplier to another on a mass scale. The global manufacturing of bearings presents challenges of its own. Nearly 80 percent of survey respondents say it has increased the risk associated with qualifying new designs or suppliers.

What enhancement in bearing application technology would be of greatest value?

Enhanced corrosion resistance	29%
Enhanced wear resistance	54%
Higher operating temperature	32%
Higher operating speed	18%

Based on responses sent to 13,000 TLT readers. Total exceeds 100% because some respondents chose more than one answer.

We failed it. We were selling a lithium stearate grease to a boat trailer axle manufacturer. Our customer called to ask if we had any issues with the grease. We said. "No, are you?" He said no. Then he switched grease suppliers. His axles were failing in large numbers, and he fired his bearing supplier, his grease supplier (us), and he changed the installation process. The real problem is not known, but it was most likely the grease: lithium stearate is not great in water wash-out, and we should have been supplying a calcium-thickened grease for better wash-out.

Our company is a lubricating oil company. A lubricant to reduce the adverse effect of wear particles is the challenge.

Very large motor rebuilds that have bearing failure during initial start-up was solved by insisting on specific name and application bearings and requiring baseline vibration testing during rewind.

Lube oil analysis result, not on par with local analyzer. (e.g., moisture analyzer)

Tailor-made bearing in steel-roll former.

Tests of porous sliding material filled with oil with BN—the phenomenon of synergy BN - C has occurred.

Heavily loaded journal bearings in mixed lubrication regime. We built a test rig.

Running life test on angular contact bearings for spacecraft is virtually impossible because they can last for more than 10 years. We have used a modified thrust bearing tester that increases the sliding-rolling ratio and, therefore, significantly lowers the lifetime to allow comparison of various lubricants.

Our issue is always ingression of some type or another of scale dirt, etc.

Pillow block bearings on conveyor systems outdoors. Used a polyurea grease and removed the grease zerks, so the bearing was sealed. Problem was over lubrication, causing the seals to fail and allowing dirt and water to enter the bearings.

Assurance that the correct amount of grease and lubrication frequency is applied. Challenge met through information gathered from the OEM, training and use of temp gun to monitor operating temperatures.

Duplicating the environment of a PTU to determine roller bearing life with different viscosity oils. We do not have a good resolution since our only test is a full-scale dyno, and this cannot be tied up for the time it takes to determine bearing life. The bearing companies will not commit to this type of testing either.

Trying to change from one bearing supplier to another on a mass scale. We created product groups based on bearing type and size. Determined which bearing sizes within each group had the highest usage and high risk of failure. Performed detailed inspection and lab testing on those bearings first. Any bearing that was in the group that was produced on the same manufacturing line also was qualified. We needed to do our homework on what manufacturing lines the bearings were made on and what applications created the highest risk, but once this occurred creating the groups was easy.

Has the global production of bearings increased the risk associated with qualifying new designs or suppliers?

Yes	79%
No	21%

Based on responses sent to 13,000 TLT readers.

We had to pass an FE9 at 160 C in a mineral oil-based grease.

Failure to a gearbox due to the ingress of water used in the process. Solved by frequently scheduled oil changes after improved seals.

Which bearing qualification tests produce the greatest reduction risk in the shortest amount of time?

Four-ball weld and four-ball wear.

Effectively reducing the pitting life test.

Vibration or bearing condition.

Oil analysis.

Compared results from two different kinds of testers for the same material coupling (and lubrication).

Temperature.

Vibration analysis is the only method I'm aware of.

For rear axles we typically take the most damaging customer duty cycle torque/speed events and run an accelerated dyno test.

ASTM D2266.

Performing a detailed bearing inspection followed by lab testing to compare empirical results between suppliers and to determine if design and material differences have a significant impact on life.

We ran PDSC and TGA to screen additives.

Highly loaded fatigue tests. TLT

Editor's Note: *Sounding Board is based on an e-mail survey of 13,000 TLT readers. Views expressed are those of the respondents and do not reflect the opinions of the Society of Tribologists and Lubrication Engineers. STLE does not vouch for the technical accuracy of opinions expressed in Sounding Board, nor does inclusion of a comment represent an endorsement of the technology by STLE.*

TLT ADVERTISERS INDEX

Company	Page	Contact	Phone	E-mail	Web
Acme-Hardesty Co.	58	Bryan Huston	(215) 591-3610	bhuston@acme-hardesty.com	www.acme-hardesty.com
Additives International	72	Gregory Jorjorian	(800) 708-9657	gjorjorian@additivesinternational.com	www.additivesinternational.com
Afton Chemical Co.	IFC, 40	Lauren Ereio	(804) 788-6081	lauren.ereio@aftonchemical.com	www.aftonchemical.com
BASF	OBC	Betsy Arnone	(973) 245-7865	betsy.arnone@basf.com	www.basf.com
Cannon Instrument Co.	17	Patricia Argiro	(814) 353-8000 ext. 267	pargiro@cannoninstrument.com	www.cannoninstrument.com
ChevronPhillips Chemical Co.	60	Amy King	(832) 813-4627	kingam@cpchem.com	www.cpchem.com
CRC Press - Taylor and Francis Group	70	Maikala del Castillo	(561) 998-2562	Maikala.delCastillo@taylorandfrancis.com	www.taylorandfrancis.com
ExxonMobil Chemical Co.	51	Caslin Lee	+65 6885 8229	caslin.hl.lee@exxonmobil.com	www.exxonmobil.com
Evonik Oil Additives	47	Richard Williams	(215) 706-5821	dick.williams@evonik.com	www.evonik.com/oil-additives
Focus Chemical	74	Kristin Anderson	(440) 686-2197	kanderson@palmerholland.com	www.palmaerholland.com
Hangzhou Sungate	33	Eric Chen	+86-571-87040747	ericchen@sungatechem.com	www.sungatechem.com
Herguth Laboratories Inc.	43	Linda Perry	(707) 554-4611	lperry@sgs.com	www.herguth.com
Huntsman Petrochemical Corp.	61	Sam Branco	(281) 719-4704	sam_branco@huntsman.com	www.huntsman.com
J.A.M. Distributing Co.	57	John Filak	(713) 844-7730	jfilak@jamdistributing.com	www.jamdistributing.com
King Industries, Inc.	62	Karen Grunwald	(203) 866-5551	kgrunwald@kingindustries.com	www.kingindustries.com
Monson Companies	21	Doug Hiple	(609) 773-0031	dhiple@monsonco.com	www.monsonco.com
Münzing	59	Alicia Colacci	(973) 279-1306	acolacci@munzing.us	www.munzing.com
Napoleon Engineering Services	24	Chris Napoelon	(716) 372-6532	cnapoleon@nesbearings.com	www.nesbearings.com
NCeed Enterprises Inc.	63	Rolly Enderes	(888) 726-3114	rolly@chemceed.com	www.nceed.com
NLGI	65	Marilyn Brohm	(816) 931-9480	nlgi@nlgi.org	www.nlgi.org
Prospector	IBC	Olivia Li	(913) 307-9010	olivia.li@ul.com	www.ulprospector.com
STLE 2014 Annual Meeting Mobile App	73	Bruce Murgueitio	(847) 825-5536	bmurgueitio@stle.org	www.stle.org
STLE 2014 Annual Meeting	67	Merle Hedland	(630) 428-3400	mhedland@stle.org	www.stle.org
STLE 2014 Tribology Frontiers Conference	75	Merle Hedland	(630) 428-3400	mhedland@stle.org	www.stle.org
STLE Call for Volunteers	77	Tom Heidrich	(847) 825-5536	theidrich@stle.org	www.stle.org
STLE 2014 Education Courses	79	Kara Sniegowski	(847) 825-5536	ksniegowski@stle.org	www.stle.org
The Elco Corp.	29	David Millin	(216) 749-2605	dmillin@elcocorp.com	www.elcocorp.com
The Lubrizol Corp.	3	Meredith F. Bruder	(440) 347-5282	meredith.bruder@lubrizol.com	www.lubrizol.com
Vanderbilt Chemicals, LLC	5	Glenn Foster	(203) 853-1400 ext. 485	gfoster@vanderbiltchemicals.com	www.vanderbiltchemicals.com

TECHNICAL BOOKS

MAINTENANCE, REPLACEMENT, AND RELIABILITY: THEORY AND APPLICATIONS, SECOND EDITION

Authors: Andrew K.S. Jardine and Albert H.C. Tsang
Publisher: CRC Press

Completely revised and updated, *Maintenance, Replacement, and Reliability: Theory and Applications, Second Edition* supplies the tools needed for making data-driven physical asset management decisions. The well-received first edition quickly became a mainstay for professors, students and professionals with its clear presentation of concepts immediately applicable to real-life situations. However, research is ongoing and relentless—in only a few short years, much has changed. New topics covered include the role of maintenance in sustainability issues, PAS 55 (a framework for optimizing management assets), data management issues, including cases where data are unavailable or sparse and how candidates for component replacement can be prioritized using the Jack-knife diagram. Based on the authors' experience, this book maintains the format that made the first edition so popular. It covers theories and methodologies grounded in the real world. Simply stated, no other book available addresses the range of methodologies associated with, or focusing on, tools to ensure that asset management decisions are optimized over the product's life cycle—presented in an easily digestable and immediately applicable way. List Price: $149.95. Available at **www.crcpress.com.**

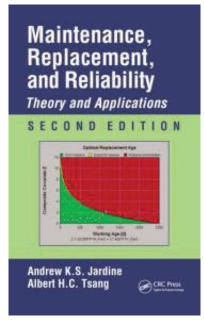

ASTM RELEASES NEW PUBLICATION ON VISCOSITY AND RHEOLOGY OF IN-SERVICE FLUIDS

ASTM International announces the release of a new publication, *STP 1564, Viscosity & Rheology of In-Service Fluids as They Pertain to Condition Monitoring*.

STP 1564 includes 11 peer-reviewed papers that provide the latest in current research and practices on viscosity and rheology of in-service fluids as they pertain to condition monitoring.

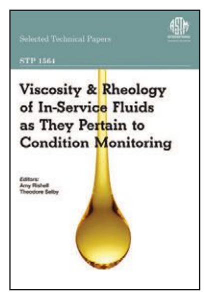

Topics covered include:

- Grease Working and its Role in Consistency Trending
- Possible Impact of In-Service Grease Mixtures with a Stress Rheometer as an Element of a Predictive Maintenance Program

- Comparison of the Effects of Normal Automobile Engine Use on the High Shear Rate Viscosity, Wear, and Volatility of Four Engine Oils
- Die-Extrusion Method for Comparing Changes in Grease Consistency and Flow Characteristics
- Application of Sensors for *In Situ* Measurements of In-Service Grease Rheology
- Absolute Viscosity and Sample Density Measurement Methods to Determine and Report Absolute and Kinematic Viscosity Values for Used Lubricating Oils
- Start-Up Viscosity of In-Service Engine Oils at Low Temperatures
- Rheological Property Measurements of Newtonian and Non-Newtonian Fluids with the Falling Needle Viscometer
- Hand-Portable Low-Temperature Viscosity Measurement to Prevent Sudden Transformer Failure upon Very Cold Start-Up
- Low-Temperature Rheological Response of Fresh Versus Used Oils Using the Scanning Brookfield Technique.

For more information, visit **www.astm.org**. List price: $76 (USD).

STLE PHILADELPHIA SECTION SPONSORS FRACKING EDUCATION COURSE

STLE's Philadelphia Section announces its 2nd annual education course on hydraulic fracturing or fracking, April 24, at the Sandy Run Country Club in Oreland, Pa.

The dramatic growth in hydraulic fracturing or fracking has led to great interest in learning more about this process in general and the lubrication challenges faced by this industry in particular.

The education course is highlighted by a presentation, "Trends in Shale Energy Development and Utilization," from David Yoxtheimer, P.G., a hydrogeologist and extension associate with The Pennsylvania State University's Marcellus Center for Outreach and Research (MCOR). Other speakers include Dave Archacki, Shrieve Chemical Products, Inc., whose talk is entitled, "Guar Gum and Emulsion Polymers and their Use in Hydraulic Fracturing Fluids," and Rob Ferguson, French Creek Software Inc.

This education course is designed to help attendees gain a better understanding of the fracking process, the types of components used in fracking fluids and the opportunities for the lubricant industry to participate in this growing industry.

For more information about the program, visit the STLE Philadelphia Section Website: **www.philadelphia-stle.org.**

Jerry L. Kennedy

Just say no to SEO

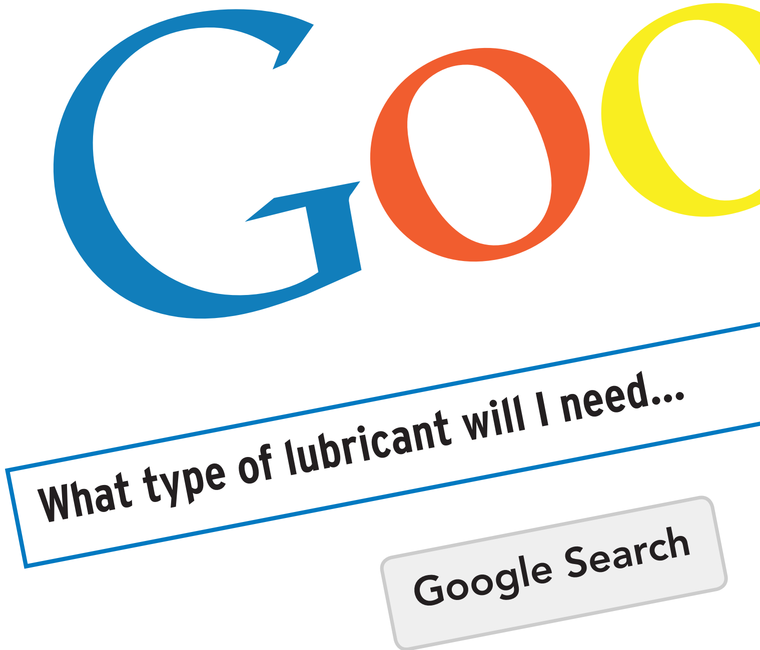

Customer service, not keyword stuffing, is the key to a successful online marketing strategy.

IF YOUR BUSINESS has any sort of online presence (and sometimes even if it doesn't), you probably receive anywhere from one or two to a dozen or more emails a week offering to help you with SEO—search engine optimization. Many of these emails are probably siphoned off by your spam filter, but a few invariably get through. You'll notice a common theme, as the messages usually indicate that for anywhere from a few hundred to a few thousand dollars a month, the vendor will make sure you get to the front page of Google's search results.

But buyer beware. More often than not such solicitations are an effort to separate you from your money in exchange for something that will have limited, if any, positive impact on your business. In fact, ultimately these services can do lasting harm to your online marketing efforts.

What is SEO and why should you take such promises with more than a few grains of salt?

SEO is well defined by Google's Search Engine Optimization Starter Guide **(www.google.co.jp/intl/en/webmasters/docs/search-engine-optimization-starter-guide.pdf).** It is the practice of "making small modifications to parts of your Website that could have a noticeable impact on your site's user experience and performance in organic search results." Sounds helpful, right? When practiced correctly, it is. The problem is that many SEO practitioners focus almost entirely on factors that, while they may be of some limited importance to search engines, give zero consideration to the folks who really matter: your clients and prospects. Ironically, shifting the focus of your content to your clients is more important in the long run than any amount of so-called optimization you could do. Why?

When I talk to groups about online marketing, one of my favorite questions to ask is,

Provide your clients and prospects with content that will answer questions and help solve their problems.

"What is Google's most important job?" Some will say selling advertising or making money, but Google couldn't do either of those things as effectively as it does without being the best in the world at one thing: answering questions. In fact, Google is so good at answering questions that its name has become synonymous with looking something up online. When's the last time you heard someone say, "I'm going to Bing that?"

The best way to get the attention of Google's search algorithm and improve your position in search results is to help Google accomplish its most important function. In other words, provide helpful answers to your clients' questions and you will begin to rise to the top of the search pile. More than anything else, this is the key to successful online marketing.

Of course, as with any endeavor, there are best practices to follow. Rather than hire an SEO firm whose interest in serving itself may override any interest in helping you serve your customers, why not go straight to the source? The SEO Starter Guide is an invaluable resource in developing and maintaining SEO best practices. The best advice in the guide, though, is this: "You should base your optimization decisions first and foremost on what's best for the visitors of your site." Right now, you might be asking yourself, "How can I do that?"

It's quite simple. Rather than providing pointless, keyword-stuffed drivel, provide your users with content that will actually answer their questions and help them solve problems. If you do, you'll not only see better search engine results, you'll come to be a valuable resource to your clients and prospects and will gain the kind of top of mind awareness that leads to increased sales.

Jerry Kennedy earned his stripes as an operations and sales manager in the lubricants industry. He is currently the co-founder of CDK Creative, a digital marketing agency that brings his real-world sales and operations experience to the world of online marketing. Learn more or request a consultation at ***http://cdkcreative.com****. Email him at* ***jerry@jerrykennedy.com.***

The common U.S. dandelion originated in Asia.

Dr. Edward P. Becker

Adhering to new processes

Ford's decision to use more aluminum on its best-selling vehicle opens opportunities for tribologists.

Adhesive bonding is critically important because the average age of a car on U.S. roads is 11 years and rising.

THE NORTH AMERICAN INTERNATIONAL AUTO SHOW (NAIAS), held in Detroit each January, is a great opportunity for industry watchers to see the latest trends from automobile manufacturers all over the world. Unsurprisingly, NAIAS 2014 showcased numerous advances in fuel economy for both the near and far term. One very interesting introduction is the new Ford F-150 pickup truck, which the manufacturer claims will weigh about 700 lbs. (320 kg) less than the vehicle it replaces. The weight savings is primarily due to the replacement of steel body panels with aluminum.

Aluminum has steadily replaced ferrous metals in automotive casting for years, and aluminum sheet metal is certainly not new. However Ford's decision to increase the use of aluminum sheet so dramatically on the best-selling vehicle in North America bodes well for aluminum suppliers. In fact, the Aluminum Association forecasts the demand for aluminum sheet for automobiles will increase from about 200,000 metric tons per year in 2011 to more than 1.5 million metric tons by 2020. That's an increase of 750 percent!

So what does it mean for the tribologist? There are two main opportunities, as I see it.

First, although pure aluminum is highly formable (you don't have to look far to find a beverage can whose bottom and sides are a single aluminum back-extrusion), the alloys needed for body panels are high-strength alloys that place severe limitations on the amount of deformation these sheets can tolerate without cracking. Therefore, die lubrication becomes even more critical. Although there are a number of known acceptable lubricants for relatively small-scale production, ramping up to automotive quantities provides a window for new lubricants to enable the kind of throughput typical in assembly plants.

Second, while steel bodies are extensively spot welded, welding of aluminum poses additional challenges. In particular, aluminum reacts with oxygen in the air, producing a thin, tenacious layer of aluminum oxide. This oxide has a much higher melting point than the alloy. Also, aluminum has a much higher thermal conductivity than iron, meaning more heat input must be very rapid, and thermal diffusion will result in a relatively large heat affected zone, a bane of all weldments.

Although it is still possible to weld these alloys, alternative means of fastening are gaining favor, particularly adhesive bonding. This is a classic tribology problem. After all, if we define a lubricant as a substance that reduces friction between two surfaces, then all we need to do is change "reduces" to "increases" and we have the definition of an adhesive!

One of the main challenges of adhesive bonding becomes apparent when you realize that the average age of a car on the road in the United States is 11 years and rising. Any adhesive bond, therefore, must be stable and reliable for decades. Perhaps some of what we know about producing stable lubricants for lowering friction can be applied to making stable, long-lasting adhesives. As we say in academia, actually accomplishing this goal is left as an exercise for the reader.

Ed Becker is an STLE Fellow and past president. He is president of Friction & Wear Solutions, LLC in Brighton, Mich., and can be reached through his website at ***www.frictionandwearsolutions.com.***

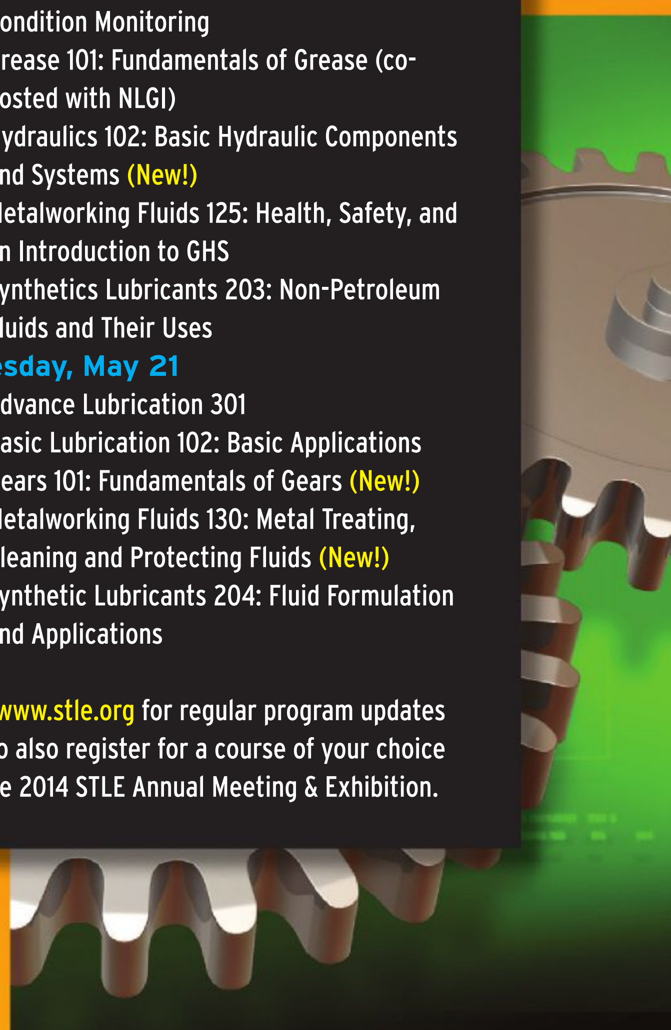

Society of Tribologists and Lubrication Engineers
840 Busse Highway, Park Ridge, IL (USA) 60068
www.stle.org • P: 847-825-5536 • F: 847-825-1456 • info@stle.org

Drs. Wilfred T. Tysoe & Nicholas D. Spencer

Split or Squeak?

A remarkably simple model goes a long way to explaining stick-slip motion.

WE ARE ALL FAMILIAR WITH STICK-SLIP BEHAVIOR, both in our professional and our everyday lives. The sound of the violin, the squeak of the horror-movie door and the shaking during an earthquake are all manifestations of this ubiquitous phenomenon. Many studies have dealt with stick-slip, and not a few attempts have been made to model it, generally focusing on the dynamics of the slider system and the slider-track interface.

In a recent issue of *Tribology Letters*, Michael Varenberg and Yuri Kligerman of the Technion-IIT in Israel published an alternative, extremely simple massless (non-inertial), quasi-static (non-viscous) approach to the problem.

In systems in which the contacting area is split among many asperities, such as under the many split protuberances in the feet of certain insects and amphibians, stick-slip has been observed to be far less likely to occur than in systems where there are few but relatively large contacts.

In Varenberg and Kligerman's model, two

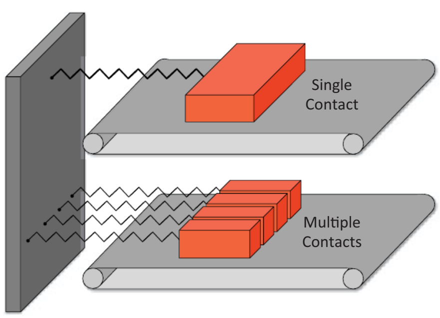

Figure 1 | **Single and Multiple Contact Cases.**

situations are considered (Figure 1). In the first case of "single contact," a block attached to a fixed wall by a spring is placed on a conveyer belt and the belt set in motion. The spring force and the friction force between the block and the belt increase (stick-phase) until the elastic force of the spring exceeds the static friction between the block and the belt. At this point, the block begins to slide, causing the tension in the spring to decrease until the dynamic friction value is reached so that the block sticks again and the cycle repeats.

In the second case of "multiple contacts," the block is divided into a number of small blocks ("sub-contacts"), each being connected to the wall by a spring. This mimics the situation where contact is split between numerous asperities. This time the stiffness and friction of each sub-contact are both fractions of the values for the single-contact case, but there exists a statistical distribution of individual values for these contacts. When any particular sub-contact enters the slip phase, as described above, the other sub-contacts may still be sticking or have already entered the slip-phase.

The sum of all the friction forces is shown in Figure 2 for the cases of the single (Figure 2(a)) and multiple (Figures 2 (b) to (d)) contacts, where here the contact is split into 2, 50 and 5,000 individual sub-contacts (referred to as *n* in the Figure). It can be seen that while the friction force displays the characteristic stick-slip behavior for the single contact, even splitting it into two contacts begins to complicate this simple behavior due to the incoherence of the two slipping blocks. When *n* reaches 50 or 5,000 sub-contacts, the stick-slip behavior is hardly detectable anymore, even though the total friction and spring force are the same as in the single-contact case.

Such a simple model cannot reproduce all the properties of a real system, but it does go a long way toward explaining why stick-slip behavior disappears in the case of contact splitting. It also helps us to understand the materials' influence on stick-slip and why, for instance, metals, with their many characteristic asperities, are less likely to produce stick-slip than rubber-like materials, which conform better to the countersurface, and therefore form far fewer contacts.

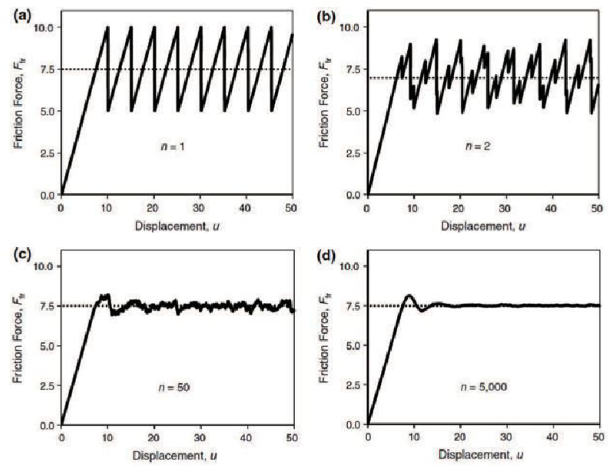

Figure 2 | **Effect on friction behavior of splitting contact into *n* subcontacts** *(reproduced from the reference below with kind permission from Springer Science Business Media B.V.)*

FOR FURTHER READING:

Kligerman, Y. and Varenberg, M. (2014), "Elimination of Stick-Slip Motion in Sliding of Split or Rough Surface," *Tribology Letters*, **53**(2), pp. 395-399.

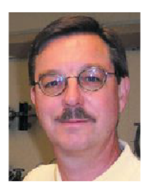

Eddy Tysoe is a Distinguished Professor of Physical Chemistry at the University of Wisconsin-Milwaukee. You can reach him at ***wtt@uwm.edu.***

Nic Spencer is professor of surface science and technology at the ETH Zurich, Switzerland. Both serve as editors-in-chief of STLE-affiliated Tribology Letters journal. You can reach him at ***spencer@mat.ethz.ch***.


We create chemistry that makes hydraulic equipment love a smaller carbon footprint.
By using high-performance biodegradable hydraulic fluids from BASF it is possible to minimize the potential impact bull-dozers and hydraulic excavators have on their surroundings. When the earth-moving and construction industry leaves a smaller footprint on the environment, it's because at BASF, we create chemistry. For more information contact us at: industrial_lubricants@basf.com
www.basf.com/lubes
BASF
The Chemical Company